Vologram

Handgemachte Volumsphysikalisierungen für die Ausbildung

DIPLOMARBEIT

zur Erlangung des akademischen Grades

Diplom-Ingenieur

im Rahmen des Studiums

Medizinische Informatik

eingereicht von

Daniel Pahr, Bsc.
Matrikelnummer 0906438

an der Fakultät für Informatik

der Technischen Universität Wien

Betreuung: Ao.Univ.Prof. Dipl.-Ing. Dr.techn. Eduard Gröller
Mitwirkung: Assistant Prof. Dr. Renata Raidou
          Hsiang-Yun Wu, PhD

Wien, 24. November 2020

_____   _____
        Daniel Pahr   Eduard Gröller

Vologram

Educational Craftworks for Volume Physicalization

DIPLOMA THESIS

submitted in partial fulfillment of the requirements for the degree of

Diplom-Ingenieur

in

Medical Informatics

by

Daniel Pahr, Bsc.

Registration Number 0906438

to the Faculty of Informatics

at the TU Wien

Advisor: Ao.Univ.Prof. Dipl.-Ing. Dr.techn. Eduard Gröller
Assistance: Assistant Prof. Dr. Renata Raidou
            Hsiang-Yun Wu, PhD

Vienna, 24th November, 2020 _____   _____
                                      Daniel Pahr   Eduard Gröller

Erklärung zur Verfassung der Arbeit

Daniel Pahr, Bsc.
Gerichtsweg 47
2540 Bad Vöslau

Hiermit erkläre ich, dass ich diese Arbeit selbständig verfasst habe, dass ich die verwendeten Quellen und Hilfsmittel vollständig angegeben habe und dass ich die Stellen der Arbeit – einschließlich Tabellen, Karten und Abbildungen –, die anderen Werken oder dem Internet im Wortlaut oder dem Sinn nach entnommen sind, auf jeden Fall unter Angabe der Quelle als Entlehnung kenntlich gemacht habe.

Wien, 24. November 2020

_____

Daniel Pahr

Acknowledgements

First and foremost, I thank my supervisors from the Research Unit of Computer Graphics. Not only did Renata Raidou and Hsiang-Yun Wu provide me with ideas and inspirations during the inception of concepts and valuable feedback in writing this thesis, but their positive reinforcement along the way also filled me with limitless motivation. I also thank Eduard Gröller who, despite my tight schedule, managed to provide me with thorough proofreading of this thesis with unrivalled preciseness, timely support, and the comprehension of the concept of the Oxford Comma.

I would never have made it this far, without the help and camaraderie of the countless colleagues I met along the course of my studies. Nor could I have reached this point without the constant motivation and support from my partner, friends, and family, who believed in me more than I did myself.

Lastly, I thank my cat Galvina
for all the biscuits.

Kurzfassung

Bereits lange vor der Verbreitung von Computertechnologien wurden anatomische Skulpturen oft zu Lehrzwecken eingesetzt. Die fortschreitende Entwicklung digitaler bildgebender Verfahren und medizinische Visualisierung haben zu einer Verdrängung von Skulpturen in der medizinischen Ausbildung geführt. Heute findet medizinische Visualisierung hauptsächlich auf Computerbildschirmen statt. Jüngste Entwicklungen in den Bereichen virtuelle, erweiterte und gemischte Reality bieten neue, interessante Möglichkeiten für die Darstellung medizinischer Bilddaten. In den letzten Jahren hat die Nutzung von physikalischen Skulpturen zur Visualisierung von Patientendaten durch das Feld der *Datenphysikalisierung* neue Beliebtheit erlangt. Im medizinischen Bereich wurde dabei vor allem versucht, die Ausbildung von Fachpersonal und Laien zu unterstützen. Dabei wird oft teure 3D-Druck-Technologie verwendet, um detailgetreue, realistische anatomische Modelle zu erzeugen. Es existieren jedoch wenige Anwendungen, um diese Konzepte in leistbarer Form für Laienausbildung zu verwenden.

Im Rahmen dieser Diplomarbeit werden verschiedene Wege erforscht, um selbstgebaute, personalisierte Physikalisierungen zur anatomischen Fortbildung medizinischer Laien einzusetzen. Wir stellen das *Vologram* Konzept vor, als passenden Kandidaten, um medizinische Bilddaten auf eine ansprechende Art für Nichtmediziner darzustellen. Dies geschieht in der Form von Folien-basierten Skulpturen. Diese können aus leistbaren und zugänglichen Materialien mit konventionell verfügbaren Mitteln hergestellt werden und erlauben einen hohen Grad von Interaktivität. Um einen anpassungsfähigen Workflow zum Erstellen dieser Figuren zu unterstützen, bieten wir eine Desktop-Applikation, die es medizinischen Laien ermöglicht, ihre eigenen, personalisierbaren Skulpturen zu erzeugen. Reale medizinische Bilddaten können damit gefiltert und auf verschiedene Arten dargestellt werden, um eine Vielzahl an optisch unterschiedlichen Resultaten zu liefern. Das Konzept wird in einer Studie im kleinen Rahmen evaluiert, um die Wirkung von interaktiven medizinischen Visualisierungen und Physikalisierungen auf das Zielpublikum abzuschätzen. Die gesammelten Resultate deuten auf ein großes Potential für den Einsatz interaktiver Fortbildungskonzepte für die anatomische Ausbildung medizinischer Laien hin.

Abstract

Long before the onset of computer technology, anatomical sculptures were already used for educational purposes. Digital imaging technology and its incorporation into the clinical workflow through the advancements of medical visualization led to a steady decline in the use of sculpture-based teaching aids. Currently, anatomical volume visualizations are predominantly presented on computer screens. Recent developments in augmented, mixed, and virtual reality offer new, exciting ways to digitally display medical imaging data. In recent years, the application of real-world sculptures to display patient imaging data has seen a resurgence through the field of *data physicalization*. Predominantly, it has been used to enhance the education of medical personnel and laymen through the use of physical models. Expensive 3D printing technology is often employed in the creation of high fidelity anatomical sculptures, with realistic look-and-feel. However, few approaches make use of affordable physicalizations in the field of layman anatomical education.

In the course of this thesis different ways to introduce self-made, custom physicalizations into layman medical education are explored. We propose a suitable concept, the *Vologram*, to display medical volume data in a visually appealing way for medical non-experts. This takes the form of slide-based sculptures, made out of affordable materials available to the general public with a high degree of interactivity, and can be produced through commonly available means. To support a customizable workflow in the creation of these sculptures, we provide a stand-alone desktop application, which allows layman users to create custom educational sculptures. Real medical imaging data can be filtered and displayed in different ways, delivering optically diverse results. We evaluate the concept in a small scale study, to determine the effect of interactive medical visualizations as opposed to physicalizations on the target audience. The results of this study point to a great potential for the application of interactive educational concepts for layman anatomical education.

Contents

Introduction

1.1 Motivation

Long before digital imaging was a possibility, 3D physical models of anatomical structures were used in medical education. This included mould-cast wax figures [RCSL10], wood, ivory and paper sculptures, or sued silk figurines [MMŽ10]. Technological developments made such methods less popular. The introduction of imaging and computer technologies provided convenient and insightful replacements. In the early stages of computing technology, visualizations were confined to screens and printouts. New modalities in visualization, like augmented and virtual reality devices, serve as an alternative to the traditional 2D methods. Parallel to current screen-based, and augmented or virtual reality visualizations, real-world representations of data still have their place. Such *physical visualizations* are called *physicalizations*.

In the last two decades, the field of physicalization is seeing a rise in popularity [JDI+15]. As public demand for information rises, current research looks into meaningful and more engaging ways of information visualization. It is argued that physicalizations possess qualities that can aid this task [ZM08]. They can convey a unique sense of scale and employ metaphors to convey their message. Examples for this can be seen in museums, where this concept is used in multiple creative ways [JDI+15]. A population density map might be more impressive for laymen to observe if the values are represented by tower-like figures, among which they can walk [JDI+15]. The inhumane conditions of slave trade might be better conveyed, if the *layout* for the arrangement of people on a ship's deck is displayed in the 3D context of a model of the ship [ZM08].

Today, the rise of new technologies, such as 3D printing, offers an alternative to expensive and difficult manual techniques, such as wax casting. Several attempts have been made to employ this, as an aid in medical education [ADS5] and surgical planning

[WPF$^+$15, HL16]. However, 3D printers are still not easily accessible to the general public. Firstly 3D printers and the materials that they use are fairly expensive. Also, those printers accept only certain input formats from often proprietary computer-aided drawing applications, which demand some experience from the user. Lastly, common 3D prints do not provide a lot of interactivity, due to their static nature. Alternative forms for creating volume visualizations with more readily available technologies have been presented [SB16, Fra], opening promising directions for the future of physicalization. If physicalizations can find their way into households, they might add value to information visualizations in a way that screen-based visualization alone can not.

1.2 Aim of the Work

In the course of this thesis, we demonstrate the potential of physicalization for the anatomical education of the general public. We propose an application for anatomical education, using readily available volume data. The target audience of this application are laymen, i.e., people from the general population with no experience in medical visualization and little anatomical knowledge. To facilitate their understanding of the anatomical data, the volumetric data will be presented in a way similar to illustrative volume rendering [LVPI18], resembling illustrations in a typical anatomical textbook. The application enables layman users to explore prominent anatomical structures, such as major organs, and to create personalized physical sculptures from regions of interest. The sculptures enhance the learning experience of the users and provide an interactive and engaging exploratory experience of the human body.

A fundamental aim is to find alternative ways, besides 3D printing, that support the creation of physical anatomical visualizations, and to facilitate the translation from digital visualizations to physical objects. Users will be provided with a way to create custom sculptures from the supplied volume data using commonly available technologies, such as desktop printers, paper, and cardboard. The application will support the assembly of the physical models, by providing step-by-step instructions for construction.

To summarize, this thesis aims to answer the following research questions:

Q1 How can the engaging properties of physicalizations be used to advance the anatomical education of laymen?

Q2 Does a combination of commonly available materials exist that can be used to create meaningful physicalizations, cheaper and faster than 3D printing?

Q3 Are physicalizations able, due to their unique properties, to complement virtual visualizations in the context of anatomy education of laymen?

1.3   Methodology and Contribution

This work is distilled into an application that allows users the creation of physicalizations of anatomical structures. Our first task along the way is to a suitable physicalization. Based on the target group, we find a style of physicalization that is both meaningful and feasible to construct with cheap and accessible methods. This is achieved by using the *holograph* physicalization style, as we will discuss in the upcoming sections. Our proposed physicalization uses transparent sheets of overhead foils, stacked in a regular interval to create the effect of a three-dimensional figure. The slides can be printed with conventional inkjet printers and are available in office supply stores.

The application to create these physicalizations uses illustrative-style volume visualization. Different organs are rendered in different colours, to be easily distinguished for laymen. We use a simple *what-you-see-is-what-you-get* approach, for selecting the parameters for the physicalization. Rotation of the volume is defined by rotating the viewpoint of the screen visualization. Parameters for the pyhsicalizations can be set and previewed before printing, so that potential waste and faulty output is kept to a minimum. Users select an inter-slice distance and a scale for the physicalization. Organs can be selected to be displayed or removed from the resulting physicalization, to reduce the visual clutter of the physicalization, while still providing sufficient anatomical context.

After parameters have been selected, the volume data is transformed into a printable template. A volume data source is created, based on the selected organs. Based on the previously selected viewpoint, the volume data is sampled in a regular interval, normal to an axis defined by the selected viewpoint. The interval corresponds to the selected inter-slice interval and scale of the physicalization. Upon completion, the result is displayed as images with the arranged slices, numbered by their order from front to back with respect to the viewing direction. Users need to select a range of slices and save the images to print them onto the foils. Afterwards, they need to assemble the slides in a regular distance, preserving the order indicated by the printout.

The *contribution* of this thesis is the conceptualization and development of a physicalization strategy for medical visualization to be used in anatomical education. This is achieved by the development of the transformation tool *Vologram*. The tool enables users to create meaningful physical sculptures of real medical volume data. The simplified and colourful *illustrative* method for visualization and the easily understandable visualization parameters are primarily targeting layman users. The resulting printables can be created without the need for expensive technology or materials, as opposed to 3D-printing. Assembly of the sculptures is self-explanatory, through the ordered labelling of the slices. A small scale study provides insight into the potential of our physicalization approach.

1.4   Thesis Outline

The following chapter provides a brief overview of the background of this thesis. Most importantly the field of anatomy education concerning the application of both digital and physical visualizations are examined. As anatomy education has an overlap with doctor-patient-communication, we also briefly introduce this field as a possible application for physicalizations. We present the concept of data physicalization and how such an approach will fit into a traditional information visualization workflow. Lastly, we go into detail about the historical and current applications of physicalization in and out of the medical field. Current approaches are compared and their examples are used to determine a suitable contribution for our work.

With these conclusions, we formulate a concept for the application of physicalization in anatomical education in Chapter 3. This includes a thorough requirements and design analysis to formulate tangible goals for our work. We examine a set of available materials that will be used in the prototyping stage and define the target audience for our application. Based on this we present the findings of our prototype designs and present the selected physicalization concept. We then present the design of the application for the creation of these sculptures and finally formulate the visualization pipeline encapsulating both. The technical aspects of the implementation are described in Chapter 4. In Chapter 5, we summarize the result of all work performed. This includes the results of the performed evaluation. Conclusively we provide a summary of our findings and possible entry points for future work in the field.

CHAPTER 2

Background and Related Work

This chapter serves as an introduction to basic concepts, as well as a review of the work related to this thesis. The following sections provide an insight into the backgrounds of anatomy education. We focus primarily on different teaching aids that are provided to anatomy students, of both physical and virtual nature. Approaches to the education of laymen are mentioned as well. Afterwards, we explain the concept of physicalization in further detail. The penultimate part of this chapter is a review of related work in the field, both in the past and present times. We conclude this chapter with a summary of the lessons learned within, as well as our conclusions on what can be contributed to the field in the future.

2.1 Anatomy Education

The teaching of human anatomy is one of the cornerstones in the education of medical professionals. Traditional anatomy atlases and textbooks play an important role here. Examples for this can be found in *Gray's Anatomy* [Gra09], a highly influential anatomy textbook, written in the 1850s and published to this day, or the more recent *Grant's Atlas of Anatomy* [AD09], published in 1991. Furthermore, anatomy education is often supported by cadaver dissection [PS18]. Such teaching methods have a historic background, dating back as far as to the beginning of medicine itself. However, the use of cadavers has been disputed by clerical authorities in different periods of history [Gho15]. Additionally, the source of cadavers for vivisection is limited [MMŽ10, RCSL10]. Anatomical models made with different materials have been a widely used alternative to cadavers through medical history [MMŽ10, RCSL10]. Wax moulds of rare skin conditions have been used by dermatologists well into the 20th century [Gei09].

Developments since the 20th century in the field of imaging have brought alternatives for many of the historic techniques. Commercial photography replaced wax moulds
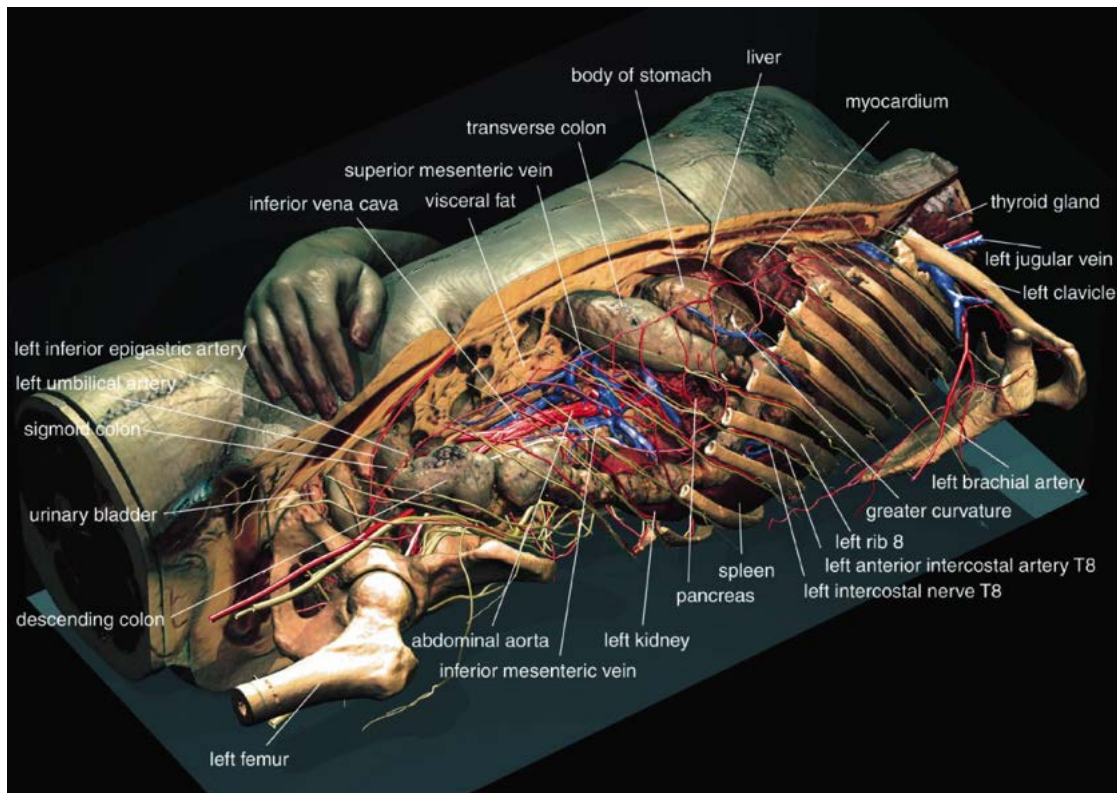
Figure 2.1: Visualization created from the *Visible Human* male dataset. It provides a realistic rendering of the data and allows arbitrary cutting and clipping. Labels are attached to the anatomical structures [PHP⁺01].

because they were easier to make and significantly cheaper [Gei09]. The introduction of X-Ray and other medical imaging modalities offer the possibility to capture structures under the patient's skin in a non-invasive way [PB13]. As those practices found their way into the medical workflow, anatomy education began to be aided by medical imaging techniques. This meant that the interpretation of medical images also became a subject of medical education [SAK10].

In recent decades the ubiquity of computing technology has led to the widespread use of screen-based visualization of medical imaging data. As a result, research in anatomical education seeks to incorporate digital visualizations as well [PS18]. Multiple interaction possibilities result from the application of virtual imaging data. Digitally stored imaging data is made widely available and many exemplary applications make use of those image sets. A very prominent example are the *Visible Human* datasets [ASSW95]. They consist of high-resolution scans of cryosected human bodies, one male and one female. When processed, this data can be represented in multiple ways that can aid the study of anatomy in different ways. Segmentation, performed on imaging data, results in different structures being labelled and presented distinctly. Three-dimensional

renderings of medical data can be rotated and filtered in real-time by users. The digital representation of the data facilitates arbitrary cross-sections and cuts through the renderings. Pommert et al. [PHP$^+$01] created a multitude of different visualizations from the *Visible Human* male dataset. One of these is shown in Figure 2.1. Such visualizations provide users arguably with more degrees of freedom in interaction with their subjects than illustrations. The high degree of detail in such visualizations allows users to examine those structures thoroughly without the need for actual vivisection. It has been shown for a specific case that 3D models can benefit anatomical education [NCFD06].

Recent years have also seen substantial developments in *virtual reality* (VR), *augmented reality* (AR), and *mixed reality* systems. The distinction here is that VR systems aim to immerse a user into a purely virtual world and AR systems project virtual objects into the real world. Mixed reality systems expand upon AR in the sense that they allow virtual and physical objects to interact. A supposed advantage of such a system is the more direct mode of interaction as opposed to, for example, with keyboard and mouse. Additionally VR and modern AR systems make use of depth perception through stereoscopic vision. Naturally, VR and AR technologies are now being applied to anatomical education in various aspects [PS18]. Some VR devices allow users more or less *direct* interaction with virtual objects through the use of joysticks. This has been shown to be beneficial for anatomy education as opposed to simple observations of 3D rendered objects [JVJB17]. An interesting approach to the application of AR technology in anatomy education has been made by Stefan et al. [SWO$^+$14]. They propose a 3D anatomy puzzle where bone structures are superimposed over the recorded images of people. This application was notably not exclusively aimed at medical professionals. The authors argue that such an application would also benefit the education of children. Chen et al. [CDTJ17] see a purpose for AR systems in both medical training and education. For the training of medical professionals, AR systems provide a way to practice some medical work practices without the danger of harming a patient. Although both VR and AR systems are still very much in a developing stage [PS18, CDTJ17], both technologies have good potential for use in medical education.

After the historical use of wax models, the recent developments in 3D printing technology show the potential of the return of physical models for anatomical education. Based on medical imaging data, models of anatomical structures can be created using 3D printers. Alternatively, modern 3D scanning technology can be of aid in reproducing existing surgical dissections [ADS5, MQMA14]. When using printing material of different colour [MQMA14], or different materials for different tissue types [HL16], models can be created with different degrees of realism. An example of this is given in Figure 2.2. An advantage of the use of 3D printed learning material over the use of dissected specimen is the ability to reproduce the models at a relatively low cost. Furthermore, some abstractions can be introduced in the printed materials, like the use of colour for different anatomical or histological regions. Finally, the durability of cadaveric materials is limited despite preparation, which does not apply to artificial materials. Lim et al. [LLG$^+$16] were able to prove that the use of 3D printed anatomical models had no significant disadvantage to
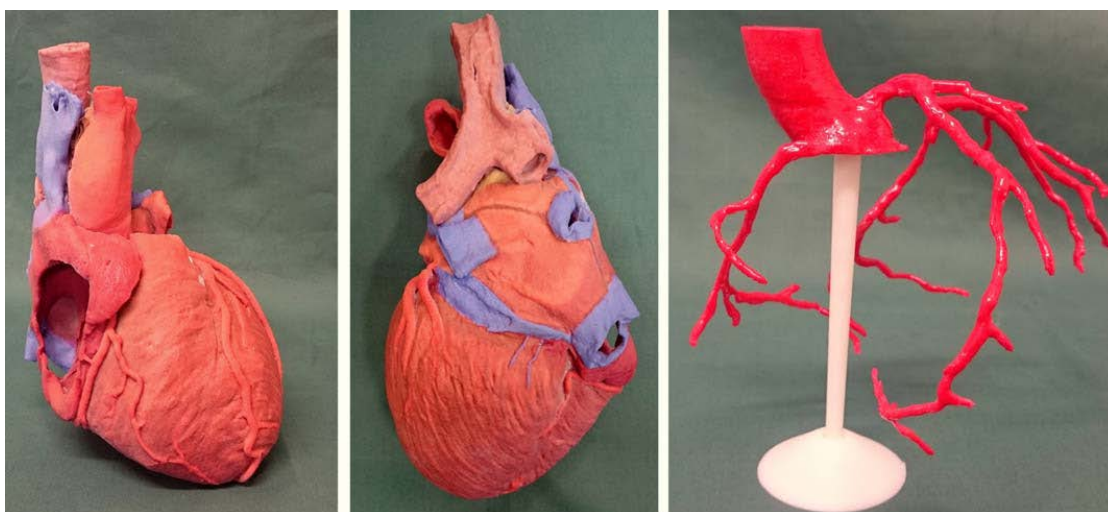
Figure 2.2: 3D Printed models of human cardiac anatomy. The models use colours for better differentiation of anatomic regions as opposed to monotonously coloured specimen from cadavers. [LLG$^+$16]

the use of cadaveric materials as learning aids for medical students.

While many of those approaches rely on 3D printing, especially when focusing on the education of medical professionals, some research is examining more cost-effective and easier reproducible ways to create anatomical models. This is often focused on the education of laymen, who normally do not have access to 3D printing technology [RGW20, SWR20].

Conclusively, nowadays medical professionals and laymen alike have access to a multitude of anatomy teaching aids, in many different modalities. Reviews on the evolution of the state of anatomy education agree that the best way to teach anatomy lies in a multi-modal approach [SAK10, EB16]. It is, therefore, worth to investigate new modalities to support tried and trusted practices.

A field that lies on the interface between medical professionals and patients is patient education or doctor-patient communication. It is seen as an important part of medical treatment. Proper doctor-patient communication can further the relationship between doctors and patients [ODHHL95] and lead to more patient satisfaction and fewer complaints [HL10]. Nowadays patients are required to consent to medical procedures. It is therefore required to communicate as much information about their condition and planned interventions as possible to patients [ODHHL95]. Additionally, communication is an important aspect of diagnostics, from both the doctor's and the patient's side. Patients need to accurately describe their symptoms during anamnesis, which can be aided by a doctor asking the right questions [ODHHL95]. Anatomical details can play an important role in patient education. As patients often lack anatomical knowledge,

visual aids can be of help here as well.

Saalfeld et al. [SSPOJ16] presented a 3D interface that can be used for the interactive sketching of vascular structures. It is argued that sketching is often used as a supplement in patient education. Although the system was primarily designed for the teaching of vascular anatomy to medical professionals, such a system could find application in patient education as well.

Applications for physicalizations that could be used in supporting informed patient consent can be found in Stoppel and Bruckner's *Vol2Velle* [SB16] as well as Raidou et al.'s *Slice and Dice* [RGW20]. They present methods to create simple and cost-effectively manufacturable printable volume visualizations. Localized visualizations of patients' pathologies could be used to communicate the underlying conditions. Both concepts are examined in further detail later.

2.2 Data Physicalization

In a general sense, data physicalization can be understood as mapping data to objects and their properties in the physical world [JDI$^+$15][Moe08]. In a historical perspective, looking at a time before computer visualizations were found everywhere, it is easy to come up with an example of such a representation. Due to the analogue nature of measuring devices, hard to observe phenomena are typically mapped to easily observable properties. A quicksilver thermometer displays temperature by allowing us to measure the thermal expansion of the medium on a numeric, distance-based scale. Abacuses represent numbers and numeric operations by shifting beads or scales along fixed axes.

Recently, physicalizations have begun to resurface, sometimes as an aid to traditional visualization [SCS17], sometimes as a replacement of digital screens [JDI$^+$15]. Where a computer screen can only communicate through the optical channel, physicalizations facilitate data exploration beyond that, allowing us the use of our other senses for data exploration. Moere [Moe08] suggests multiple categories for "non-screen" information displays, such as:

- **Ambient Display:** Displaying information by altering physical properties of matter, such as water ripples or rising/falling water levels.

- **Pixel Sculpture:** Replacing pixels with real-world equivalents, like lamps, water bubbles, or flames.

- **Object Augmentation:** Using the properties of objects to display a specific state, such as coloured lamps to indicate water temperature.

- **Wearable Visualization:** Information displays that can be worn by humans, indicating specific data to themselves and others around them.
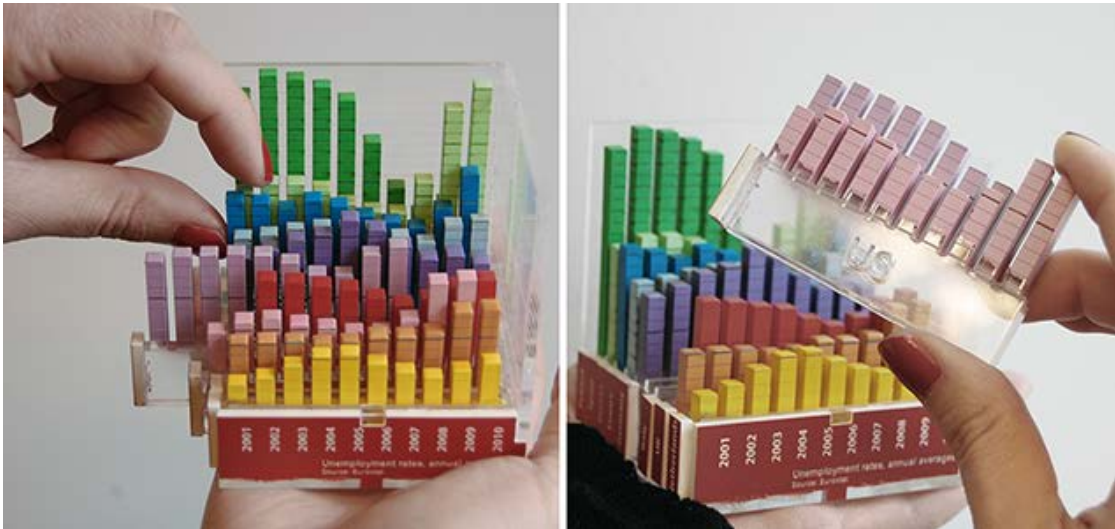
Figure 2.3: A tangible, interactive 3D bar chart [JDF13]. A typical example for a sculpture representing abstract data.

- **Data Sculpture:** Contrary to the previous categories, data sculptures have no purpose besides displaying the data to the observer.

- **Alternative Modality Display:** These focus on using different senses to convey their meaning besides vision. Examples are sound and olfactory displays.

From here we will focus on *data sculpture* and (hybrid) *alternative modality displays*, for which applications in the field of medical visualization can be found. Furthermore, we will also consider 3D sculptures of medical imaging data as data sculptures.

2.2.1 Main Facilitators of Data Physicalization

Historical examples [RCSL10] show that tangible sculptures were used with a benefit in the past. In this section, we will motivate the future use of such concepts. We will use three central arguments to underline this. For once, it can be argued that tangible objects have at least different, maybe even advantageous properties to virtual images [JDI+15]. Furthermore, it is necessary in the current world to provide means of access to a multitude of information to a non-expert audience [ZM08]. Lastly, we argue that technology has advanced since the onset of digital visualizations and new ways to create meaningful physicalizations efficiently have been developed[RMVTK+10].

Advantages over traditional visualizations

When Jansen et al. [JDF13] evaluated the efficiency of physicalizations, they use a digitally manufactured, physical bar charts. The form was specifically chosen to appeal

to non-expert users, with little experience in data analysis. The bar charts consisted of 100 bars, made from laser-cut acrylic, displayed in front of a transparent scale. Each of the bars represented the magnitude of one specific fact in a specific country in a specific year. Each country was additionally assigned one colour for its bars. The bars were ordered by time. The models are compact enough to be lifted and observed in one hand. Interactivity was additionally enabled by the possibility of rearranging the series of bars by country. One such bar chart can be seen in Figure 2.3. The study showed an advantage of physicalizations over virtual 3D visualizations in the examined context. These findings also emphasize the importance of tangibly conveying information to non-expert users [ZM08]. The interaction possibilities of the previously named example are also an aspect that screen-based visualizations do not provide. Unique properties of physical representations such as physical properties, material, and nuances that can not be produced with digital screens are mentioned as opportunities for such tangible visualizations. Also, the opportunities provided by the use of visual metaphors are more numerous in physicalization. [ZM08]. 3D objects that exist in reality can convey a sense of scale that can not be displayed on screens. Depth perception is also a factor that computer screens can only simulate. Some findings argue that this is another beneficial aspect of physicalizations [ASS+19]. 3D printing technology can create a single model with multiple materials. Some of those materials can serve as a good simulation of the tactile feedback from actual organs [VMML17]. Another advantage provided by physical sculptures is their ability to serve as a reproduction of tangible objects, such as organs. Medical education [ADS5, RMVTK+10] as well as diagnostics [HL16, KNSV15, RMVTK+10] can benefit from this.

Empowerment of laymen

Zhao [ZM08] cites the *democratization of information access* as a big motivation behind the application of data sculptures. Early concepts of information visualization mostly dealt with the presentation of data to expert users. They argue that, due to the higher demand of non-expert users to information, we must look for suitable ways to present data. Doctor-patient-communication is one example of this. It is argued that due to their properties, physicalizations are well suited for this purpose [RMVTK+10, SB16]. Patients are required to give informed consent on procedures performed on them. Thus it can be argued that such communication should be meaningful. Attempts have been made to facilitate this communication by way of providing tangible visualizations [SB16]. Another exemplary for laymen empowerment was provided in the previous chapter, where data sculptures were used to communicate facts to a non-expert audience [JDF13].

Technological advancements

It can be argued that in the field of printing, the onset of 3D printing technologies is similar to the development of VR and AR technologies in visualization. Both technologies essentially add another dimension to the output of already existing modalities. The recent advancement in 3D printing is often mentioned as a universal facilitator for the feasibility

Figure 2.4: A 3D printing (right) of a segmented anatomical volume visualization (left). showing an aortic aneurysm (see arrows) [RMVTK+10].

of physicalizations [KNSV15, RMVTK+10, ASS+19]. Some 3D printing technologies are even similar to the nature of medical 3D imaging data, in that they create the models slice by slice. An example of this can be seen in Figure 2.4 where a digital segmentation is compared to the resulting 3D print. Various 3D printing technologies exist with different degrees of fidelity. Uses for 3D printing in medicine can be found in the fields of education and surgery planning. 3D printing is steadily becoming more affordable and production times decrease. Models can be produced in around 24 hours and the only major cost factor are complicated materials. Wax models like moulages, which were carefully hand-crafted, were replaced by photography for cost and convenience reasons. As soon as a 3D printing will reach a higher level of convenience this could mean that the inherent advantages of physicalization could make such a technique attractive to medical practitioners. Additionally, the interactivity of physical data embodiments is argued to profit from the advances in microchip technology. The decrease in size of computation
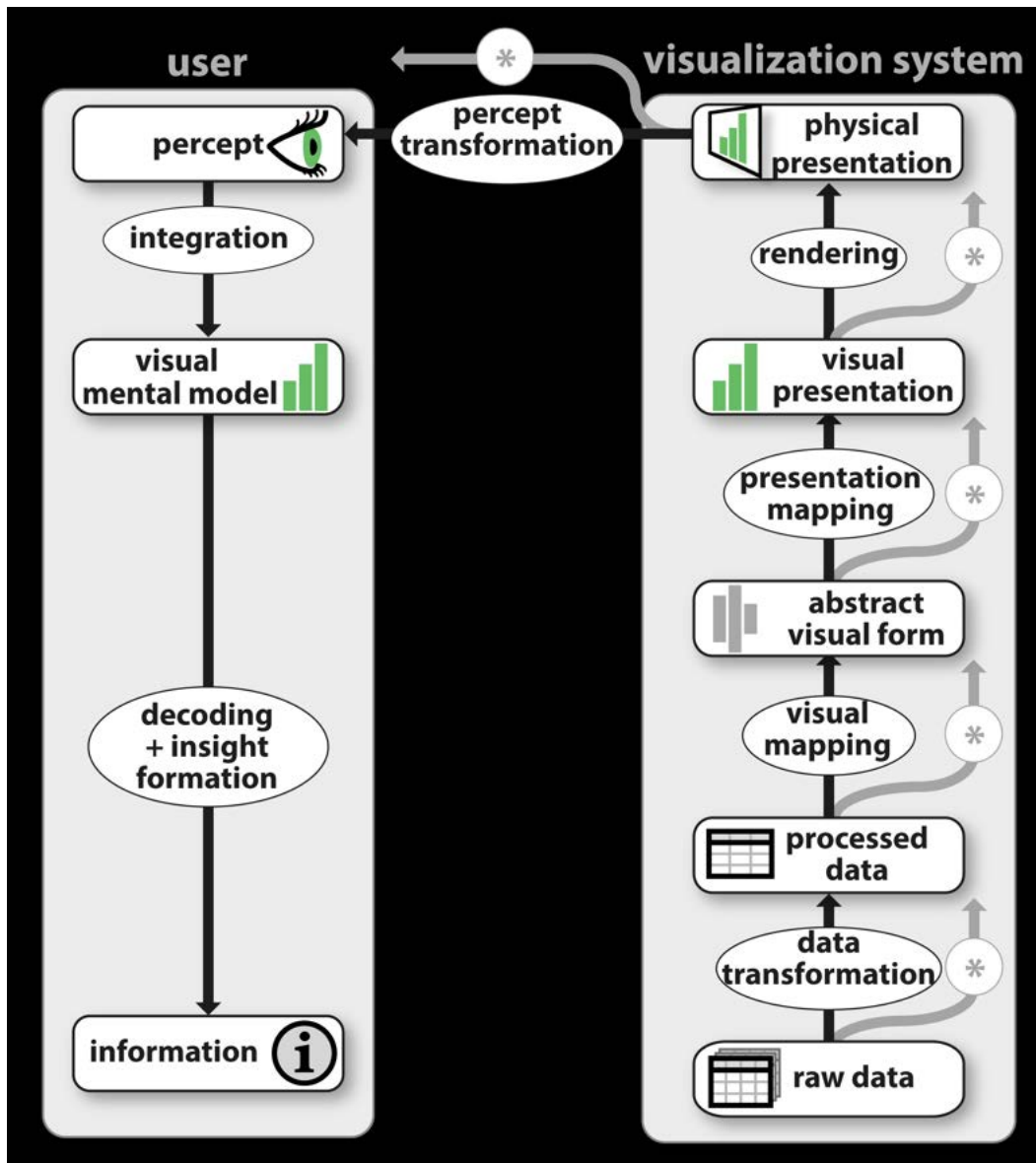
Figure 2.5: An updated version of the information visualization pipeline, proposed by Jansen et al. [JD13]. It contains an added emphasis on the perceptive side.

devices can further aid the interactivity of physicalizations. [ZM08]. Although there are also applications outside the field of visualizing data, such as creating surgical prosthesis for patients [RMVTK+10], here we will focus only on the benefits of physicalizations for visualization.

2.2.2   From Data To Sculpture

The field of information visualization has traditionally been dealing with the transformation of raw data to a *visual* representation of the data that can be explored by an observer. To extend the traditional information visualization pipeline to incorporate the fabrication of physicalizations, Jansen et al. [JD13] presented an adapted version of the workflow which can be seen in Figure 2.5. A notable extension they provide is a higher emphasis on the (usually) final part of the pipeline, the rendering, in which the visualization is normally created. The creation of information visualizations starts by transforming the raw data by essentially picking out what subset of the data one wants to visualize. In the visual mapping stage, the processed data is transformed into a visual abstraction. Typically this means a specific form of visualization is chosen, for example, a type of graph. In the end, the visual presentation is created by customizing the chosen abstraction, selecting scales and colours, rearranging aspects of the visualization, and providing visual decorations such as axis figures. At this point, a complete displayable digital form of the visualization exists. By performing the final step, this form is presented to the user, but this task is not limited to the display of the data on flat digital screens. The representation can also be created by using specialized physical displays, or 3D printing.

Furthermore, a whole new side to the visualization pipeline is added, describing the users' observation of the data and the process of extracting information. The perceptual side of the model aims to describe the processes that occur after a representation of the data is rendered. It begins with the perceptual transformation of the rendered object. This constitutes the act of perception, such as looking at a screen or perceiving a physical sculpture. The perceived stimuli are integrated into a visual mental model of the data which is then decoded to yield the actual information the user can extract.

A user's manipulation of the information visualization pipeline is defined as *interaction*. Physicalizations offer notably different possibilities compared to 2D and 3D visualizations. A user can touch a sculpture, determine the weight of individual parts, physically rearrange components [JDF13, JD13], or add audio signals in relation to physical or digital sculptures [SCS17], to name a few possibilities.

2.3   Historical Medical Physicalization

Medical research has begun long before the age of computers and even the rise of analogue photography. Hand drawn anatomical illustrations can be found in textbooks that predate digital imaging such as the *Tabulae Anatomicae* from 1627 [CB32] of which an illustration can be seen in Figure 2.6 and the *Syntagma Anatomicum* by Johannes Vesling from 1647 [Ves47]. Even then, people have been looking for alternatives to those pictures, of which anatomical education for emerging doctors and surgeons could benefit. The only way for a person to see an organ in real life was, of course, the dissection of a human specimen
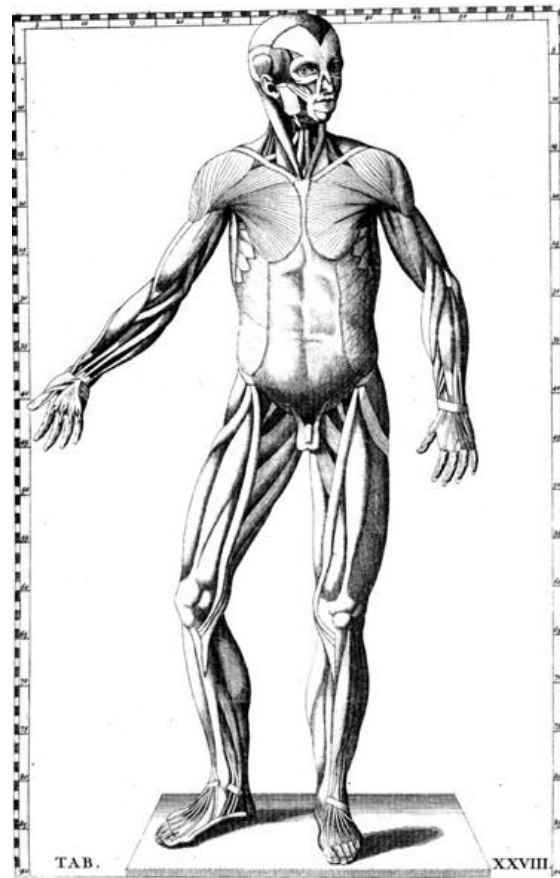
Figure 2.6: Eustachius: Tabulae Anatomicae (1714): Tab. XVIII. A classical example for a historic anatomical drawing [CB32].

or conserved preparations.

In the 17th century medical professionals began to see the need to produce anatomical sculptures to eliminate the need for performing dissections for medical students. Wax sculptures, produced by moulding and casting the organs of dissected cadavers, became a popular method for teaching anatomy. One example of such a wax sculpture can be seen in Figure 2.7. The generally *aesthetic* nature of such works becomes apparent by the details of the figure like for example the tranquil facial expression. These wax figures were based on limited knowledge of human anatomy and histology. Nevertheless, the sculptures provided a reusable and durable alternative to preparations [RCSL10]. To this day most people will have seen some form of anatomical sculpture.

Other prominent examples of sculptures being used in medicine are the so-called *moulages*. They were officially introduced in the late 19th century by dermatologists. Moulages are wax cast models of pathological conditions occurring on the surface of the body. They were used predominantly by dermatologists, both as teaching aid and case documentation.

15

Figure 2.7: Wax statue *deep lymphatic vessels in a female subject* by Susini, 1794. A Typical wax figure created from molds by an artist [RCSL10].

Due to the increasing availability of photography, the widespread use of moulages for medical purposes ended in the mid-20th century [Gei09].

After the discovery of X-Ray, and the invention of sonograms and various tomography technologies, resulting images were incorporated into the workflows of medical practitioners [PB13]. X-Ray images result directly in 2D photographs, sonograms are displayed live on monitors and also display a 2D cross-section of the body, and computed tomographies produce digital imaging data. This eliminates the necessity for a physical manifestation of the data in the first place. In recent times the abundance and ubiquity of computer technology led to further digitalization of medical data, as hospitals and doctors keep and communicate files primarily on digital media. Many applications for three-dimensional visualizations of anatomical data exist today, for multiple purposes, largely taking the space of physical models in education [PB13]. In aiding diagnosis such technologies have the immediate advantage of representing actual patient data in a time and cost-efficient manner, which the historical wax models never could. Emerging virtual and augmented reality systems, in light of their ability to display images in a 3D space, are also used in growing abundance.

The use of physical representations of anatomical and also abstract data has thus naturally decreased. In some fields like diagnosis, treatment planning, and education the modern computer technologies have established. However, in recent years, research into data physicalization has persisted and evolved. Some physical visualizations have proven effective, sometimes even more than their virtual counterparts [JDF13]. It should be noted that representations of abstract data can be physicalized as well, as opposed to sculpting more or less realistic images of anatomical structures. Many current works that focus on data physicalization do not explicitly focus on medical application [Moe08, ZM08, JDI+15],

Figure 2.8: Carcinoma faciei, manufactured by Dr. Carl Henning, 1894 (Foto: Mag. Anatole, 2013). A moulage on display in the pathoanatomical collection of the Natural History Museum Vienna [Mou].

however, some examples can be found. Both in the augmentation of visual data through sound [SCS17] and the preparation of creative, off-screen, volume visualizations [SB16] we find uses for not (exclusively) screen-based data representations. Due to the recent developments in the field of 3D printing, many attempts have been made to put this technology to use for medical applications. Uses for 3D printing in medicine can be found in education [ADS5] and surgery planning [WPF⁺15, HL16]. In light of these circumstances, we will present the current state and opportunities of physicalization for medical visualization.

2.4 Concurrent Applications of Physicalization

Societal factors and inherent capabilities of physicalizations [ZM08] as well as advantages over certain digital visualization techniques [JDF13] point to various applications for the use of physical data representations. We will provide multiple examples for the current use of physicalizations. Applications notably exist in the form of data sculptures. This concept deals with physical objects that represent only the data and no more[Moe08]. Data sculptures typically do not possess a hidden or contextual meaning. They can

deal with abstract data representation [JDF13] and the embodiment of spatial data [RMVTK+10]. Abstract data in this context are such data that have no *natural* counterpart. On the opposite side, spatial data can be understood as imaging data, especially in the context of medical visualization. Hybrid visualizations, previously introduced as *alternative modality displays* are another potential application for physicalization in medical visualization[SCS17]. We employ the term *hybrid visualization* because for the given examples the alternative modality is provided in addition to a visualization. The following section will provide an overview of some of these examples.

2.4.1 Data Sculptures

A physicalization is called a data sculpture, when it only represents the underlying data, without adding additional context to the representation. Data sculptures have proven to be useful alternatives to 3D visualizations [JDF13]. We will distinguish between two variations of data sculpture, embodiment of *abstract* and *spatial* data. Visualizations, where the mapping between the raw data and the representation in the sculpture are arbitrary, like for example bar charts and graphs, will be categorized as *abstract* data embodiment. On the other hand, applications where the sculpture is a direct representation of the data, like in the visualization of medical imaging data, will be named *spatial* data embodiment.

Abstract Data Embodiment

To examine the efficiency of physicalizations compared to 2D and 3D visualizations, Jansen et al. [JDF13] performed a study where these three distinct modalities were set side-by-side. They focused on sets of data that could be compared using bar charts, as those require relatively little experience with visualizations. The datasets contained some facts that were to be examined over 10 years in 10 countries, leading to 100 distinct values. Participants were given three different modalities to interact with the data and complete different visualization-related tasks, like ordering data or determining value ranges over a specific dimension. In the 2D variant, the participants were given a multi-modal 2D visualization that showed the whole dataset in a matrix display with squares, filled proportionally to the magnitude of the values. Additionally to that, the matrix view could be filtered along both axes individually to provide a *flat* bar chart for one selected *slice*. The 3D visualization was a 3D bar chart rendered in an interactive visualization, controllable with a PC mouse. Finally, a physical version of the 3D bar chart was created, using digital manufacturing technologies, the result of which is shown in Figure 2.3. The bar chart sculptures were of a fixed size with an $8\,cm \times 8\,cm$ base and $5\,mm \times 5\,mm$ bars. This allowed for easy physical manipulation, like lifting, touching, and turning. The observation was made that after initially having some reservations to do so, participants started to take full advantage of the sculptures by lifting and rotating them. Comparatively, the more indirect mapping of the object manipulation techniques for the virtual 3D visualization proved more difficult to handle. Despite some advantages, like dynamic transparency, the participants reported some trouble with this variant. The

Figure 2.9: An interactive physicalization using lego bricks. Used by General Motors to visualize problems in the manufacturing line [gmL]

2D visualization was found to be the most efficient for the task. However, compared to the virtual 3D visualization, the physicalization proved to be the better method. In a second experiment, the 3D visualization and the data sculpture were examined in direct competition more closely. Here the study found that, through physical interaction with the sculpture, the participants were able to use their fingers as memory aids. This helped them to complete tasks more quickly compared to mouse interactions, further exemplifying the usefulness of physicalizations. It was therefore concluded that, if a 2D visualization would not be feasible for a given problem, the use of physicalizations can be beneficial.

A good example of an application for tangible visualizations comes from the automobile industry. A General Motors executive became frustrated with the limitation of 2D visualizations for 3D problems [gmL]. Within only a few days, they could prototype and use a physical representation of their data. Stacks of bricks in different sectors of a board denote irregularities in manufacturing. Figure 2.9 shows an analyst working with the model. The colours of the bricks are used to denote the different areas of a

Figure 2.10: 4D physical visualization of cardiac blood flow, using 3D flow lines [ASS+19]

car, their sizes corresponding to the severity of the problem. Due to the nature of the used material the bricks can easily be rearranged. This communicates on a metaphorical level [ZM08] that these problems can be mitigated and the board's shape will change again.

Physicalizations are not limited to display static 3D objects. Where it might be possible to add movement to a sculpture, like for example using animation, movement can be implied differently. Where in digital imaging, the passing of time is mostly represented by animation, there are ways to depict moving objects over time with static methods. These methods can be used to create static data sculptures that illustrate dynamic movements. Ang et. al. [ASS+19] developed a physicalization of cardiac blood flow to explore this concept. 4D MRI data was used which records anatomical structures over time and captures movement. Such data are typically viewed as a video like an animation on a computer screen. Arguing that a physicalized representation of the data may bring advantages over the on-screen depiction [JDI+15], Ang et. al. [ASS+19] set out for a model to incorporate those benefits. The 3D printing technology they used combined two materials with different colours in one sculpture. This was incorporated in the physicalization, by using a white background material for the anatomical context and a foreground material in red, to simulate the blood flow. Specifically, the left ventricle

and the blood flow therein were examined. Blood flow can be modelled as a vector field and the representations sought to benefit from this fact. Two variants of static depictions of moving processes were chosen to explore, a *glyph* based representation and a *streamline* model. The glyph model directly displayed underlying vector field data, each glyph (with an arrowhead shape) represents the flow at a specific point in space, with their size corresponding to the magnitude. The more complex streamline shows a more direct representation of flow paths in the vessel. First, a flow line model is computed and then the flow lines are reduced to facilitate printing and avoid complications. Both variants are placed into anatomical context by using equidistant slices of semitransparent material, representing the volume's shape and serving as a support for the glyphs and flow lines. A flow line model can be seen in Figure 2.10. The concept was evaluated in a study that found positive implications for the glyph based variant. It was shown that the participants needed less time to solve tasks when using the physicalization compared to a 3D screen-based visualization. The results of the evaluation of the flow line model were less conclusive, however, citing limited interaction opportunities for the participants with the model and some view obstructions, for example. It was concluded that the models provide a valid proof of concept for future work, for use both in professional and patient education as well as opportunities for applications in diagnostics.

It should be noted that these physicalizations contain spatial data as *shell* depicting the anatomical context. However, the main purpose of it is to illustrate the flow of blood inside the heart. This is achieved by abstracting the time component of the flow into vectors and flow lines. These graphical elements do not exist in reality and can not be captured as spatial data. Therefore we argue that this method depicts abstract data.

Spatial Data Embodiment

Areas that can benefit a lot from the use of physicalizations are applications where the data are a representation of tangibly existing objects. Medical imaging is a tool aiding medical professionals in their work and education [PB13] and can serve as a visual aid for patient communication. Many modern medical imaging modalities inherently produce 3D data. This fact is put to use in some current applications and research [SB16, RMVTK+10, KNSV15, HL16, WPF+15]. Modern 3D scanning technologies are also employed with some success [ADS5]. This section presents some notable examples for physicalizations of anatomical imaging in various ways.

3D printings of anatomical regions, for surgical planning, have been employed with some success [WPF+15, HL16]. Two studies examine small prototype settings. The Boston Children's Hospital Simulator Program evaluated the use of 3D printed vascular structures in preparation for cerebral surgery [WPF+15]. For suitable candidates, 3D prints of the malformed vessel and their surrounding vessels were created. The volume data were created from routinely performed MRI scans. A criterion for the suitability of the vessel was that it could not be too small ($< 2\,mm$) so that accurate 3D prints could be constructed. This meant that surgeons had the opportunity to examine the

Figure 2.11: A 3D printed (partial) heart and the removed artificial tissue from the practice procedure, compared to the tissue removed in the actual operation[HL16].

area of interest before the operation in a tangible way. For each patient, multiple models could be created to show different aspects of the regions of interest. This method led to a reduction of operation time in some cases. While it was a very small study with only five patients, it was argued that the positive results warrant further exploration of applications of 3D printed physicalizations in surgical planning. Hui and Lee [HL16] researched a similar application for 3D printed anatomical models in the field of cardiac surgery. They aimed to create anatomically correct models of patients' hearts with 3D printing. The models should have a similar feel as compared to their physiological counterparts. This meant to employ materials that can mimic human histology, as far as providing a similar feel when being cut with a scalpel. The 3D models were created by 3D printing a scaffold based on segmented CT data. Special hydrogels that mimic the histological properties of the heart muscle were then injected into the scaffold. A silicone layer was added for stability as well. Those models were then given to surgeons to practice the actual operation in a realistic setting. The concept was evaluated in a study with two patients with hypertrophic cardiomyopathy. Participating surgeons report a good sense of scale and a somewhat realistic feel. It could however not be proven that the procedure profited from practice on the 3D model. The authors argue, however, that such procedures are too sparse to provide regular examples for medical students. Thus they propose that it could be beneficial to employ such physicalizations techniques for training purposes. In Figure 2.11 one of the produced heart models can be seen. The operational procedure was performed on the model, leading to removed tissue that can be seen next to the model. After the actual operation, the tissue removed from the patient was placed next to the model as well. It shows a remarkable similarity in the removed

pieces.

A similar argument was made by AbouHashem et al. [ADS5]. Similar to the historic application of anatomical drawings and wax sculptures [RCSL10], they study the use of 3D printing in anatomy education. They argue that bones, in particular, are suitable for easy reproduction, using 3D scanners and printers. This is mainly because of their solid shape and monochromatic texture, which is easily simulated by modern 3D printers. The scarcity of demonstrable subjects with rare bone conditions to handle for medical students further exemplifies the need for this. By scanning specific bones from cadavers and reproducing them with conventional 3D printers, first successes were made in cost-effectively producing sculptures with sufficient realism for use in medical education.
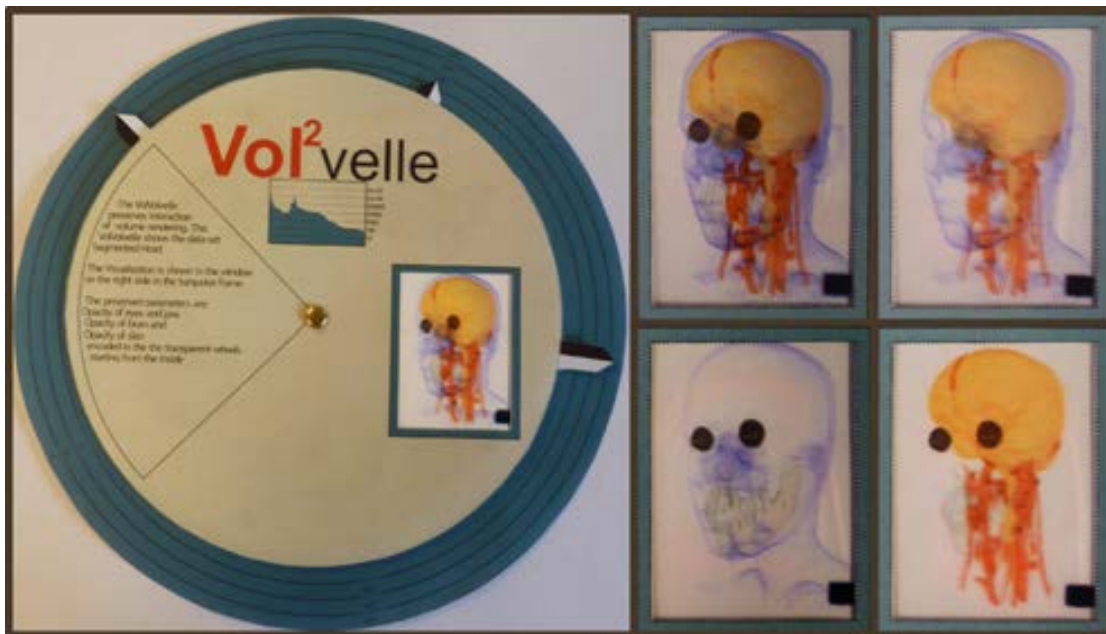
Figure 2.12: A printed volvelle with transparent layers showing 3D volume Data [SB16]. This is an example of spatial data representation without the use of 3D printing.

An example of a modern application of a long-existing concept can be found in the work of Stoppel and Bruckner [SB16]. The authors present a tool for the creation of print-out volume visualizations, using *volvelles*, called *Vol2Velle*. Volvelles are interactive wheel charts that can historically be found in many applications, even to this day. They consist of concentric, superimposed disks that can be freely rotated by the user. An existing volume visualization tool is employed to select anatomic regions that a user wishes to examine on the volvelle. Multiple parameters are adjusted in advance to produce one wheel chart per visualization. The upper disk contains a window where, depending on

(a) Rendering of an aneurism dataset.   (b) Physicalization of the same dataset.
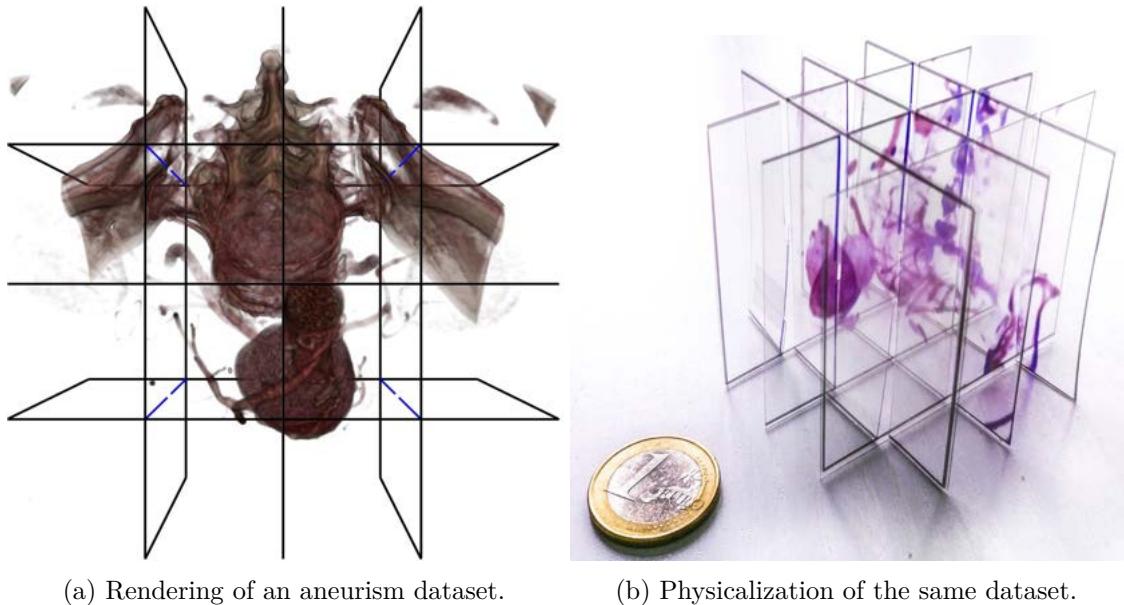
Figure 2.13: A *Slice and Dice* sculpture (b) created from a dataset showing an aortic aneurism (a) [RGW20]. The intersection of the slices is placed close to the centre of the aneurism to accurately display it.

the current orientation, a version of the selected volume is shown. By drawing lines from regions of the window, specific regions can be mapped to regions of a reference image. Regions in the window can be mapped to specific points in a reference image on the disk by connecting them with a line. This can serve as an orientation aid for observers. The parameters of the volume rendering transfer function are mapped to the rotating axis of the disk so that the user can examine the selected region in varying detail by rotating the disk. As an extension to the simple paper volvelle, multiple transparent disks can be used to display superimposed images of different segmented anatomical regions. Each of the individual transparent disks can contain samples due to a different transfer function. This allows users a more detailed examination of selected anatomical regions. The method embodies a creative alternative to 3D sculpting and through careful tuning of the sampled transfer functions can display meaningful data for users that are not proficient with the use of volume rendering software. This can aid in patient communication, another field that can be addressed as a target for the democratization of information access [ZM08], through informed patient consent. Due to the use of paper as the medium, this method is especially cost-effective and the production of the wheel charts is easily facilitated by conventional desktop printing.

Raidou et al. [RGW20] have also focused on creating a do-it-yourself workflow for physicalizations. They created a way to transform medical volume data or surface renderings into 3D sculptures. The process, called *Slice and Dice* uses an octree-based partitioning system to identify important structures based on a specific transfer function.

Figure 2.14: Sculptures created with the *Anatomical Edutainer* workflow [SWR20]. Filters for different colours are employed to emphasize different anatomical structures.

This can be used, for example, to emphasize important structures such as specific organs or pathologies, while removing focus from less important structures that serve as anatomical context. From the resulting orthogonal slices, they then create a printable form, prepared for easy assembly. The individual parts of the sculpture are then automatically arranged on a template, which can be produced with conventional printers and subsequently cut out and assembled. The results are palm-sized, cuboid figures such as the one displayed in Figure 2.13. The figure shows that the sculpture conveys a 3D dimensional appearance despite being made from 2D materials. In an evaluation, participants were asked to identify specific structures in different sculptures and static visualizations respectively. The participants reported generally positive experiences when using the model and also remarked that it could be an attractive educational tool for children. From the participants' reaction, it was also summarized that the tool could be of aid to medical personnel explaining medical image data to patients.

As a final example for cheap and easily manufacturable anatomical physicalizations serves the *Anatomical Edutainer* by Schindler et al. [SWR20]. Aiming to create a way to allow medical laymen the exploration of the human body, they proposed a process to construct
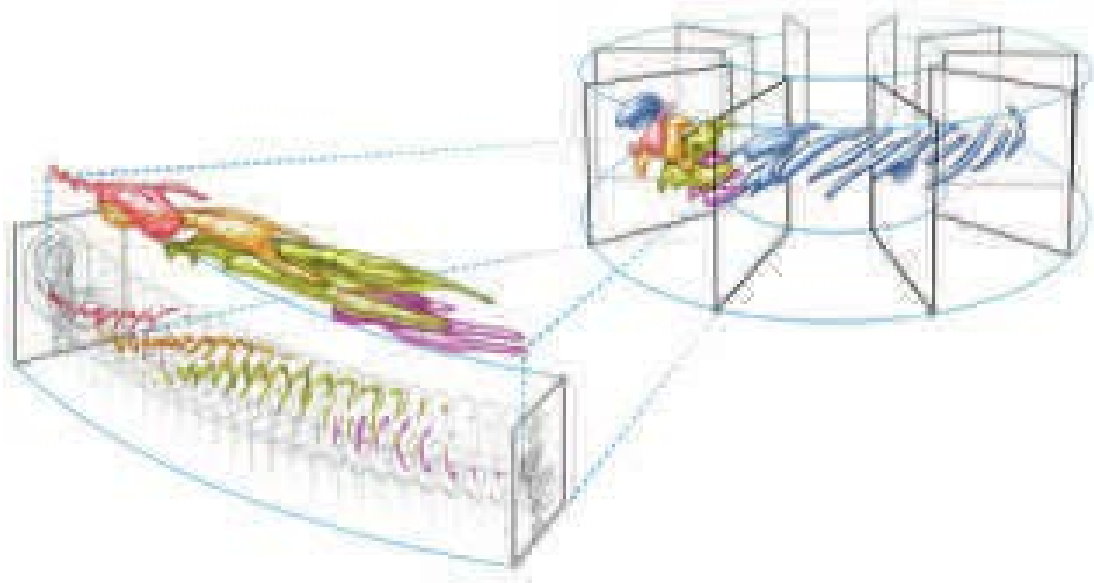
Figure 2.15: A proposed, carousel-like display for examining cerebral aneurysms proposed by Steinman et al .[SCS17]. The user stands in the centre of the circular display and observes the animation, while sounds corresponding to the flow of blood in the vessel are played.

multi-layered papercraft visualizations. In the workflow, a combination of three surface visualizations of human anatomy, for example, bones, muscles, and vessels, of the same anatomical region are rendered. Different colours are used per structure and the images are blended into a common texture. They use cyan, magenta, and yellow as the distinct colours to facilitate colour blending on white backgrounds. Furthermore, red, green, and blue colour filters are easily obtainable in the form of coloured-light or transparent sheets. The resulting object is then unfolded on a flat plane, to be printed with a conventional printer and reassembled. If the object is observed while using a colour-filtering technique, only one region remains visible, creating the effect of looking inside the object. This effect is shown in Figure 2.14. The authors also propose the possibility of using a light source located within the object to make the approach more attractive and remove the need for using an external colour filter. One big advantage of this method is that it can be accomplished with a very small number of technical means. The sculptures can be printed with regular colour printers and standard paper. While this approach may still have limitations, future potential additions including the utilization of more base colours and more complicated colour filters add to the concept's potential.

2.4.2 Hybrid Visualizations

In Zhao's categorization [ZM08] hybrid visualizations as physicalizations fall both under the term *alternative modality display* and *data sculpture*. Since the example we provide

is not using a single physical channel, but rather a combination of a visual display and a physical aid, we use the term *hybrid visualization.*

Steinman et al. [SCS17] provide an interesting example of such a hybrid visualization. Their research focuses on aiding clinicians in decision making. For their proposed application, they chose the subject of examining cerebral aneurysms and deciding if surgical intervention is needed. This is normally done by examining the blood flow through the aneurysm. This means the data has to be presented in a 4D way to the observer. Citing *image fatigue* they propose a way to aid a doctor's examining of the data without focusing entirely on screen-based images. Additionally, through a carousel-like display, higher immersion into the visualization is sought. Steinman et al. decided on a hybrid approach and proposed a circular display that surrounds the user, showing the vessel in detail and providing sound cues depending on which frame is examined. The sound cues were proposed to in some way encode the amount of shear stress inside the blood vessel. This concept is shown in Figure 2.15. In agreement with doctors, who are trained in *auscultation* when examining patients, it was decided to use more realistic sounds that occur naturally within the human body. The approach serves notably as an example for a more abstract visualization than typically used.

2.5 Summary

The application of 3D sculptures in medical education can be found before the invention of medical imaging techniques [RCSL10]. In recent times, a renaissance for this concept is taking place. In the field of information visualization, the term physicalization is gaining a certain popularity [JDF13, JDI+15, JD13, ZM08].

Providing a sensible categorization [ZM08], we identify the types of *data sculpture* and *mixed modality display* as promising candidates for medical applications. We argue that multiple reasons for the application of physical visualizations exist, identifying their advantages over screen-based visualizations, their potential for laymen empowerment, and current technological advancements as core facilitators. Furthermore, we present a formal model for the inception of information visualizations that facilitates the incorporation of data embodiment besides traditional screen-based forms [JD13].

For data sculptures and hybrid visualizations, we provide examples of current applications and research. For visualizations of *abstract* data, we examined the Study of Jansen et al. [JDF13], where a 3D bar chart is employed. The physical data sculpture proved to be superior to a similar screen-based 3D visualization. The approach was partially inspired by General Motors' use of a Lego brick-based technique [gmL]. The interactivity of this visualization is another interesting subject and the metaphorical character of the brick sculptures is theorized to be another beneficial factor. Applications for abstract visualizations can also be found in the medical field [ASS+19]. Glyph and streamline based vector field visualizations are augmented by placing them in a spatial context. This allows an informative visualization of blood flow patterns, which is also proven to

be superior to screen-based visualizations.

Spatial data physicalizations profit a lot from modern imaging technologies. The modalities for medical data storage and capture have similarities to 3D printing technologies [RMVTK+10]. This was also employed in two different studies concerning the application of 3D printing in surgical planning [HL16, WPF+15]. Both studies show some positive aspects for the application of physical sculptures. It was indicated that surgery planning can be improved using 3D printed props of regions of interest. For surgery practice [HL16] it was found that the direct impact on the procedure was not measurable, but that it could be beneficial to employ the technique for educational purposes. This theory is further examined by AbouHashem et al. [ADS5]. They point out the scarcity of anatomical preparations of bones with specific rare conditions as a motivation for the use of 3D printed physicalizations. Finally, we present examples of physicalizations of spatial data not using 3D printing. Stoppel and Bruckner [SB16] use the existing concept of wheel charts to create printable interactive volume visualizations. This is notably not thought of as a tool to aid medical professionals in diagnostics or training. Instead, they propose the possibility to use these visualizations in doctor-patient communication, due to their relatively low cost and easy manufacturing. Likewise, Raidou et al. [RGW20], and Schindler et al. [SWR20] employ readily available and low cost means to create anatomical physicalizations for layman education. Lastly, we inspect hybrid approaches between multiple physical communication channels. Steinman et al.'s [SCS17] proposition of a multi-modality display using sound effects generated from 4D anatomical data serves as an example for such methods.

With current technologies, sculptural physicalizations are mostly static objects. Single parts can be exchanged [JDF13] and figures can be animated using motors and the like. Different materials can be used in the construction of a sculpture to create a more realistic tactile feedback [VMML17]. However, the principal properties of the parts remain static. Jansen et al. [JDI+15] discuss the possibilities for future developments in the field of *programmable matter*. This could give further agency to create interactive data sculptures. Many studies performed on the subject serve as proof of concept efforts. As the new-found enthusiasm for physicalization in information visualization is still relatively young, it remains to be seen where research will be going.

In our opinion, the field of physicalization has a lot of potential. The application in surgery planning undoubtedly needs further study. In the few examples that we showed, it is explicitly mentioned that their scale was very small. The high, at least currently, price of 3D printing and the relatively long production times of 3D prints are another limiting factor here. Foremost, we see the potential of physicalizations in education. Besides their already widespread use in museums around the world, we think that they could make their way into private homes. This is why we find that manufacturing methods different from 3D printing have to be explored. Through their unique

hands-on feel, which can currently not be reproduced by AR or VR, physicalizations show their true strength. Simple hand-made physicalizations, as shown in Figure 2.16, can be produced at minimal cost with widely available tools. Despite the figure's rather simple composition, we think it shows aspects of the underlying data in a way which can not be reproduced with screen-based visualizations.

Figure 2.16: A handcrafted physicalization displaying a human skull at 50% scale. Made from layers of cardboard, stacked on a wooden spike. The spatial data was taken directly from a DICOM image. The sculpture was created as a prototype in the course of this thesis.

Design

In this chapter, we will examine the requirements for our solution and target group based on our formulated research questions. We formulate a description of tasks, based on the imposed requirements, which we aim to accomplish in the course of the thesis. The physicalization concepts we explored are explained in detail. Based on the form of physicalization we choose, we propose a suitable visualization for data selection. Finally, we explain in detail the full visualization pipeline of the concept, based on the extended visualization pipeline proposed by Jansen et al. [JD13]. An illustration of this pipeline is given in Figure 3.9.

3.1   Design Analysis

3.1.1   Target Audience

Zhao and Vande Moere [ZM08] propose that physicalizations, especially in the form of data sculptures are well suited to educate layman audiences. They cite the *democratization of information access*, i.e. the growing demand of non-expert audiences to information access, as an important driving factor for the development of information visualization. Jansen et al. [JDI+15] concur with this notion and point out that public speakers who aim to engage mainstream audiences, as opposed to scientific audiences, use physical aids to engage their audience.

The target audience for our research is comprised of medical laymen, which we intend to engage with the help of physicalizations. We do not want to focus on a particular age group, because medical education can be needed in different stages in life. Children might benefit from a more engaging way to visualize medical data during their education. Designing educational tools and evaluations thereof would require the active involvement of children educators. The physical and hands-on nature of physicalization might be

a positive factor for a young audience [NMA12]. Elderly, in turn, who are likely to be subjected to medical treatment and often not as proficient with the use of computer technology might similarly profit from such learning aids. Many elderly people are not as familiar with computer screens or smartphones as younger people are. Proper patient communication is, of course, a factor for people of all ages, which can contribute in a positive way to the treatment experience [HL10, ODHHL95].

The focus on laymen education will lead to a simplified, illustrative approach [PB13] for the anatomical visualization. Experts, like medical practitioners, or researchers, are not the target of our research. They could still find application for our physicalizations for patient education and communication. Our approach will likely lead to the loss of at least some detail present in the data, which would not be acceptable for a diagnostic aid. The reduced level of detail should not impact its potential for educational use.

3.1.2   Imaging Data

For an audience of medical non-experts, who might be confronted by medical imaging at some part in their life, it might be interesting to be able to examine real human medical data. Therefore, we want to use medical volume data, which can be a direct result of medical imaging technologies like computed tomography (CT) or magnetic resonance imaging (MRI) [PB13]. As opposed to surface data, volume data provides an insight into internal structures as well. Additionally, this would mean that it could be possible, to use patient-specific data as input.

Many sources for medical imaging data exist on the internet. A notable example is the *Visible Human* dataset [ASSW95], made accessible to the public in 1996. It contains volume data of a male human cadaver, comprising of photographs of the cryosected slices of the body, as well as CT, and MRI images. During the same project, a female human dataset was introduced later. Figure 3.1 shows a photograph of a cryosection, as well as a CT image from the Visible Human male dataset. This dataset was used by Pommert et al. [PHP+01] to create a comprehensive segmentation of the human head and torso. The data are publicly available and has been provided to us for use in the course of this thesis.

3.2   Requirements Analysis

In Chapter 1, we formulated three research questions **(Q1-Q3)**. To answer them, we present a list of requirements, to be fulfilled by our work. The first three requirements **(R1-R3)** are concerned with the specific target group of the project. Our analysis identifies non-experts in human anatomy of every age as the target group. The data should be presented in an easily understandable way and we will require our solution to be accessible to people with little knowledge in both anatomy, visualization, and computer technology. The requirements **(R4-R6)** result from **(Q2)**. The third question **(Q3)** will
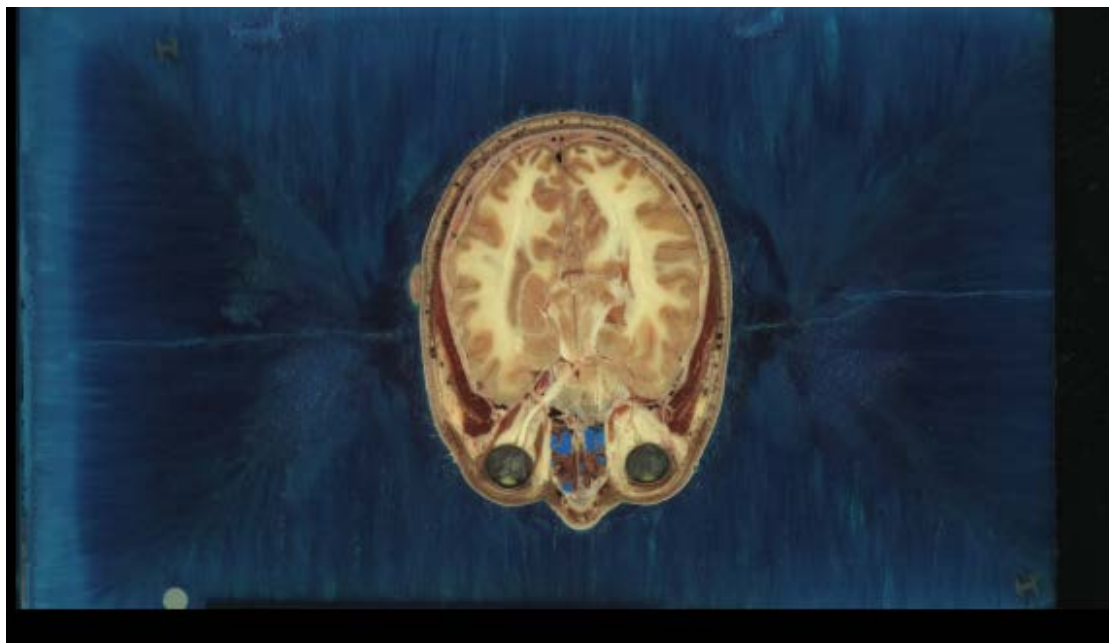
(a) Cranial slice photo.
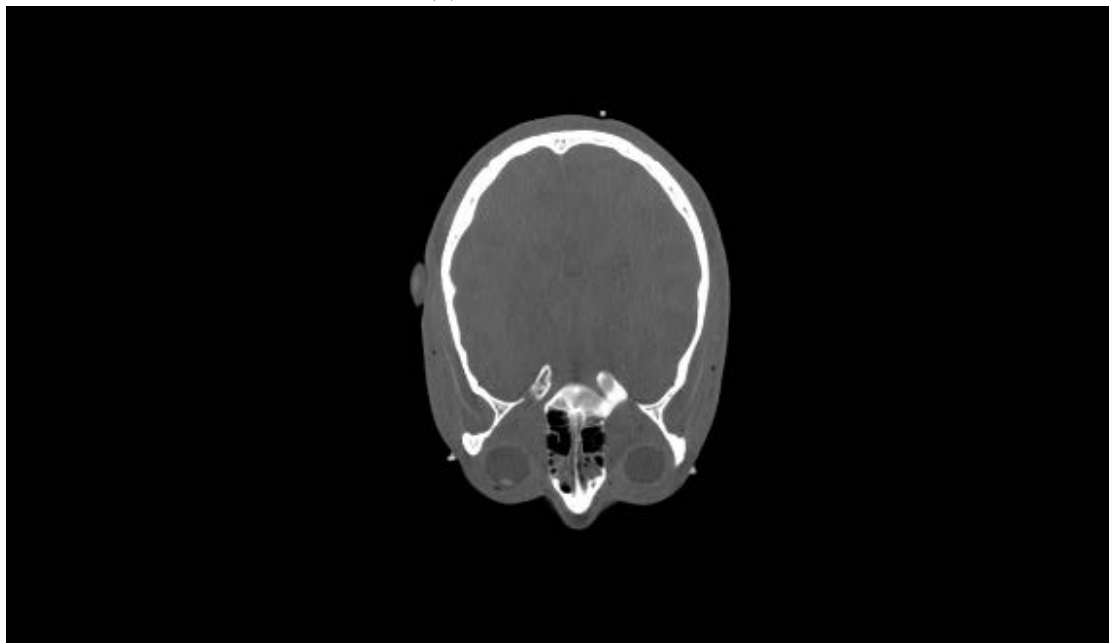
(b) Cranial slice CT image.

Figure 3.1: Two different captures of the same slice from the *Visible Human* male dataset [ASSW95]. (a) shows a cranial slice from the cryosected cadaver, (b) shows a CT image from the same slice.

be answered by an evaluation; thus, **(R7)** encompasses the need for comparability between an on-screen visualization and the resulting physicalization. The list of requirements for our following work are summarized as follows:

R1 The application should cater to the layman target group's needs for anatomical education.

R2 Data selection and processing should be feasible and automatized, for people not proficient in medical visualization and image processing.

R3 The application should convey basic human anatomy.

R4 The input data is real medical volume data from CT or MRI data.

R5 The materials used should be affordable and available to the general population.

R6 The physicalizations should be easy and quick to assemble.

R7 The visualization and the physicalization should be optically comparable.

3.3   Task description

After formulating a list of requirements for a potential solution, we combine them with the research questions and formulate our tasks. The first task is to find a suitable physicalization concept for our approach. Users should be able to construct the physicalization with relative ease and the materials should be affordable and readily available **(R5-R6)**. Having found a suitable physicalization concept, we will develop an application that provides a workflow to create the sculptures from medical volume data. For this task, it will be important to consider the target group, with regards to their abilities to use computers as well as their illiteracy in medical visualization **(R1-R4)**. In the end, we will answer our third research question, by performing a small scale study. In the study, the visualization of the medical data will be contrasted to the resulting physicalization, to identify if either approach provides a distinct advantage. We summarize our tasks in the list below:

T1 Identify a physicalization approach which satisfies **(R3, R5, R6)**.

T2 Design a robust and interactive workflow to create the physicalization, satisfying **(R1-R6)**.

T3 Evaluate the proposed approach with regards to usability and user performance, addressing **(R7)**.

3.4 Physicalization Concepts

The first stage in our research, as stated above, is to find a suitable physicalization concept to satisfy the set requirements. We investigate three different concepts in this stage and compare them to the requirements to determine their suitability. As a suitability metric, we determine for each potential solution if it fulfils requirements **(R3)**, **(R5)**, and **(R6)**, which directly refer to the physicalization part of the workflow. The following section summarizes our findings from this investigation. Each concept is introduced with regards to its inspiration. We then briefly propose a workflow for the creation of the sculptures. Afterwards, we list possible materials for the realization of the concept, followed by a discussion of its suitability for our purpose.

3.4.1 Slicer Concept

During our research into physicalizations, we looked for inspirations in fields other than the medical domain. A popular field of application for physical models can be found in architectural design. Hull and Willet [HW17] describe how architectural models can inspire data physicalization design. One aspect of architectural design, to which they refer as *context models*, is used to depict the surroundings of a proposed structure. Models of the actual design can be embedded in their environments to provide a simulation of the structure in its natural surroundings. A typical context for architecture can simply be a topological landscape, which can be modelled by contour lines at different heights, creating a stair-like appearance. An example of an architectural model in a topological context model is shown in Figure 3.2a

Medical volume data created through tomography result in 2D images which are combined into a 3D structure, by arranging the axial images in a regular voxel grid. Interpolation is sometimes used to lessen the step-like artefacts in those images, which result from the inter-slice distance. Without interpolation, rendering low-resolution data has an appearance very similar to topological context models. An example for this can be seen in Figure 3.2b. While the resolution in the image is reduced, one can still clearly recognize the shape of the human skull. We, therefore, propose that a physicalization, created from stacked slices of constant thickness, could provide an insight into the shape and size of different anatomical structures, such as organs or body parts. This led to the first physicalization concept, the *Slicer*.

Concept

First, a single structure has to be extracted from the source data. The concept is only suited for larger, homogeneous structures, such as bones or larger organs. Finer structures, such as vessels, are not suited to be displayed this way. Because 3D CT and MRI imaging data are created from multiple parallel slice images through a volume [PB13], there are two different resolutions to consider. On the one hand, there is the resolution of the

(a) Architectural model.
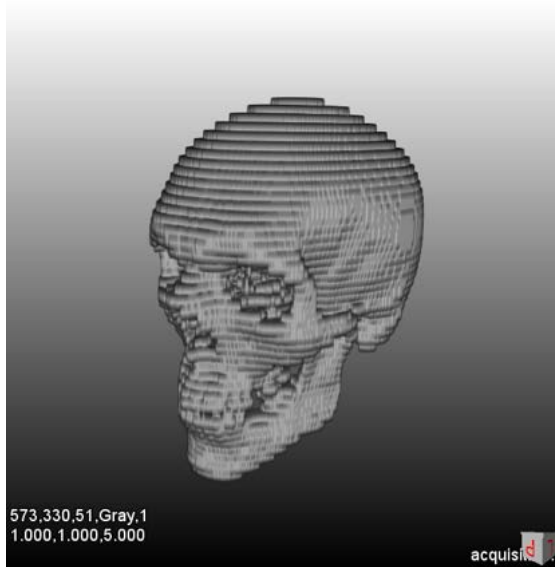
(b) Low resolution skull render.

Figure 3.2: (a) Model of the Lethbridge University campus [Let]. The campus buildings are embedded in their topological context. (b) Low resolution render of the skull from the *Visible Human* dataset [ASSW95, PHP⁺01], the vertical resolution was reduced by a factor of five, to achieve an appearance similar to the context model.

individual slice, which we will refer to it as the *horizontal resolution*. On the other hand, exists the resolution representing the distance between the axial slices, which we will refer to as *vertical resolution*. We propose to decrease the *vertical* resolution of the data. Through this, a set of slices through the volume can be obtained, with a thickness equal to the inter-slice distance. The slices are then transformed into silhouettes of the volume. For this, we propose to first use a smoothing algorithm, like the *Sigma* filter [Lee83], to reduce
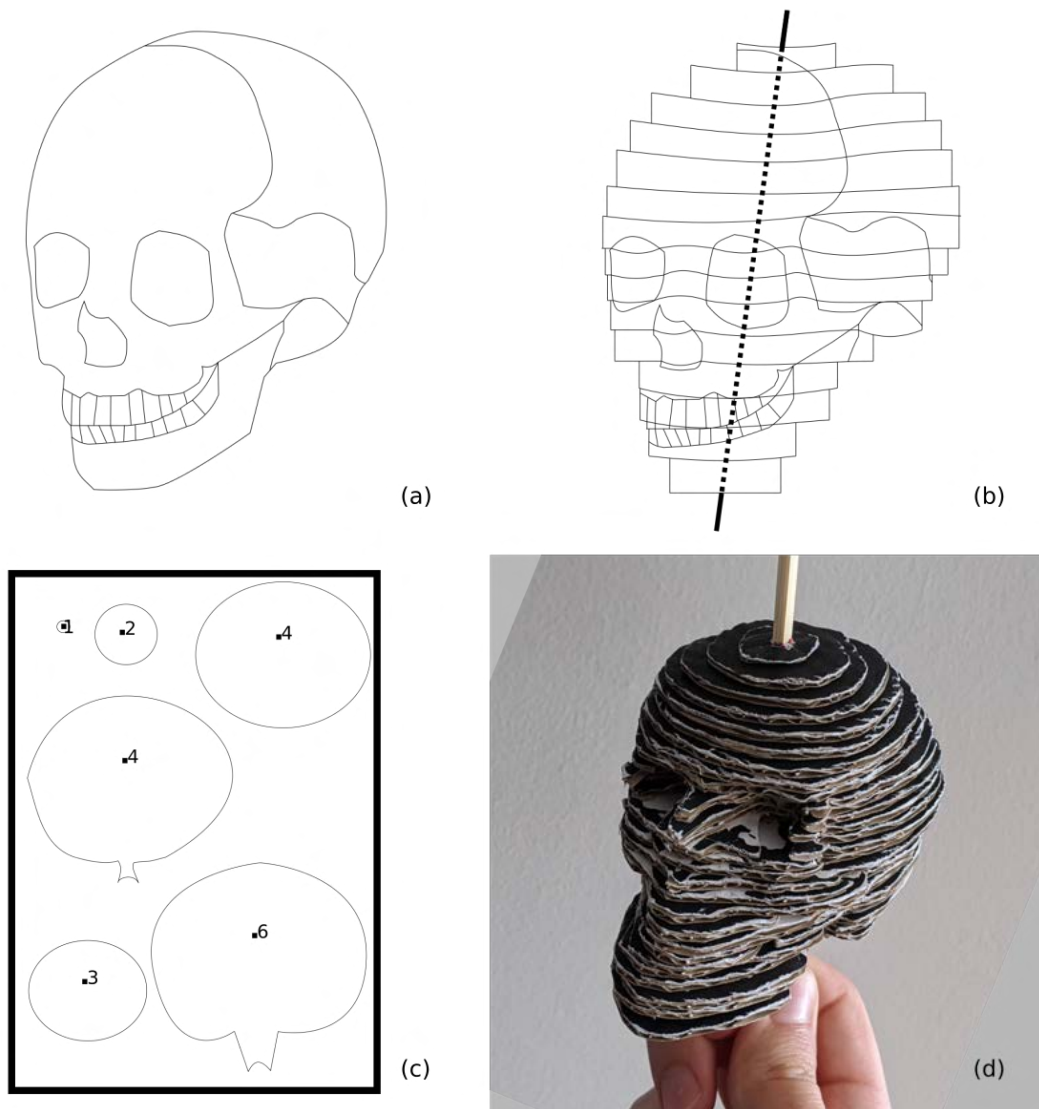
Figure 3.3: Concept of the *Slicer* workflow. (a) The volume data is filtered to display one distinct, homogeneous structure. (b) The filtered volume is processed, slices are created by axial downsampling, with the stacking axis displayed. (c) The results are multiple pages of printable stencils for printing and subsequent cardboard cutting. (d) Finally the cardboard slices are assembled by stacking them on a spike, along the predetermined axis.

image noise. Smoothing will also lead to a flatter, less complex surface for the structure. To obtain silhouettes from the individual slices, edge detection can be employed. An

candidate for this is the *Sobel* filter [VF$^+$09]. The result of this is a set of silhouette slices. The individual silhouettes can be arranged on a page, to be printed with a conventional desktop printer. The slices are then cut out and glued to the cardboard material. This provides a stencil for cutting out the cardboard. Afterwards, the individual cardboard slices have to be assembled to produce the sculpture. One difficulty in assembling the slices is to preserve the correct orientation. We propose to use a rectangular spike in the core of the model, which would prohibit rotation of the individual slices. This only requires to print the rectangular cross-section of the spike on a slice. If only glue was used to connect the slices, there would be an indication required on each slice on how to orient the following slice, for example, the silhouette of the following slice. If a slice is placed on top of a slice which it fully covers, such an indication would not be possible. The placement of the spike is a crucial component of the model. Every single slice needs to be connected along an axis. For this, the principal axes transformation of the volume data can be utilized. Principal axes transformation has been used as a registration method in the past by Alpert et al. [ABKC90]. It is computed by performing the eigenvalue decomposition of the volume's inertia matrix. The eigenvalue decomposition results in the principal moments of inertia, as well as the rotation of the principal axes. Using a straight line along the direction of the largest moment of inertia, passing through the volume's centre of mass, a candidate for the stacking axis is obtained. The position and orientation of the spike is indicated on the printouts. Another factor that complicates assembly is to keep the correct order of the slices. As a solution to this problem, we propose to include a number on the printed silhouettes which are glued on the slices, to indicate the order of assembly. An illustration of the slicer workflow is shown in Figure 3.3.

We require our physicalization to consist of affordable and obtainable materials. One of the cheapest and most abundantly available material in many homes are cardboard boxes. The cardboard has a constant thickness throughout one box. We found multiple delivery boxes, with thicknesses from 3-5mm. Alternatively, cardboard is readily available for a low price in paper stores, where thickness can be selected. To achieve additional insight into the structures, a transparent material would have to be used instead of the cardboard. Transparent plastics or glass are a possible alternative. However, those are not as cheap and easily available. As a connecting spike, we propose the use of rectangular barbecue skewers. These are also cheap and available in many supermarkets.

Discussion

The *Slicer* workflow is very quick to implement and very cheap to execute. The materials are cheap and available to most people, satisfying **(R5)**. We think the idea to display organs in their original size is very interesting from the standpoint of a layman. Simple thresholding can quickly isolate bone matter, making it an interesting tool for users to examine their medical image data, for example in the course of a fracture.

However, the concept delivers only an outside view of the structure and does not permit a view inside. The processing required for obtaining the silhouettes also leads to a loss of

detail. For those reasons, we consider the concept to only partially fulfil **(R3)**.

An interesting addition could be the use of translucent material instead of, or in addition to, cardboard. This would enable users to see internal structures of the region of interest. Transparent material of constant thickness is, however, harder to obtain and not as easy to cut as cardboard. The devices required to process this material is not readily available to the general public. Furthermore applying the stencils to the transparent material would complicate assembly. Using a transparent, printable overhead sheet, would mitigate this, however, the application of the sheets to the slide material would need glueing, which would decrease the visibility of inside structures and issues with colour. The inserted spike would also be visible and obscure the view.

Placement of the spike inside the sculpture also prevents interactivity for this concept. If a spike with a circular cross-section is used and positioned outside of the structure, it could be allowed to perform a hinge-like rotation for individual slices around the spike. This complicates assembly and adds an artificial part to the anatomical structure, where the spike is placed.

The use of a single, straight, spike disqualifies the concept for the display of more complex, or branching structures. The principal axes are not a feasible candidate for the spike insertion in structures like the bowels. Here the use of materials like bendable wires further complicates the concept for a layman user.

Finally, the material use for even smaller structures is considerably high, because the full volume of the structure has to be cut out of the cardboard. This also leads to many separate pieces to assemble, resulting in a tedious and long construction of the model. This is contrary to **(R6)**.

3.4.2 Cuber Concept

The *Slicer* concept, while being affordable and providing a nice overview of the shape and scale of anatomical structures, is inflexible. With the next concept, we try to overcome some of the *Slicer's* weaknesses. We mainly target the desire of looking inside structures and more possible interactivity.

After taking an MRI scan in 2008, Neil Fraser created an interesting physical model of the data [Fra]. He used 60 cubic wooden blocks, one inch in size, to create an elaborate anatomy puzzle. The data were subsampled at a regular distance and partitioned to fit on the cube faces. Then the individual slice images were glued to the cubes so that when assembled they allowed observers different views inside the skull. An example of this is shown in Figure 3.4. This could also be used for other structures than the head. When a user interface for selection and parametrization is added, the concept can be adapted to create custom physicalizations for layman anatomy-education. Based on this, we formulate the *Cuber* concept.

(a) Saggital view.

(b) Coronal View.
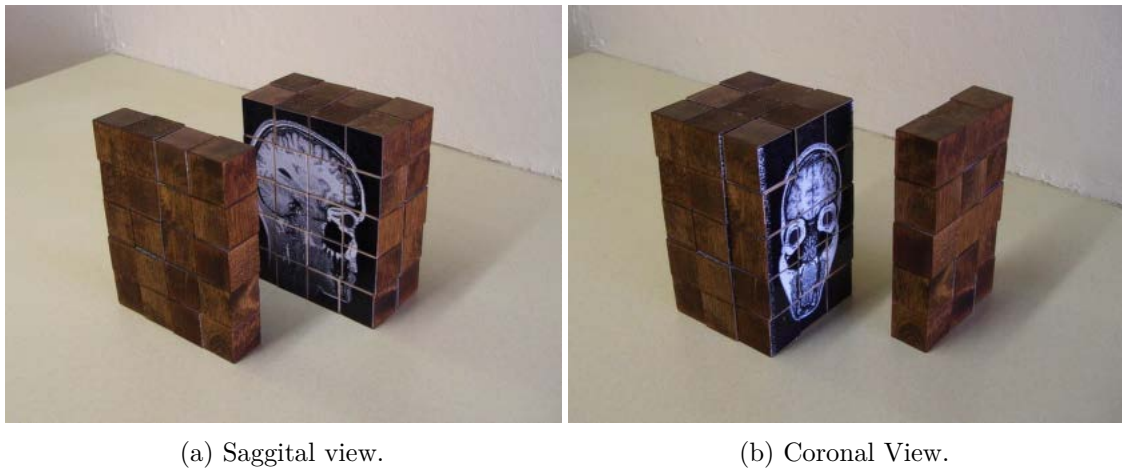
Figure 3.4: Different views into Fraser's brain cube model [Fra]. The sculpture can be taken apart and reassembled to show different parts of the skull, along axial, saggital and coronal planes. A view along the axial direction would be similar to the usual way of doctors to examine CT data.

Concept

Fraser uses his own MRI data for the creation of his sculpture [Fra]. While it might be interesting to examine personal medical data, we propose that for anatomical education, pre-segmented data is more helpful. The general population do not have sufficient knowledge to discriminate the greyscale encoded structures as CT and MRI images capture them [PB13]. With sufficient pre-processing through segmentation, different internal structures can be distinguished by using different colours in the rendering. Users select a desired area and viewpoint for their custom sculptures. For example, one might want to examine the organs in the upper torso or the anatomy of a single leg. Every organ, as well as different bones and muscles, are assigned different colours. Users can select a size for the resulting cubes, as well as a scale for the model. Before processing, the number of resulting cubes is displayed, to prevent users from having to assemble too many cubes. Fraser used 60 cubes for his model [Fra], which we would consider a soft upper barrier concerning feasibility. The amount of cubes depends on two parameters: the scale of the structure, and the selected cube size. While it might be an interesting exercise for some people, other parts of the target demographic would be deterred by the complexity of these puzzles. Children, which do not possess much anatomical knowledge, as well as the elderly which often have motoric difficulties or visual impairments, are an example of this. Different cube sizes can make the model fit for different target groups. After specifying the necessary parameters, printable stencils for the cubes are generated. A cube provides six different viewing angles, one for each of the cube faces. Fraser uses parts of cross-sections from the imaging data as faces for his cubes. We argue that it is more helpful for anatomical education to use a projection of the volume rendering behind the cube surface. This provides a view of the structure's inside area instead of
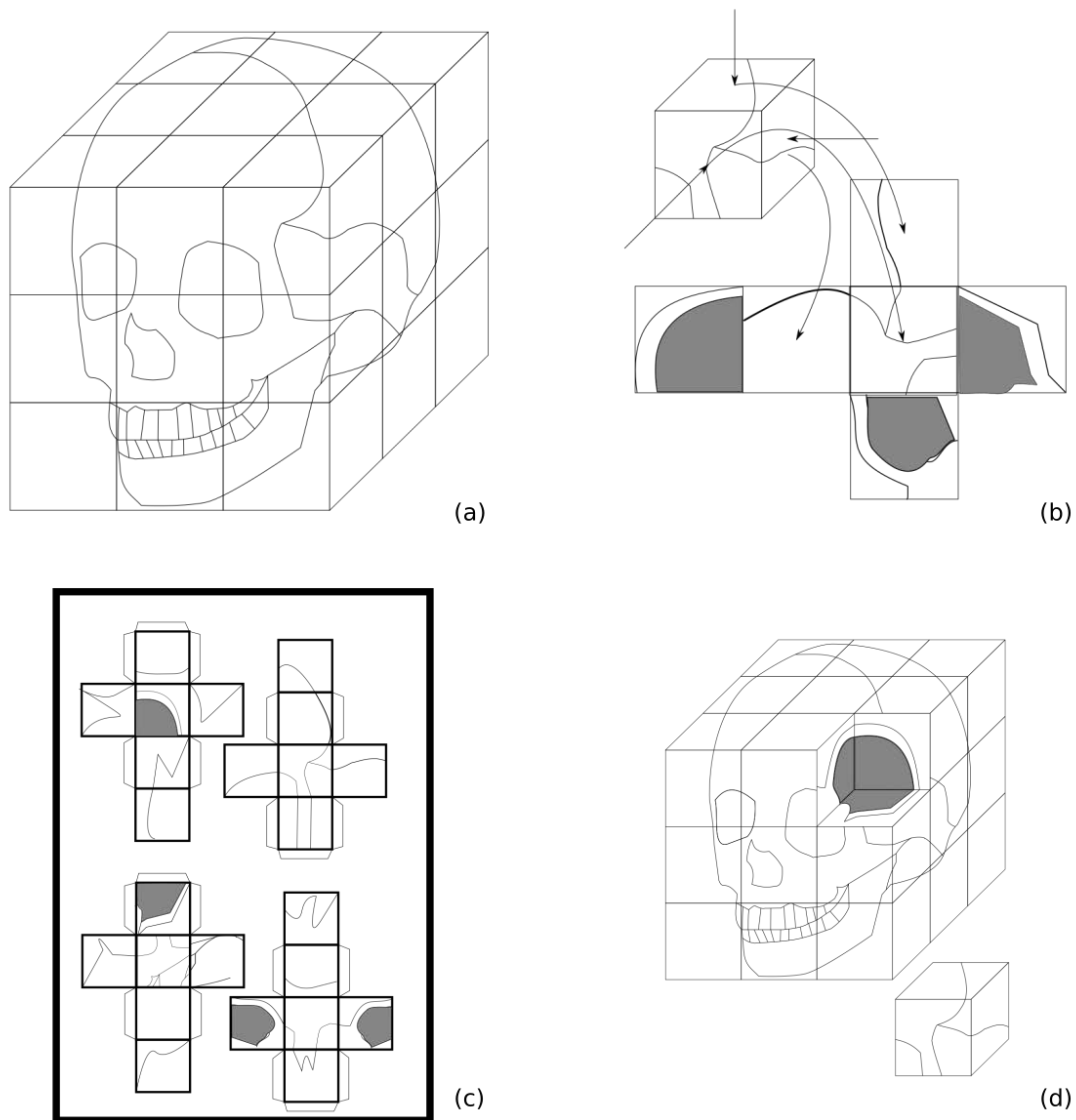
Figure 3.5: Concept of the *Cuber* workflow. (a) The volume data is partitioned into cube-shaped parts. (b) A texture for the cube faces is generated. For each face, a rendering of the volume data is created using an orthogonal perspective. (c) The cube textures are arranged onto a printable page. (d) The cubes are constructed and the sculpture is assembled from the individual parts. Removing layers of cubes reveal different parts of the internal structure of the volume, adding interactivity to the sculpture.

a flat planar slice of imaging data, which is more difficult to interpret for laymen. We propose to use an orthogonal projection into the volume from the cube position as to face texture. A rendering with a suitable transfer function ensures a 3D appearance with a front-to-back view. The orthogonal projection has the effect that structures along neighbouring cube faces fit together. Also, instead of showing only one slice in the volume, a projection shows a more complete view of the different structures. The cube stencils are then arranged on the printout pages. Every printout contains several cube stencils, depending on the desired size. The printed stencils are then cut out and built individually and subsequently assembled to the finished model. The workflow is displayed schematically in Figure 3.5.

While wood would generally be more stable, it is not trivial to obtain several cubes of a certain size. We propose to use cubes made out of printing paper because a cube shape can be easily folded and should be stable enough to support the weight of the sculpture. Paper can be directly printed upon, and the necessary reformation to obtain unfolded cube meshes is computationally trivial. Similar to Fraser's wooden blocks, the customizable cube size would furthermore enable users to employ blocks of any material and use the printed cubes as textures. During our research, we found ready-made styrofoam cubes, which would have to be purchased from online vendors. Such cubes could serve as additional support and help with the construction.

Discussion

The *Cuber* concept addresses some of the weaknesses of the *Slicer* concept. The more interactive nature of the model allows users different perspectives from inside the volume. Engagement of the target group can also be improved through this interactivity [NMA12]. The use of different colours provides users with additional insight into the composition of the human body.

While Fraser uses 60 cubes for his model [Fra], we think it beneficial to limit the number of cubes in some cases. A high number of cubes are more difficult to assemble and require more guiding of the users. This can be done by numbering the cube faces, which in turn obstructs the view into the structure with the visible numbers. A lower number of cubes, however, will limit the granularity of the model considerably. Smaller organs might vanish behind larger ones.

The model created by Fraser uses cross-sections of the volume data. Therefore the outside faces of the cubes on the border of the model do not display anything. Using projections for the outside facing cubes would mean that users could at least see from which side they are viewing the sculpture. However, a cube from which different faces can be seen shows different perspectives. Only faces that use the same viewing direction show a consistent image. This would reduce the 3D effect of the sculpture. For the *Cuber* concept, we see **(R3)** and **(R6)** only partially fulfilled. Smaller cubes allow displaying the data in greater detail, but the higher number of cubes increases the assembly time

dramatically. The cheapness and availability of paper fulfil **(R5)**.

3.4.3 Vologram Concept
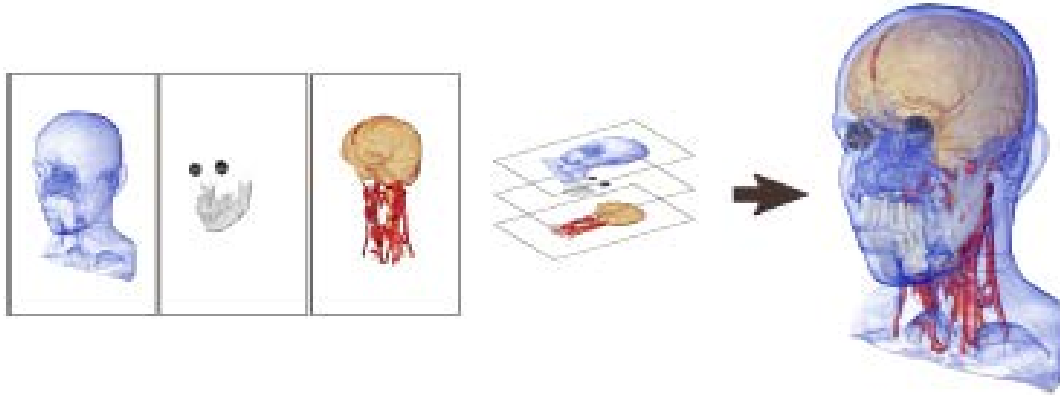
(a) Composition of a layered *Volvelle* image.
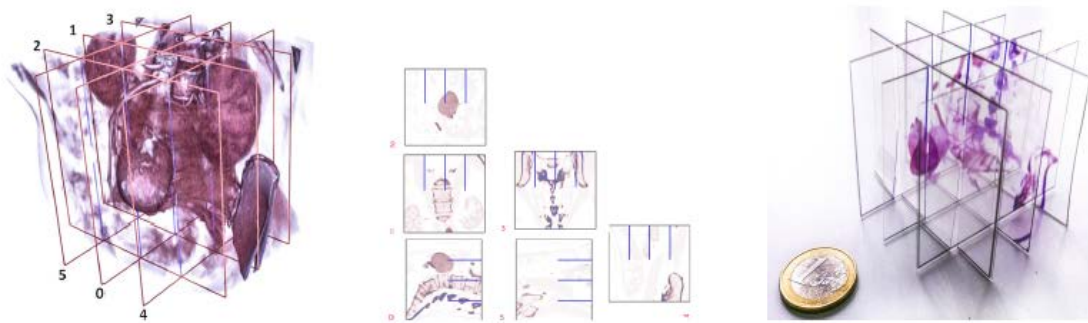
(b) Composition of a *Slice and Dice* sculpture.

Figure 3.6: Inspirations for the *Vologram* concept. (a) A multi-layered *Volvelle* figure by Stoppel et al. [SB16]. Every layer shows different versions of the same data part, if superimposed they create a composed image. (b) Composition of a 3D *Slice and Dice* sculpture [RGW20]. Multiple individual transparent parts are stacked using an octree, to create a 3D effect.

Previous approaches and their limitations provide us with some clear goals. In the final concept, the *Vologram*, we combine aspects of the *Slicer* and the *Cuber*, while overcoming some of their key weaknesses. We aim to achieve a similar level of insight in internal structures that the *Cuber* provides while overcoming the tedious assembly process of it. For this, we make use of transparency in the materials. The main goal of the *Vologram* is to display *vol*ume data as hol*ogram*-like sculptures. Simultaneously, we aim at providing a similar granularity of axial resolution than the *Slicer*.

Stoppel et al. [SB16] use transparent materials to create composite images from different

layers. Each layer contains a volume sampled with different transfer function parameters. This composition is only usable for a 2D-representation of 3D data. An example for this can be seen in Figure 3.6a. Similar to the *Slice and Dice* approach [RGW20], as shown in Figure 3.6b, we utilize stacked transparent media to achieve a 3D-like appearance of the volume renderings. We focus on displaying many different structures, through illustrative volume rendering of segmented structures [PB13], instead of direct volume rendering of volumetric data. We use a fixed inter-slide distance in our concept and do not focus on a selective partitioning of the volume data, but aim to provide the user with a more interactive approach in creating the sculptures. Physicalization parameters and the perspective direction the volume is shown in should be customizable by users, to accommodate differences in available materials. Additionally, we want to allow users some interactivity, by making individual slides easily removable.

Concept

We propose a physicalization consisting of two parts. The first parts are the semi-transparent slides containing the actual imaging data, that are stacked equidistantly in parallel. The second part is the supporting structure we call the receptacle, in which the slides are placed. It serves to keep the distance between the slides and support interactivity by enabling users to remove individual slides. To achieve the desired level of customization of *Vologram* sculptures, users are provided with an interactive user interface that helps them to select the scale, inter-slide distance, viewing direction and receptacle placement. As an input to the physicalization workflow, medical CT or MRI data are suitable **(R4)**. We propose to use pre-segmented volume data as an input for the workflow. This provides a basis for the creation of volume filters, to allow users to select parts that they wish to include in the resulting image. This can be used to prevent structures that a user is not interested in, to obscure more interesting details. The inter-slide distance has to be selected before creation because it determines the content of the individual slides. The viewing angle is selected as well, to allow users to choose a perspective interesting to them, as opposed to imposing a pre-selected viewing direction. Additionally, the scale of the data is selectable by the users. This helps them to use the material efficiently, and to make interesting structures more visible on the limited space of a slide. When a user has decided on the desired parameters, the workflow continues automatically. Single images are taken in a constant spacing along the viewing direction. This results in an equidistant positioning of the slides in the *Vologram.* These slides are created by rendering an orthogonal projection of a one-voxel layer sampled at positions defined by the inter-slide distance. As opposed to a perspective projection, which creates the impression of a central observer when viewing renderings on a screen, we chose an orthogonal projection for the individual slides because the 3D effect of the *Vologram* results from the users perspective of the sculpture in the 3D space. The colours of the individual pixels are assigned by a transfer function similar to the preview volume rendering in the user interface. This ensures that the visualization is comparable to resulting visualizations, to satisfy **(R7)**, for a later evaluation. The images are then arranged on a printable page. Assembly order is indicated by assigning numbers to the

Figure 3.7: Concept of the *Vologram* workflow. (a) Users select a viewing direction and the image is resampled along the viewing axis. (b) In a regular interval, images are sampled along the viewing direction and mapped to a rectangular plane. (c) Sub-images are arranged on a printable page. (d) The stencil is printed out and cut along the predefined lines. Images are assembled in order, in a constant distance. This creates a 3D hologram-like appearance.

individual slides. After printing, the individual slides are cut out and arranged in the previously selected interval. To achieve this, a user constructs a receptacle that keeps

the slice distance constant. Receptacle design is discussed in the following section. The resulting figure resembles the volume in a 3D-space. A hologram-like appearance is achieved and —depending on the receptacle— multiple viewing angles are possible. An overview of the *Vologram* workflow can be seen in Figure 3.7.

This concept is dependent on translucent materials, which can be printed on. As stated in our requirements, we focus on materials available to the general public. This disqualifies any means of creation that require specialized hardware. Overhead foils are a suitable candidate for the transparent medium. They can be bought in paper stores, and are available for printing with both laser and inkjet printers. Cutting the material is possible with regular scissors. We propose to use cardboard as a base for the receptacle because it provides a flat surface. It can also be easily cut with scissors or box-cutter knives. For an inter-slice distance of around 2 mm, wooden sticks that resemble icecream-sticks can be found at paper- and craft stores can be used as spacers to create slots for inserting the slides. A rectangular hole can be cut in a cardboard base, wide enough to fit the width of the sticks and long enough to support several sticks, arranged in close succession. A structure like this supports quick assembly for different *Vologram* sculptures with the same slide dimensions.

Discussion

The *Vologram* concept combines several advantages of both previously proposed approaches. Sculptures allow observers an inside view of structures like the *Cuber* concept, while their assembly is as simple as the construction of *Slicer* sculptures. A *Vologram* also requires less time to assemble than both *Slices* and *Cuber* sculptures. Receptacle construction takes about 30 minutes but does not have to be repeated for subsequent figures, because receptacles can be reused. One *Vologram* sculpture takes about 15 minutes to assemble. The sculptures still achieve similar resolutions as the *Slicer*, of around 2 mm inter-slice distance, depending on the receptacle design. The individual slices, also allow the user a degree of interactivity. Individual slices can be easily removed and examined, to provide an overview of the different anatomical structures on the same plane. The spatial resolution creates step-like, low-resolution 3D appearances, similar to the *Slicer*, while the translucent nature of the material does not hide the inside structure. The slice distance can be varied, to create bigger holograms at the cost of resolution. A single receptacle can accustom physicalization of different characters and can be reused. For bigger inter-slice distances, users can simply skip one or more slots of an existing receptacle.

Vologram fulfils all requirements of a suitable physicalization concept. The used materials are inexpensive and sold in paper and crafting stores **(R5)**. A quick and easy assembly is supported by the two-part design. The reusable receptacle can support multiple slide sets. The slides are simply printed with desktop printers and can be cut out with regular scissors **(R6)**. *Vologram*s are capable to display anatomical data, captured with CT or MRI **(R4)**, in an accurate enough way for a layman target group **(R1)** to convey

the positions of organs and their spatial relationships in the human body **(R3)**. The workflow requires little user input and is not dependent on a user's ability to navigate complicated medical visualizations **(R2)**.

3.5 Concept Summary

Table 3.1 summarizes our suitability evaluation of the three proposed concepts, according to the requirements. It should be noted that all three distinct approaches benefit from an interactive application, where users can customize their physicalizations, by altering the different parameters. These applications should provide a *what-you-see-is what-you-get* workflow **(R2)**, and use segmented CT or MRI data as input **(R4)**. All three concepts also communicate basic human anatomy in different aspects. *Slicer* can communicate organ shapes and sizes. *Cuber* deals with the spatial relationships of anatomical structures, as well as medical image analytics by using three perspectives that are also used in medical imaging: axial, lateral, and sagittal. *Vologram* shows anatomical structures spatial relationships, by showing the relative positions and sizes of organs **(R3)**. The inter-slide distance is similar to the *Slicer* and smaller than the *Cuber's* cube size. The proposed concepts all use only readily available, relatively cheap tools and materials in combination with desktop printing technology **(R5)**. Easy and quick assembly can only be guaranteed by the *Vologram* concept, through employing a reusable receptacle, with which different sculptures can be created. Construction for the other two concepts is more tedious and repetitive because the construction has to be repeated every time **(R6)**. For the optical comparability of visualization and physicalization, to facilitate the eventual evaluation of the concepts, *Vologram* and *Slicer* fulfil this criterion. *Cuber* can not be easily compared with a volume render, due to too much possible obstruction **(R7)**. Thus, we select *Vologram* as a suitable physicalization concept for our work **(R1)**. The following section contains an overview of the concept of the workflow to create such sculptures, from data selection to user interaction.

Requirement	*Slicer*	*Cuber*	*Vologram*
(R1) Meets needs for anatomical education	✗	✗	✓
(R2) Data selection and processing supported	✓	✓	✓
(R3) Conveys basic human anatomy	✓	✓	✓
(R4) Uses real CT or MRI data	✓	✓	✓
(R5) Affordable materials	✓	✓	✓
(R6) Quick assembly	✗	✗	✓
(R7) Visualization and physicalization comparable	✓	✗	✓

Table 3.1: Examination of the suitability of different physicalization concepts, according to the predefined requirements. Requirement text is shortened for readability.

(a) Receptacle schematics.

(b) Receptacle design.
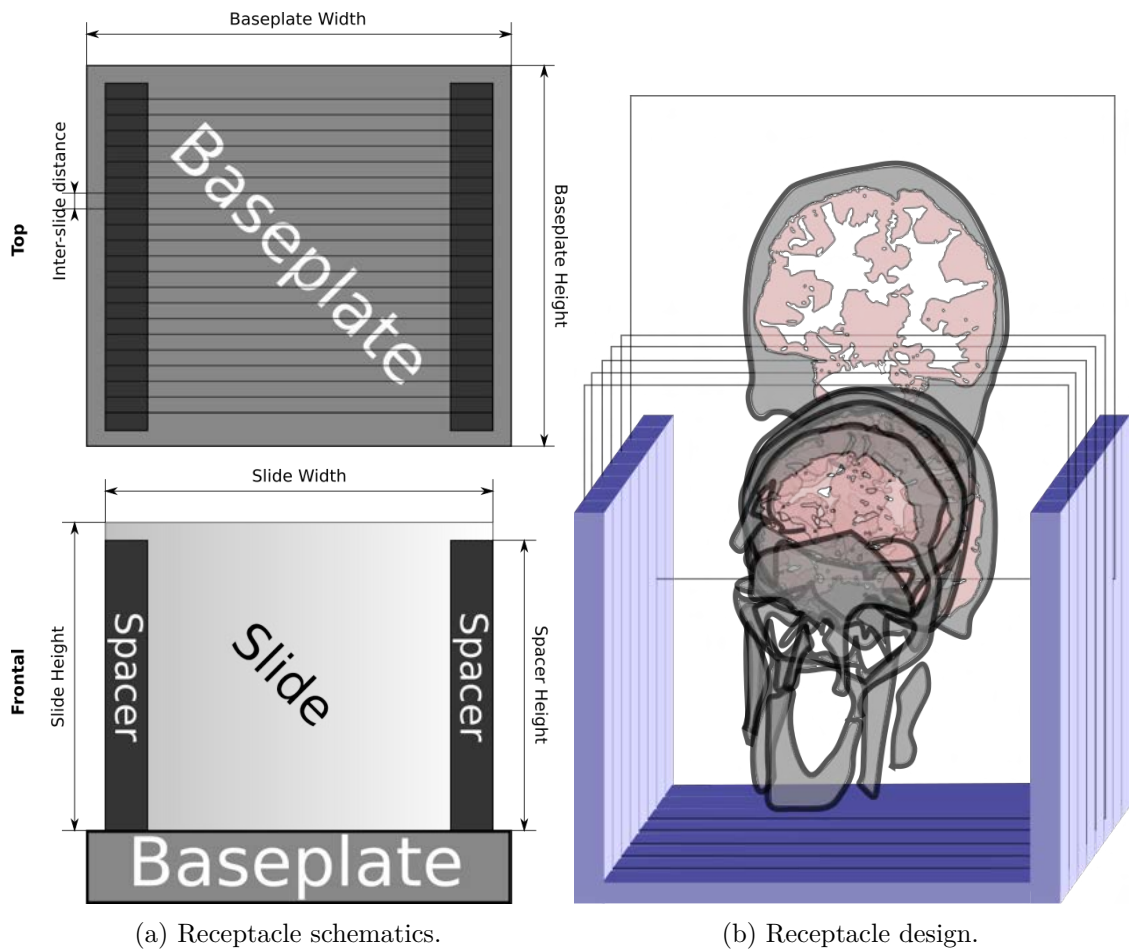
Figure 3.8: Design of the *Vologram* receptacle. (a) Design schematics. Components are labelled, and important measurements are emphasized. (b) The finished design. Sildes are inserted between the spacers and rest on the baseplate. A slide in the back is slightly elevated to emphasize potential interactivity.

3.5.1   Physicalization Design

For the realization of the *Vologram* concept, we propose a two-part design. Aside from the slides that contain the volume data, a receptacle is used to support the structure and facilitate interactivity. The physical properties of the receptacle bring different parameters with them, some of which are required as user-input in the underlying visualization. This section lists the different parts and parameters resulting from the concept. Design schematics of the proposed receptacle are shown in Figure 3.8a. Figure 3.8b shows a possible design for a receptacle.

Sildes

Slides are the core of the *Vologram* concept. To ensure the 3D effect is achieved correctly they have to be assembled in parallel, keeping a constant distance. Slide height and width are an important factor to consider. Too small slides can only support images at a very high scale, leading to bad visibility. Too big slides, lead to increased material use. The slides have to be made of a transparent, printable material, for which we propose to use overhead foils.

Baseplate

The baseplate serves two purposes: it supports the spacers and provides a plane surface for the slides. It should be made of a durable material that can be easily processed. We propose the use of thick cardboard. Baseplate width and height should exceed the slide width and the total spacer width if the spacers are pocketed in the base. For this, a rectangular hole is cut into the baseplate, and an appropriate number of spacers are inserted.

Spacers

Spacers are the vertical support for the sculptures. They serve to keep the slides apart at a constant distance. Therefore, they determine the inter-slice-distance through their width. For this, they are required to be durable and firm. Wooden sticks provide sufficient support for holding the slides. They also have to ensure the deformable slide material is kept planar. Therefore, it is beneficial for the spacer height to be equal or greater than the slice height. This has to be kept in mind also if the spacers are inserted into the baseplate. A material of sufficient height needs to be used so that the slide height is covered by the spacer to ensure stability.

3.6   A Medical Physicalization Pipeline

After deciding on a suitable candidate for our physicalization, we present a formal workflow for the process of creating *Vologram* sculptures from medical imaging data. First, the raw data is processed to create a set of filters for users, which they can use to include and exclude specific structures from the visualization. The intensity values of the volume data are transformed to suit one of three different representation method: discrete, continuous, and realistic. This is done to make it possible to use a single transfer function in the renderings. In the cases of continuous and illustrative mapping, we aim to create a more abstract appearance for our renderings. The transfer function for this mappings can be automatically generated from colours and opacity values assigned to individual structures. For the realistic mapping process, a piecewise linear transfer function has to be defined manually. After these steps, users are presented with a rendering of the volume data. Using this rendering, they can select viewing direction, scale, and slide distance for the physicalization. These parameters serve as input for the
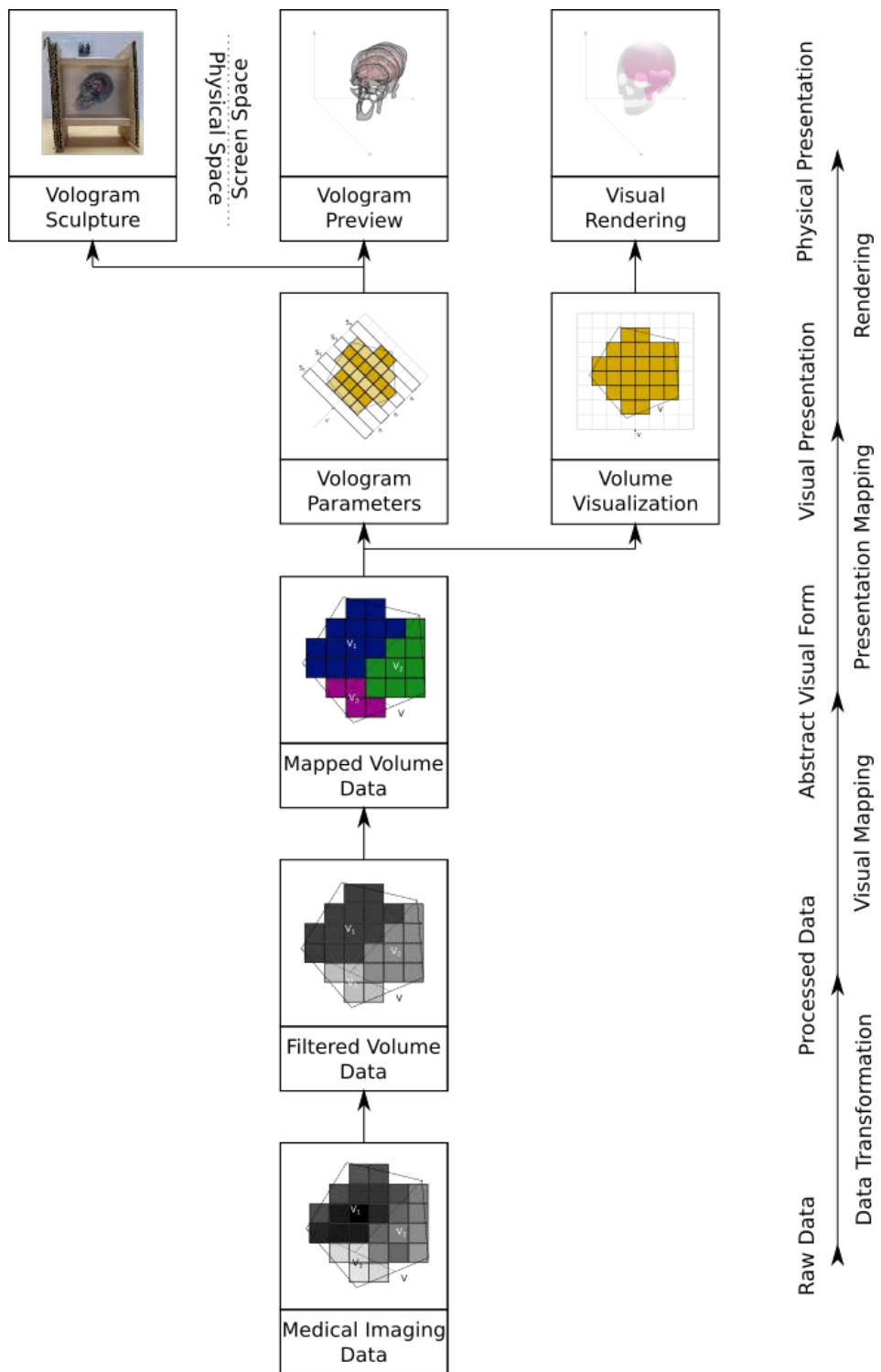
Figure 3.9: Overview of the full pipeline, adapted from Jansen et al. [JD13]. The bottom-to-top flow is consistent with Figure 2.5.

Vologram transformation of the data. After executing the transformation, users are shown a rendering of the resulting volume data. This rendering can be used to preview the resulting physicalization. If users are not satisfied with the appearance of the result, they can return to the volume rendering display and alter the parameters again. Lastly, when all parameters are supplied, the transformed volume data is brought into a printable form. Users can then print the resulting pages, cut out the slides and assemble the physicalization. We show a sketch of this pipeline in Figure 3.9.

3.6.1 Data Transformation

(a) Source volume. (b) Filters for Segmentation. (c) Partitioned volume.
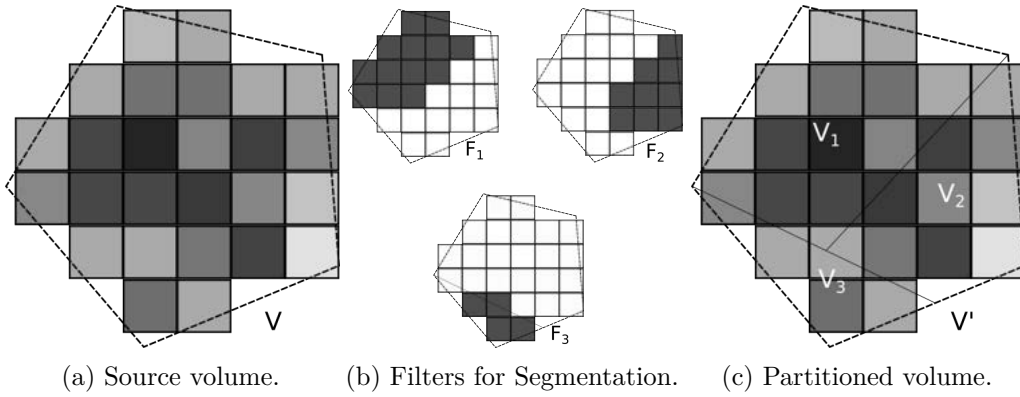
Figure 3.10: 2D representation of volume data segmentation. (a) Volume data consisting of different intensity values represented by different grey values. (b) 3 Filters provided to discriminate different structures. (c) Filters provide a partitioning of the volume into 3 disjoint sub-volumes.

The first step in Jansen and Dragicevic's extended information visualization pipeline is *data transformation*. This step is responsible for transforming *raw data* into *processed data*. In our case, the raw data corresponds to CT or MRI image data. Such data comprise of discrete intensity values for each voxel of the volume data [PB13], arranged on a regular 3D cartesian grid. The values correspond to tissue properties at the voxel's positions. For the explanation of the subsequent processing of the raw data, we define a volume data set as the 3D matrix V with elements (v_{jkl}), with the dimensions $m \times n \times o$. The elements of the matrix represent the integer intensity values at the different positions (j, k, l) on the cartesian grid:

$$V = (v_{jkl}) \in \mathbb{Z}^{m \times n \times o} \tag{3.1}$$

(R4) states that the input for the proposed application should be medical volume data, created by CT or MRI imagery. Users, as stated in **(R2)**, are not expected to be proficient in medical visualization. Data need to be prepared in advance. We propose, to

provide medical volume data, segmented into major organs and structures.

For data transformation, filters have to be obtained for each organ to be displayed in the visualization. For filtering the volume data we use binary segmentation masks which correspond to structures of interest. We define a *Filter F_i*, with elements f_{jkl} for a volume V, as the 3D matrix :

$$F_i = (f_{i_{jkl}}), \; f_{i_{jkl}} = \begin{cases} 1, & \text{if } v_{jkl} \text{ is part of the desired structure.} \\ 0, & \text{otherwise.} \end{cases}, i = 1, 2 \ldots, n \quad (3.2)$$

We define the volume data as processed when a set of filters F is provided alongside V, where F contains filters F_i for all structures of interest to be available for subsequent volume filtering.

$$F = \{F_1, F_2, ..., F_n\} \quad (3.3)$$

Users have the option, to select a subset of filters, containing filters for the regions they desire to display. The subset F' is the final input for the transformation. It is defined as:

$$F' \subseteq F \quad (3.4)$$

An illustration of the partitioning process of a volume data set is shown in Figure 3.10. We propose three different filtering algorithms that can be used to transform the volume data according to the selected filters. We define a discrete filtering method, that results in a volume data set comprised of single integer values corresponding to the selected structures. Later, a transfer function is created using these values as intensities, assigning one colour per filter. We also define continuous filtering, where the intensity values of the structures defined by the filters are remapped to a fixed interval. One colour and an opacity range are assigned to the resulting intervals, resulting in the structures being coloured in a single colour with intensities according to structural properties. Every structure is assigned a different interval so that different structures can be rendered in different colours. Renderings created from datasets that are processed with these methods have an abstract, illustrative appearance [PB13]. The third method keeps the intensity values from the source data intact for selected structures and removes all other intensity values. Using a manually defined, piecewise linear transfer function for direct volume rendering [PB13] this can create a more realistic look for the resulting image. We refer to this method as realistic volume filtering. The three proposed algorithms transform the original volume according to the selected method so that a single volume dataset V' is created and only a single transfer function is needed for the rendering.

Discrete Volume Filtering

In this variant of the filtering process, the volume data is transformed according to the following equation:

$$V' = \sum_{F_i \in F'} i * F_i \tag{3.5}$$

This results in a volume composed of discrete values i for every selected filter. This provides the base for a rendering with distinct, colours for each structure. In the source volume V, the distinct structures typically are comprised of points with discrete intensity values that encode tissue properties. In this variant, such intra-structural variations are lost in the filtering process. This results in a volume composition as shown in Figure 3.11a. The loss of intra-structural variations can be mitigated by using the following technique.

Continuous Volume Filtering

To provide the possibility to display intra-structural density variations, we propose this second variation for the volume filtering process. Intensity values of distinct structures are remapped to a predefined interval $[0, 100]$ and offset according to i. For the clarification of auxiliary parameters for this operation, we define V_i with elements $v_{i_{jkl}}$, as the volume data corresponding to the filter F_i with elements $f_{i_{jkl}}$.

$$V_i = (v_{i_{jkl}}), \; v_{i_{jkl}} = \begin{cases} v_{jkl}, & \text{if } f_{i_{jkl}} = 1. \\ 0, & \text{otherwise.} \end{cases} \tag{3.6}$$

The set containing the individual filtered volumes is named $\mathbb{V}$.

As an auxiliary variable for the transformation we define the matrix $V_{i_{min}}$. It contains the minimum value of V_i at every index. It is used to represent the subtraction of a scalar value from all intensity values of a volume dataset. Additionally the values $v_{i_{min}}$ and $v_{i_{max}}$ represent the scalar minimum and maximum value of V_i. With the help of these variables we define the result of the data transformation as follows:

$$V' = \sum_{V_i \in \mathbb{V}} 100 * i * (V_i - V_{i_{min}}) * \frac{99}{v_{i_{max}} - v_{i_{min}}} \tag{3.7}$$

This maps the intensity values of every distinct structure of interest to an interval $[i*100, i*100+99]$. A rendering resulting from this transformation shows inter-structural differences well. A possible volume composition resulting from this is shown in Figure 3.11b. This provides a more varied look than the discrete filtering technique.

Realistic Volume Filtering

Typically, when creating a volume rendering from medical imaging data, the intensity range of the full volume is considered. A distinction between different types of tissue is approximated by defining a piecewise-linear colour transfer function. In this method, we

consider the possibility of creating a direct volume rendering with a realistic appearance from filtered volume data by applying the following transformation:

$$V' = \sum_{V_i \in \mathbb{V}} V_i \tag{3.8}$$

Here, simply the intensity values of all distinct structures defined by the filters are combined into a single volume. Intensity values of the individual structures are not changed. Structures that are excluded in the filter selection are discarded. An example of a volume data set filtered with this method is shown in Figure 3.11c. This algorithm can be used to create renderings akin to direct volume rendering [PB13]. Organs and tissue can be assigned realistic looking colours. Anatomical non-experts might be disadvantaged through this because individual structures are harder to discriminate between in such renderings.

(a) Discrete filtering. (b) Continuous filtering. (c) Realistic filtering.
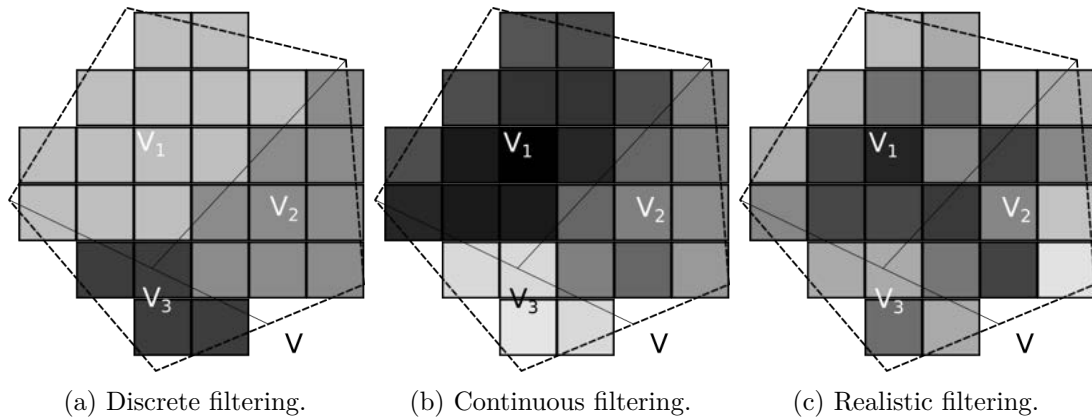
Figure 3.11: 2D representation of volume filtering. (a) Each structure is assigned one intensity value, according to the index i (represented by a single grey value) of the corresponding filter. (b) The index i determines the grey level range for the data. (c) Intensity values are taken directly from the source volume.

3.6.2 Visual Mapping

The next stage in the pipeline proposed by Jansen and Dragicevic [JD13] is *visual mapping*. In this step, the processed data is brought into an abstract visual form. In our case the visual form is fixed, only volume rendering is considered. Alternatively, iso-surface extraction could be performed on the processed data, to use a surface rendering technique. In this step, colour and opacity values are assigned to the individual intensity values of the volume.

(a) Discrete Transfer Function.

(b) Continuous Transfer Function.
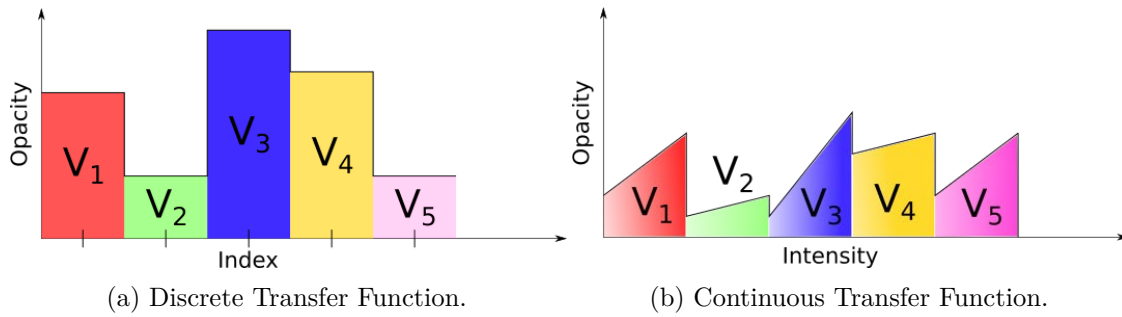
Figure 3.12: Different versions of automatically generated transfer functions for assigning colours and opacities to intensity values. (a) Colours and opacities are assigned per index of filtered structure and do not vary within the structure. (b) Colours are constant for each structure, but opacity increases linearly with the intensity values within one structure.

(a) Discrete mapping.

(b) Continuous mapping.

(c) Realistic mapping.
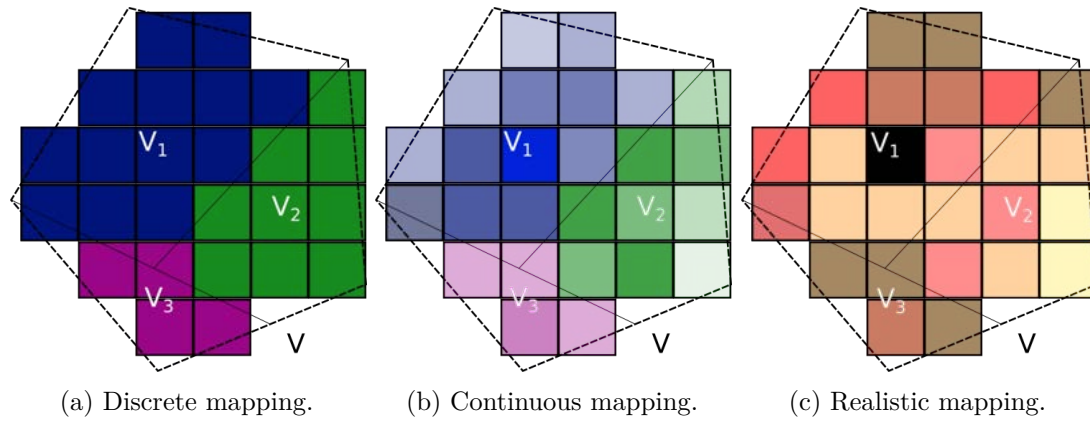
Figure 3.13: 2D representation of colour mapping. Individual transfer functions are provided for mapping opacities and colours to intensity values. (a) Each structure is assigned exactly one solid colour and one opacity value. (b) Structures are assigned one solid colour and an opacity gradient mapping for the individual intensity values. (c) Colours are assigned independent of structure.

Colour Mapping

Before creating a rendering of the filtered volume data V', a transfer function is applied to assign colour values and opacity values to intensity values. We illustrate two types of transfer functions, used for the illustrative rendering variations, in 3.12. The different variations of this mapping are exemplified in Figure 3.13.

The generated transfer functions are defined by a set of parameter vectors. For the case of discrete volume filtering, the transfer parameters simply correspond to the index i of the individual filters. For each i there needs to be a vector $p \in [0,1]^4$ defining the

individual red, green, blue and opacity value corresponding to each i. These values are defined per filter in advance. An example for one such transfer function is illustrated in Figure 3.12a, an example for a resulting mapping is shown in Figure 3.13a.

Using continuous volume filtering, intensities are mapped to piecewise linear functions. Two points are required to assign an opacity interval to a structure. The minimum and maximum opacities for the interval are assigned to the adjusted intensity interval borders per structure, the minimum adjusted intensity value $i * 100$ and the maximum adjusted intensity value $i * 100 + 99$. The transfer functions parameter vectors for this filtering method have to contain the minimum and maximum opacity for the assigned structure, in addition to the three colour values. This means $p \in [0,1]^5$. Figure 3.12b serves as an example for a transfer function of this type. A resulting mapping using a function of this type can be seen in Figure 3.13b.

The transfer function for the realistic volume mapping has to be defined manually beforehand. Users may assign any number of points corresponding to intensity values original to the source volume. The intensity values of the volume data are not altered, apart from setting the intensity values of not selected areas to 0. Figure 3.13c shows a typical outcome for such a mapping.

3.6.3 Visualization Presentation Mapping

In this stage, the final parameters for the visual presentation are assigned. The pipeline branches into two distinct paths here. The first path is the presentation mapping for the volume visualization. Default values are assigned for viewing direction and scale in this step. The visual rendering is created to aid users in selecting the parameters for the physicalization.

3.6.4 Visual Rendering

The rendering stage of the pipeline has three distinct branches. In the visual rendering part, users are presented with a rendering of the filtered volume data, using either the transfer function created in the visual mapping stage or the manually defined transfer function for the realistic method. The scale is assigned a default value and the viewing position is set parallel to the volume's z-axis, towards the center of the volume. This rendering serves for the parameter selection of the physicalization preview mapping. This view also serves as a virtual comparison for the physicalization in the evaluation phase, as according to **(R7)**. This variant is illustrated in Figure 3.14a.

For the presentation mapping for the physicalization, users have to specify a scale factor f for their sculptures, this will be typically a number less than 1 for smaller receptacle sizes. Another parameter to select is the inter-slide distance d in voxels. It represents the physical distance between individual slides in the physicalization. It

(a) Visual rendering.

(b) Physicalization preview.

(c) Volgram sculpture.

(d) Physical sculpture.
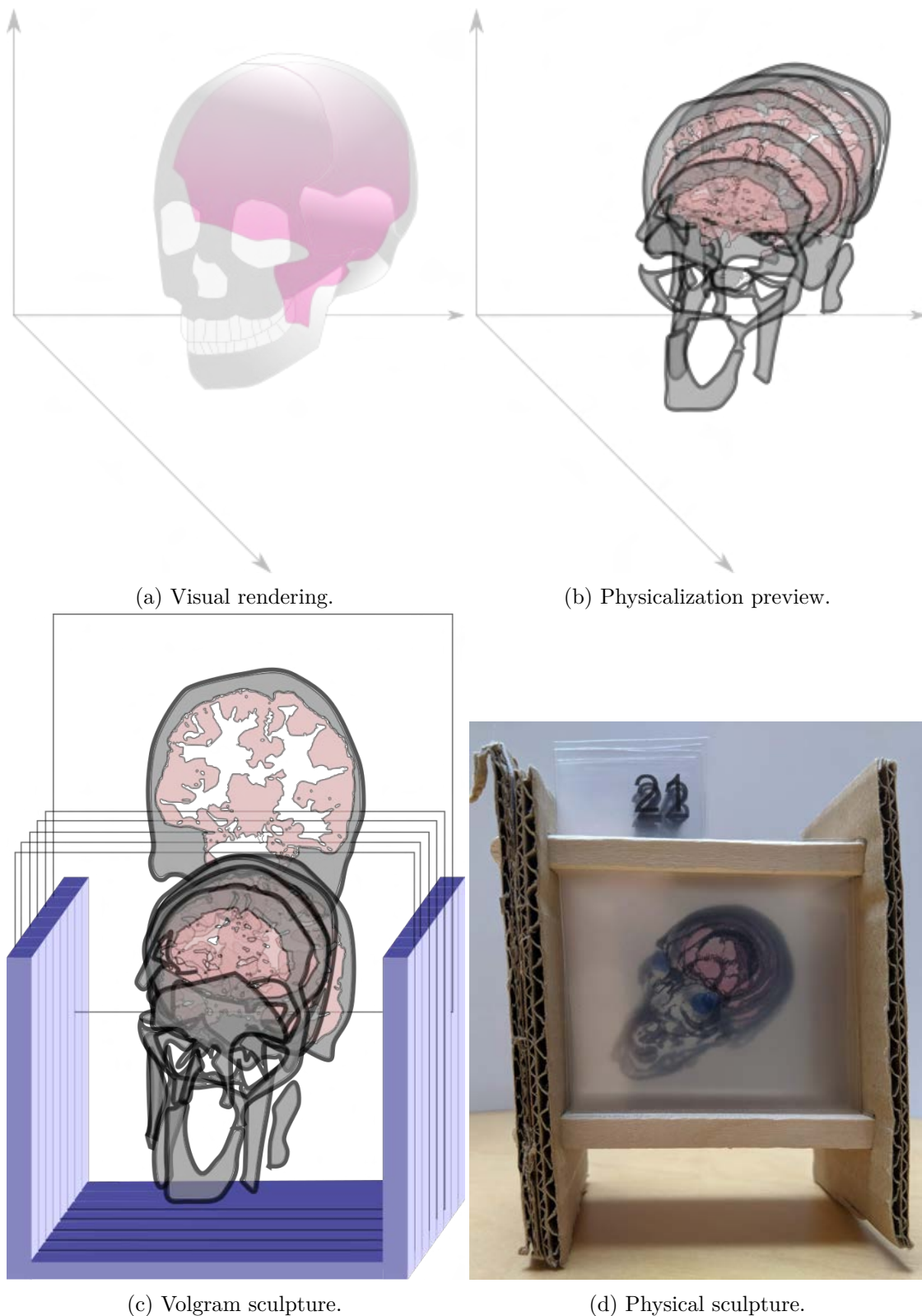
Figure 3.14: Different rendering outcomes. (a) The visualization render. The volume is rendered in perspective according to the mapping. (b) The Preview for the physicalization outcome. The Volume data is transformed according to the physicalization parameters. (c) The assembled form of the printed slides. (d) A finished *Volgram* sculpture.

depends on the chosen physical inter-slice distance in millimeters d_{mm}, as well as the voxel spacing s_v in viewing direction. It is calculated as follows:

$$d = \frac{d_{mm}}{s_v * f} \tag{3.9}$$

Users select a viewing direction by altering the viewpoint of the visualization rendering. A rendering of the volume data with centre c is displayed for this in a 3D space. The voxel data can be viewed as a set of values, aligned in a rectangular grid. The user can control the camera vector k', with the vector representing the viewing direction v' always pointing to the object centre c. We define the initial camera vector k pointing along the z-axis of the coordinate system. When a suitable viewing direction is selected, this results in an angle θ between k and k'. A normal vector k_n for the plane spanned by k and k' can be obtained by using the cross product of the vectors. A schematic view of this is shown in Figure 3.15.
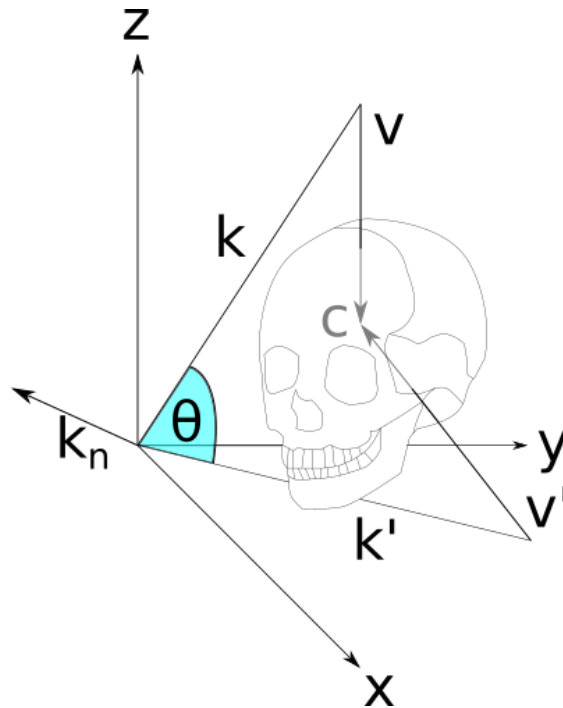
Figure 3.15: Schematic view of the parameters for the reslice transformation.

Parameter Discussion

The (*Vologram*) transformation of the prepared volume data into *Vologram* sculptures consists of two parts: the reslice transformation and the subslice extraction. It requires different parameters, which can be freely chosen by the users. Apart from these parameters depending on the constraints introduced by different materials used in constructing the

sculptures, like the size of the slides and the width of the spacers, users also have to make sure that their used parameter combinations are well balanced. The scale factor is used to fit the visible area of the data into the receptacle. It determines the influence of the slide distance on the subslice extraction as well. A scale factor, approaching 1:1 limits the slice distance to the voxel spacing of the data. Such a scaling means also that more slides are required to achieve the same resolution. 1:1 sculptures of larger structures would need a lot of slides and would be very expensive. Conversely, a smaller scale creates smaller sculptures. While smaller sculptures can use smaller inter-slice distances to achieve a comparable resolution to larger figures, such a scaling also decreases the size of the image. Finally, the viewing angle is an important consideration. Primarily it is desirable to maximize the amount of information shown by the sculpture. Users need to consider to fill the image area resulting from the view angle while taking into consideration how much slides are needed to display the desired area. The preview rendering shows a simulated appearance of the physicalization. This can be used to examine the effect of the chosen set of parameters.

3.6.5 Vologram Presentation Mapping

(a) Source volume.   (b) Reslice transformation.   (c) Sub-slice extraction.
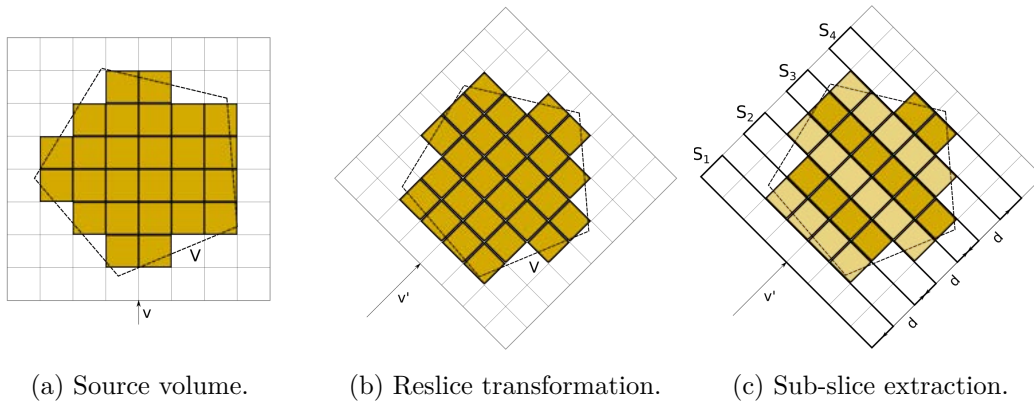
Figure 3.16: 2D representation of the *Vologram* transformation for the visual mapping for the physicalization preview. (a) The default camera position is given by a viewing vector v. (b) The reslice transformation rotates the voxel grid of the volume data to fit the chosen viewing direction v'. (c) The individual slices are extracted according to the inter-slice distance d.

After selecting the parameters for the physicalization, the transformations are performed. The process is illustrated in Figure 3.16 The parameters for this transformation are chosen by users using the rendering performed using a default mapping.

Using θ and k_n, a rotation matrix R can be defined. Furthermore, a translation matrix for moving the object centre c into the origin of the coordinate system shall be named T_c. We concatenate the transformations to obtain a transformation matrix T for our volume as follows:

$$T = T_c * R * T_c^{-1} \qquad (3.10)$$

Applying the transformation to the volume results in a transformed volume V_T', where the voxel grid is rotated in the angle θ around the vector k_n. The viewing direction vector v' resulting from the selected viewpoint vector k' stands orthogonal to the plane spanned by the x and y-axis of the voxel grid.

To create the preview of the physicalization and the *Vologram* sculptures, another step for transforming the data is necessary. The content of the individual volume slides S_i has to be obtained. For this, we collect a subset of voxels along the transformed viewing direction v' in intervals with a length of d. Each S_i represents the content of one slide.

3.6.6 Vologram Preview Rendering

After choosing the parameters, and executing the transformation of the data, a simulation of the *Vologram* sculpture is rendered as a preview, using the same colour mapping as the visualization. Users are shown a rendering, closely resembling the final form of the physicalization. This is accomplished by rendering the result of the physicalization preview mapping. For this rendering, the set of slides obtained in the previous step is used to construct a new volume data set. The slide content is put into a voxel grid. Voxels between the slides are added with an intensity value of zero, to simulate the space between the slides in the physicalization. With this rendering, users can preview the effect of their parametrization on the physicalization. When not satisfied with the outcome, they can return to the visual rendering and alter the parameters. Figure 3.14b shows a possible outcome of a physicalization preview rendering.

3.6.7 Physicalization Rendering

The actual physicalization is rendered on printable overhead foils. For this, the individual slice data S_i are rendered individually and automatically aligned on a printable page. For the rendering, orthogonal projection is used, as opposed to perspective rendering, which uses a central focus point. Depending on the size of the receptacle used, the images are aligned on the slides, images exceeding the receptacle area are cropped. The position of each slide on the page has to be determined manually. The slides need a rectangular space for image placement to fit the receptacle design. Additionally, guiding aides, in the form of rectangular tabs with the slide numbers printed on, can be added to the slides. After printing, the slides are cut out and inserted into the receptacle, completing the physicalization. Spacers serve to guide the slides into the correct position, resting on the baseplate of the receptacle. This process is illustrated in Figure 3.7. Figure 3.14c shows the arrangement of the slides in a receptacle, Figure 3.14d shows a real, constructed *Vologram* sculpture.

Implementation

With a suitable physicalization concept in mind, we now continue to propose a software application, to support and automatize the creation of *Vologram* sculptures. To cater to the needs of the target group **(R1)**, parameter selection should be feasible for non-experts in visualization **(R2)**. While conveying a basic aspect of human anatomy **(R3)**, the application also has to use real medical volume data as input **(R4)**. The *Vologram* concept provides a cheap **(R5)** and quickly constructible **(R6)** solution for this. To satisfy **(R7)**, the application has to ensure that the result of the workflow sufficiently resembles the selected volume data, to provide comparability for the evaluation. Our application consists of two parts. First, the raw medical imaging data is transformed and a set of segmentation masks is created to facilitate the volume filtering. This process is done in two separate *MeVisLab* [Mev] pipelines. This procedure is not suitable for laymen in medical visualization and has to be done by experts. The outcome of this pipeline is then used as input for an interactive *python* application, *Volcraft*, with a graphical user interface suited for the target group.

4.1 MeVisLab

To facilitate the use of medical imaging data, using the filters proposed in Chapter 3, preprocessing the source data is necessary. This is achieved manually by creating a specialized pipeline for every data set. In this section, we show an implementation of this first step of the workflow in *MeVisLab* [Mev]. The input data for this workflow has been provided by *Voxel-Man* [Voxb]. The data set is comprised of cryosection photographs and CT slice images from the publicly available *Visible Human* male dataset [Vis] from the National Library of Medicine. Additionally —and crucial for our workflow— *Voxel-Man* provide a segmentation of the inner organs [Voxa] for the *Visible Human* male dataset. The segmentation is based on the CT data of the *Visible Human* male. It is made up of individual images. The slices are provided as `.tiff` image files. The segmentation

is provided as a single dataset containing indices corresponding to the assigned labels. In the segmented inner organ data set, every distinct structure found by the algorithm used to segment the ct data set [PHP⁺01], is assigned one index. The assignment of the indices to structures is provided as a separate text-file.

In Chapter 3, we present a set of algorithms that are suited to filter distinct structures in a volume dataset. These methods require the full volume dataset, as well as a segmentation mask for each structure. Here we present a pipeline, to obtain these components from the *Visible Human* male dataset.

4.1.1   Volume Data

The CT-data of the *Visible Human* comprise of individual image files in `.tiff` format. For further processing it is beneficial, to create a single volume data file, readable by visualization frameworks, such as the *Visualization Toolkit (vtk)* [VTK]. Additionally, the *Visible Human* data have a voxel resolution of $1\,mm \times 1\,mm \times 1\,mm$, which is relatively high for such data. Hence, it is necessary to perform downsampling by a factor, to increase the performance of later parts of the pipeline. We determined that downsampling by a factor three would result in an adequate compromise between resolution and performance. For this, we use a three-part pipeline. The first step in this pipeline is to create a 3D volume out of the individual image files. For this we use the *MeVisLab* function `Compose3DFrom2DFiles`. Secondly, axial downsampling is applied to the data to achieve a lower resolution. This is achieved by the `Resample3D` function, using a scale factor of $1:3$. Lastly, the data are saved in the `.vtk` file format, with the `itkImageFileWriter`.

4.1.2   Structure Filters

The data for the filters are extracted from the segmented inner organ data, as provided separately by *Voxel-Man*. These data are generated in such a way that multiple different indices can apply to one organ or structure. Furthermore, because the target group comprises of anatomical laymen, it is beneficial to merge some structures into a single one. An example of this is the skeleton. The *Visible Human* segmented inner organ data contain indices for multiple different bones. As we want to focus on organ structures and positions, we merge all skeletal structures into one. For this, we specified to require one distinct binary mask per structure, where all voxels that correspond to that structure have intensity 1. All other voxels have intensity 0 for this specific filter. We achieve this by using another *MeVisLab* pipeline, which can be repeated similarly for every filter. In addition to creating 3D data and to resampling as in the volume data processing, a threshold needs to be applied for every index assigned to the specific structure. We do this by using the `IntervalThreshold` function, with the lower and upper bound of the interval set to the index and the output of the threshold filter set to 1. If a structure comprises of multiple indices, the output data from multiple threshold filters need to be combined to create a single dataset. Depending on the number of different indices,

we use the *ImageArithmetics* function, with a varying number of input connections for this. Finally, each filter created is stored as individual `.vtk` file. The pipeline to create the segmentation masks is shown in Figure 4.1. This pipeline can be easily adapted by visualization experts to fit different data, so it can be used to create new input data for the application to be supplied to laymen.
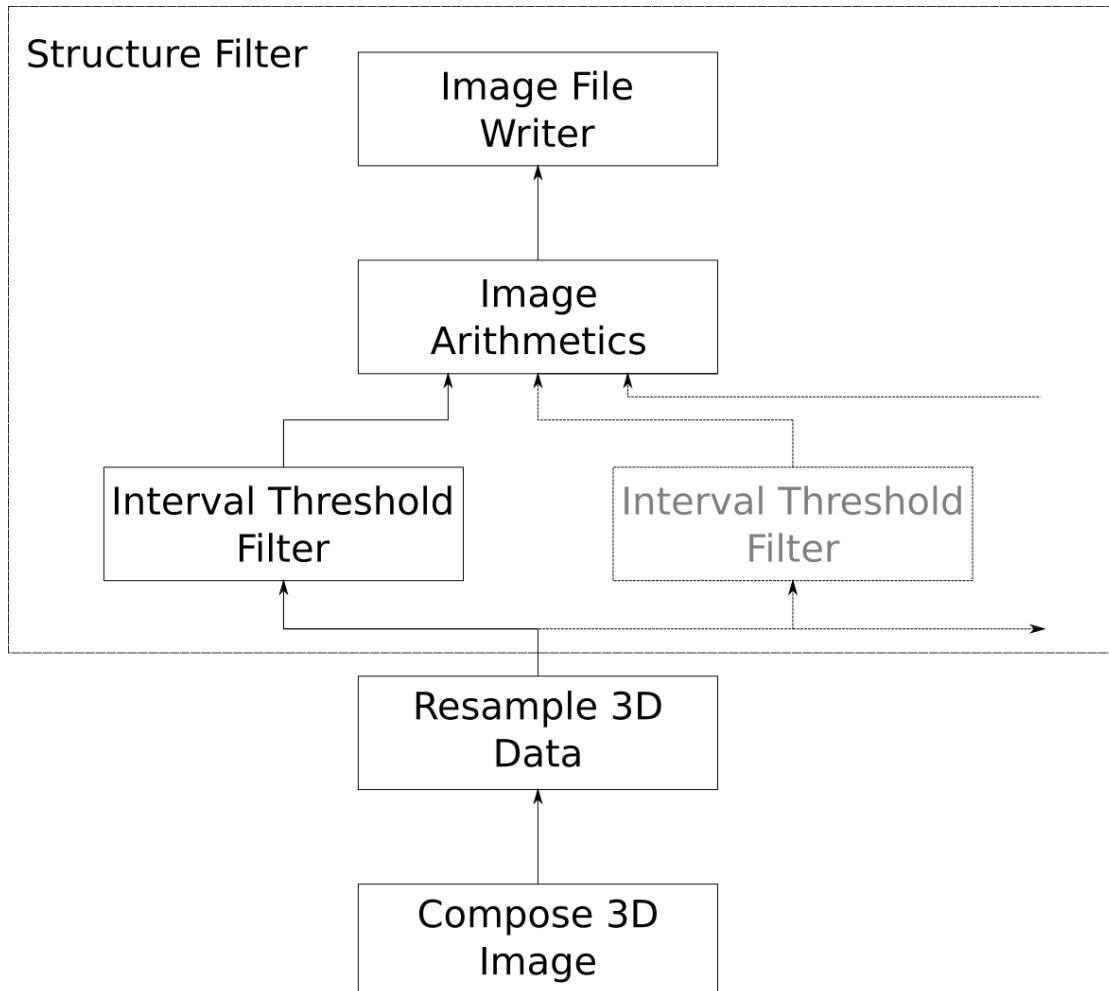
Figure 4.1: The *MeVisLab* pipeline for filtering. The segmented inner organ data are downsampled with the same factor as the volume data. Thresholds are applied for each index assigned to the structure and the results are summed up to create a filter for one specific structure. One `.vtk` file is created for each filter.

4.2 Python Development

After preparing the volume data and segmentation masks, both are loaded into a *python* 3.9.0 application [Pyt] named *Volcraft*. For volume rendering we use *vtk* 9.0.0 [SML06].

The user interface is created with *PyQt5* [pyq]. Additional image processing is handled by the *Python Imaging Library (PIL)* [PIL], and data array processing is done using *numpy* [num].

4.2.1   Interface Design

Requirement **(R2)** implies the necessity of a user interface not targeted to an expert audience. We use pre-segmented volume data that are prepared before they are presented to users. The largest space of the interface should encompass the rendering of the volume data, a preview of the results of the transformations occurring, or a display of the result. We reserve the right side of the visualization for this. The volume rendering, or result display, should make up most of the user interface (UI). Users can interact with this visualization via pan and zoom. This is controlled exclusively with a mouse, using click-and-drag gestures to rotate, and the mouse wheel for zooming in and out of the volume rendering. The remaining space, on the left side, we reserve for the parameterization. It is beneficial to provide users with a self-explanatory, step-by-step workflow. We suggest a top-down order of functions, according to the respective step in the workflow. At the top, we place rendering options, for the customization of the visualization. These are limited, to not overwhelm users with options, for example regarding the segmentation, which they would not understand. Rendering options include the filters for anatomical structures, as well as the display of visual aids in the renderer.

An important function of the user interface is the customization of the physical properties of the sculpture. Inter-slide distance, as well as scale, contain feasible default values that correspond to the measurements of our prototype. When changed, the differences should be presented to the users, as fast as possible. Scale values are directly reflected in the visualization. The inter-slide distance value influences the preview. The viewing direction is defined by the camera position the users choose. In this way, we achieve a *what-you-see-is-what-you-get* parametrization, avoiding confusing or unknown terms for layman users. The users the *Vologram* transformation is executed by pushing the *execute* button, after generating a preview, or can alter parameters until they are satisfied. The interface shows a bounding box after the transformation, in the relative size of the receptacle. This size is freely adjustable by users, depending on their material constraints. This warns users of areas that do not fit into the receptacle size, which would be cropped out of the resulting image.

After the transformation, the users are directly shown the printable page. They can freely select a set of slides to save. This allows them to exclude areas that do not contain visual information, or that are not interesting to them. The start and end slide selectors are limited to the actual number of generated images. Selecting *Save* causes a dialogue to appear, where users can select the target location of the printable page. Results can then be printed via the operating system's integrated printing dialogue. Users can return to parameter selection anytime, to create a different physicalization. A detailed sketch of the proposed user interface is shown in Figure 4.2.
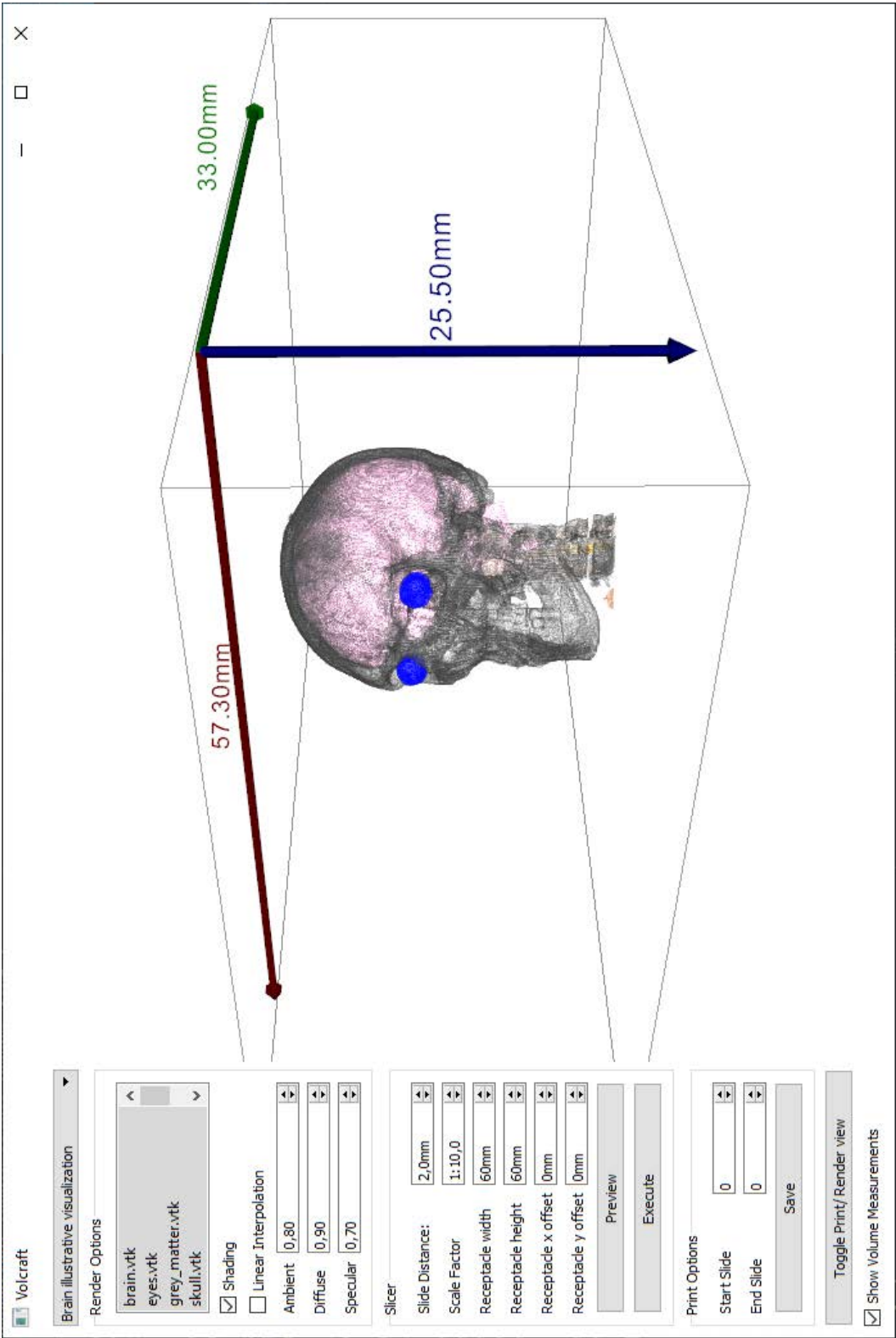
Figure 4.2: *Volcraft* interface. Parameters are depicted on the left side, while the volume rendering is given on the right.

4.2.2 Program Structure

The object-oriented *python* implementation follows a class structure as illustrated in Figure 4.3. Data wrapping for the volume and filter data and pagination, the process of creating the printable pages, make use of abstract classes, serving as an interface for the rendering part. The most important individual parts of the implementation are described in this section.

Volume Data Wrapper

Data wrapping in *Vologram* serves to provide a common interface for different kinds of segmented volume data. The classes `DiscreteVolumeWrapper`, `ContinuousVolumeWrapper`, and `RealisticVolumeWrapper` are implementations of the three different pre-processing concepts introduced in Chapter 3. They implement the `VolumeDataWrapper` interface, to make the individual implementations independent from the rendering stage and to ensure replaceability of the components, for possible future modifications. This component handles data processing and visual mapping, supplying the abstract visual form for the visualization.

The volume wrappers are required by the interface definition, to implement methods to present the available filters, set and reset different filters, and to deliver the processed volume data. The method `getAvailableFilters` returns a list of available filters, corresponding to individual organs or other structures. Through `setFilter`, a filter can be toggled *on* or *off*. This determines if the structure represented by the filter is included in the final data set. Using `getData` the current composition of the dataset, according to the state of the different filters is obtained. The wrappers also determine the appearance of the rendering. Transfer functions have to be provided for this. In the case of the discrete and continuous wrapper classes, these transfer functions are generated based on additional parameters, assigned to the filters. For the realistic wrapper, the transfer functions have to be defined manually. The parameters for this have to be set at compile-time, as the UI has no function for this.

Vologram Rendering

The core of the implementation is the `VologramRenderer` class. Besides supplying the renderers of the volume data for exploration and parameter selection, as well as the preview rendering for the physicalization, it also manages the slide projection, the process of rendering the images of the individual volume cross-section, for the printable pages. It is responsible for the visual presentation component of the rendering pipeline, as well as the presentation on the screen side.

The renderers are created in a *vtk* pipeline, which can include the proposed visual aids from Chapter 3. Besides creating a direct volume rendering of the volume data, with the properties supplied by the data wrapper, a reference frame, representing the receptacle dimensions of the sculpture, as well as reference measurements depicting the sculpture
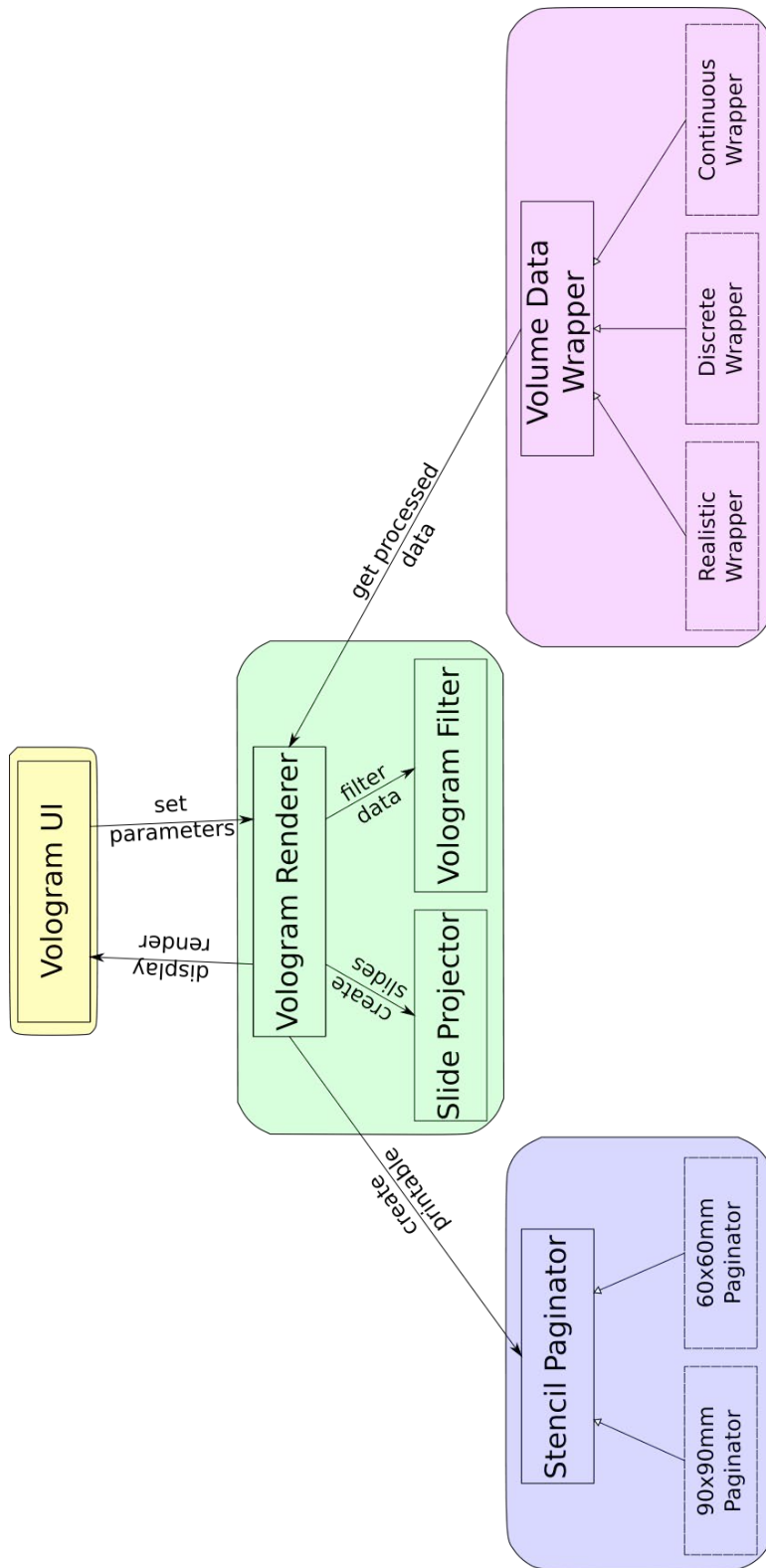
Figure 4.3: *Vologram* program structure. Yellow: the user interface. Renderings are displayed and users alter the visualization and physicalization parameters. Purple: wrapping. Volume data and filters are processed according to different methods. Wrappers implement a common interface and can use different methods for volume filtering. Green: rendering. The volume renderings are created for display on the screen. Volumes are displayed as illustrative renderings or as a preview for the *Vologram* sculptures. Blue: pagination. Printable templates for *Vologram* sculptures are created from processed volume data. Paginators implement the common interface and can use different methods for slide placement.
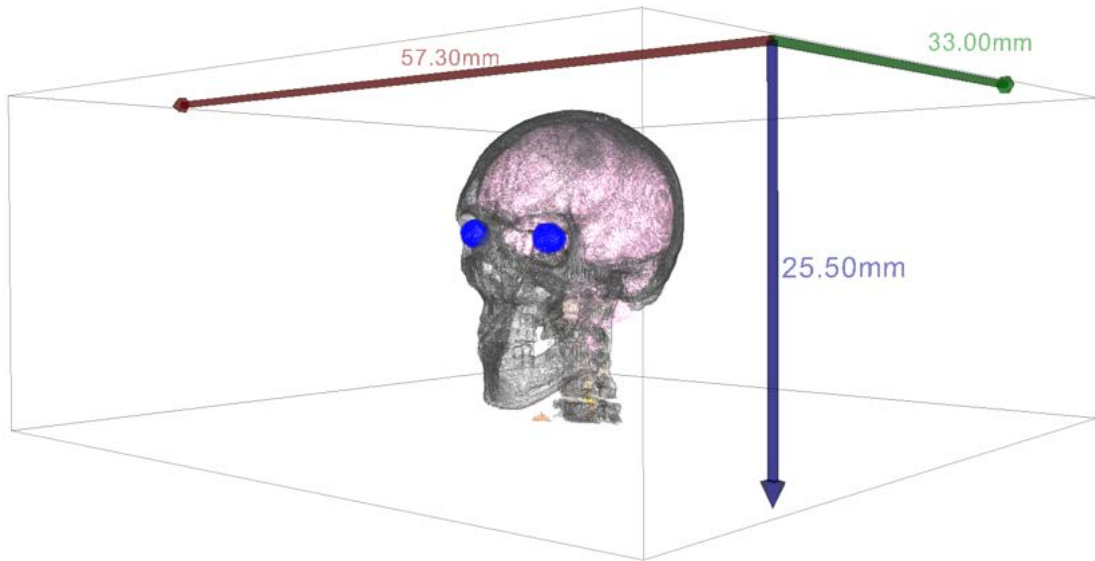
Figure 4.4: Volume rendering, augmented with the receptacle reference frame (grey), and coloured arrows showing the true-to-scale measurements of the data.

scale can be included in the form of coloured arrows. Additionally, when displaying the *Vologram* preview, a filter to create the simulated appearance of the sculpture is included in the pipeline. This is illustrated in Figure 4.4

Vologram Filtering

The class `VologramFilter` follows an implementation similar to other filter components in *vtk* [SML06]. We decided not to use *vtk's* included `ProgrammableFilter` class, for simplicity. The `VologramFilter` takes a slice distance, as well as a transformation matrix as input. The transformation matrix represents the selected viewpoint for the reslice transformation and is interactively selected in the user interface. The filter performs the vologram transformation by combining the reslice transformation and the slice subsampling from the presentation mapping. The output of the filter is a virtual representation of the *Vologram*. Additionally, this component holds an array of 2D volume slices, which can be used as input for the slide projector.

Slide Projector

After the *Vologram* transformations, users can review the selected settings in the preview of the visualization. If they are satisfied with the preview and wish to create a *Vologram* sculpture from it, the `SlideProjector` class is used. The slide projector uses the slide array, created by the `VologramFilter` as input. To create a 2D image from the volume data cross-sections, a separate *vtk* pipeline is required. This pipeline creates a rendering from the 2D data. The distance from the camera to the volume cross section's centre

is the same for every slice. Orthogonal projection is used, as opposed to a perspective projection, to prevent the resulting images from being distorted. A comparison of these two projection modes is illustrated in Figure 4.5. This process is repeated for every subslice. The result is a set of `.png` images, stored in a temporary folder on the hard drive. The images have a resolution of $1\,mm$ per pixel. The resizing of the images, according to the user's chosen scale, as well as receptacle placement is performed by the paginator.

(a) Perspective projection.   (b) Orthogonal perspective.
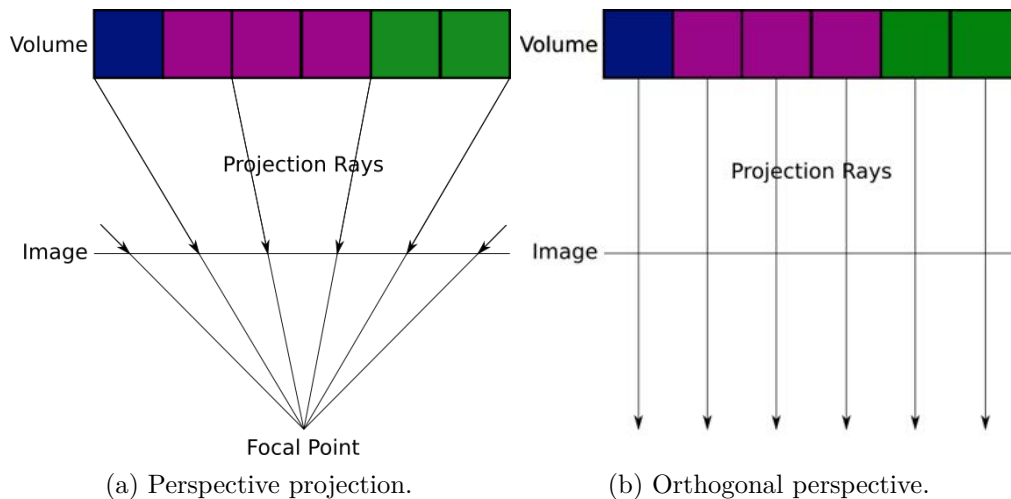
Figure 4.5: Comparison of two modes of projection. (a) Viewing rays converge at the focal point, creating a similar projection result than the human eye. (b) Viewing rays run in parallel.

Stencil Paginator

The paginator is responsible for the physical rendering part on the physical side of the visualization pipeline. The interface `StencilPaginator` sets the prerequisites for classes that create printable templates for the sculptures according to different methods. We implemented two versions of the pagination process, both performing slide placement according to a manually defined page layout. They use the *Python Imaging Library (PIL)*, to process the images created by the `SlideProjector`. Users can determine a start index, as well as an end index for the slides that are to be placed on one page. The paginator also handles the image scale, by increasing or decreasing image sizes, depending on the selected scale. Additionally, if a user selected an offset for the receptacle placement, this is accomplished by positioning the rendered image on the slide. The result is cropped, to prevent overflowing of one image to another slide. Our implementations use manually defined positions and rotations for the slide placement. Cartesian coordinates as well as rotation are defined for each image by hand. With this, we manage to use the paper space optimally, while also adding rectangular tabs placed on top of the slides. Our paginators also places slide indices on the tabs to help with sculpture assembly.

4.3   Physicalization Assembly

To display and interact with *Vologram* sculptures, users need to construct a receptacle. A schematic for this is shown in Chapter 3. In this section, we describe the materials and assembly process we used for our prototype receptacles.

4.3.1   Materials

We use three different materials for the different parts of the receptacle. For the baseplate, we use cardboard sheets of a thickness of around 3 *mm*. Stability is important for the baseplate because it needs to support the spacers. For spacers, we use flat wooden sticks that can be bought at craft stores. We found two different variants, which we both used for different prototype receptacles. The first, shorter version is 75 *mm* long and 5 *mm* wide, The longer version is around 110 *mm* long and 10 *mm* wide. Both versions are about 2 *mm* thick. Lastly, for the slides, we use transparent overhead projector slides in A4 size. The used materials are shown in Figure 4.6. The materials for the receptacle components can be substituted by users, depending on available means. This only results in the necessity to adjust the transformation parameters for the physicalization.

Figure 4.6: Materials used for the construction of the *Vologram* receptacle and slides.

4.3.2 Construction

We want to display as much image space as possible, without endangering the stability of the *Vologram* sculptures. This led to two different receptacle designs, each using one variant of the sticks for spacers. The smaller variant is designed for quadratic slides of a size of $60\,mm \times 60\,mm$, the taller one for $90\,mm \times 90\,mm$. Using the thickness of the sticks as a reference, we decided on a fixed number of spacers for each receptacle. We then used a box-cutter to remove two rectangular parts of the baseplate, as wide as the spacers and as long as the total number of spacers multiplied by $2\,mm$. We decided to use an additional layer of cardboard for the baseplate for additional stability. Between the far ends of the rectangular holes, we left enough space to fit one slide exactly. We then inserted the required number of spacers into the holes, stacking them to ensure an inter-slice distance equal to their thickness. Coincidentally, the taller sticks were sold in different colours. We decided to use the colours in alternating succession, to give users a better indication for slice placement. The prototypes can be seen in Figure 4.7
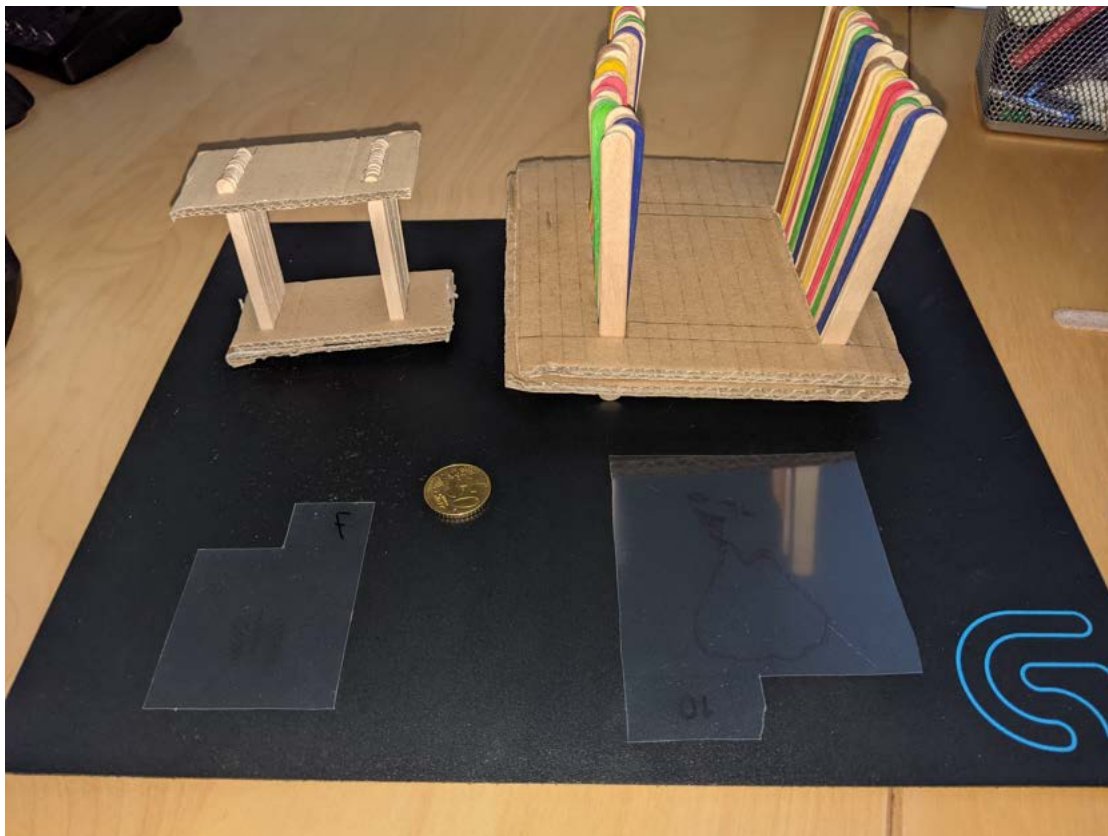
Figure 4.7: The two receptacle prototypes with their respective slides. The small version has a cardboard cover for additional stability. Spacers of different colours help with slide placement in the taller version. Compatible slides are shown in front of the respective receptacles for reference.

Results

After implementing *Vologram*, we created multiple sculptures from different datasets, with different parameters, to explore the application's potential and test its limitations. For the input data for all prototypes, we use the processing procedure on the *Visible Human* segmented inner organ data. The *Voxel-Man* segmentation provides two different areas with separate segmentations: the head and the torso area. We also conducted a study to evaluate the performance and user experience aspects of the physicalization concept in comparison to computer visualization. This chapter summarizes the results of this.

5.1 Demonstration of Physicalizations

This section describes different realizations of *Vologram* sculptures. Different processing methods and parameters were employed in the creation of the physicalizations. Furthermore, multiple combinations of parameters are explored, and material differences are examined.

5.1.1 Skull Dataset

In the course of this thesis, we always use the example of a frontal perspective rendering of a human skull. With a complete implementation of our workflow, we are now able to present the steps in creating the corresponding *Vologram* from start to finish.

The head region is one of the two distinct datasets provided by *Voxel-Man*. We defined a volume wrapper with the necessary filters, assigning the bone structures grey, the brain pink, and the eyes blue as colours. The respective opacities for each structure are mapped to the interval $[0.5, 1]$. The viewpoint is moved to create a similar appearance to the illustration we used in the previous chapters. Figure 5.1a shows the resulting volume rendering.

Parameter	Value
Receptacle	$60\,mm \times 60\,mm$
Rendering method	Continuous illustrative
Scale	1:5
Slice distance	2 mm
Vertical receptacle offset	0 mm
Horizontal receptacle offset	0 mm

Table 5.1: Parametrization of the skull in *Vologram*

(a) Illustrative rendering of the skull.   (b) *Vologram* preview of the skull
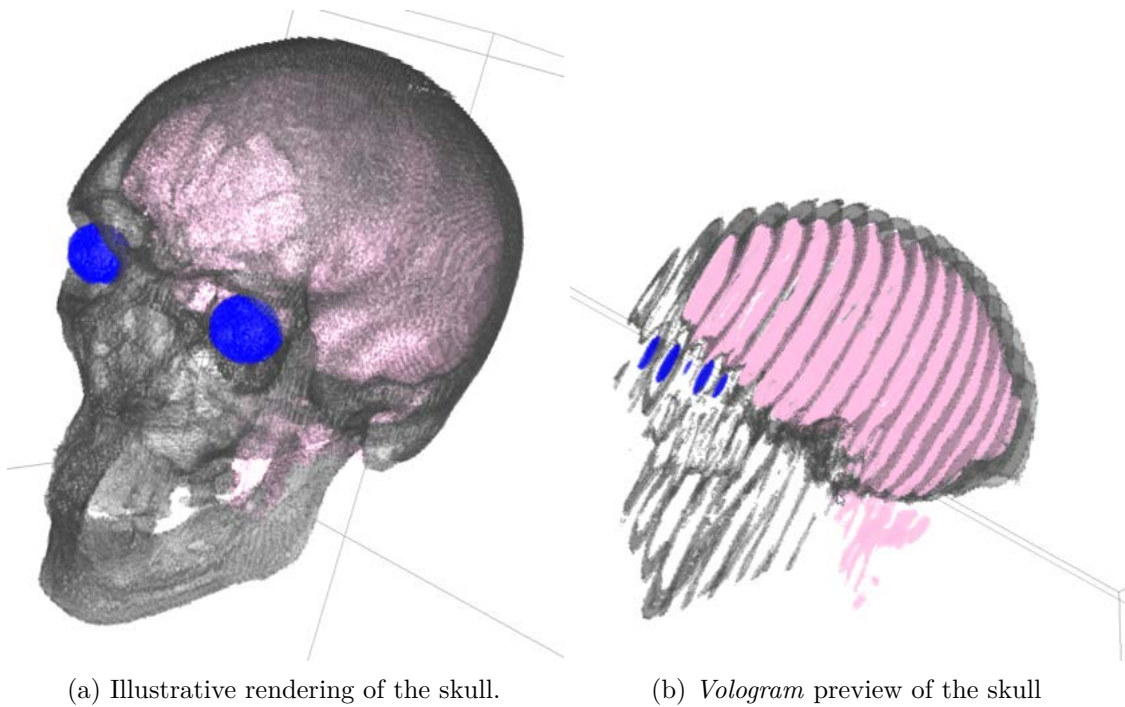
Figure 5.1: Renderings during the process of creating a skull *Vologram* sculpture. (a) Illustrative volume rendering of the data. (b) Preview rendering for the *Vologram* transformation.

To recreate the appearance of the illustrations we use in the previous chapters, we selected the skull including the jawbone, the brain and the eyes for display. The head without torso fits the small receptacle at a scale of 1:5, maximizing the area of coverage for the given receptacle dimensions. A full list of parameters can be seen in Table 5.1. Figure 5.1b depicts the preview visualization for the selected parameters. Figure 5.2 shows various *Vologram* transformations, to exemplify other possible viewing directions and outcomes.
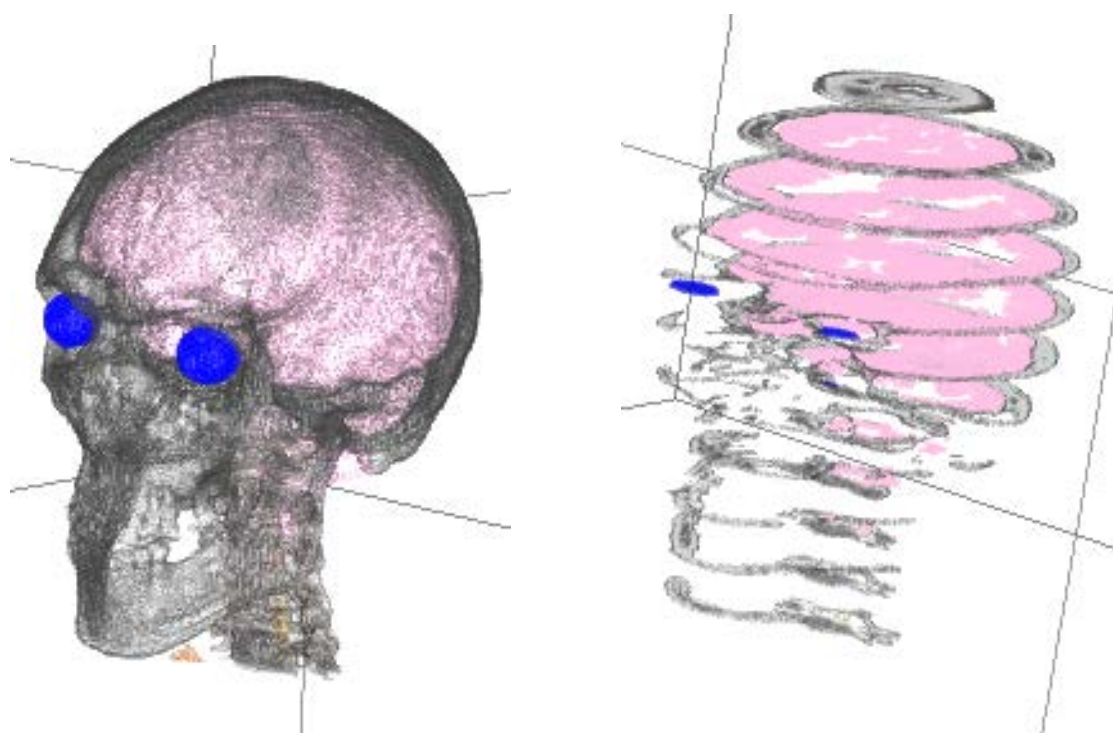
(a) Illustrative rendering of a skull.

(b) Axial *Vologram* transformation of a skull.
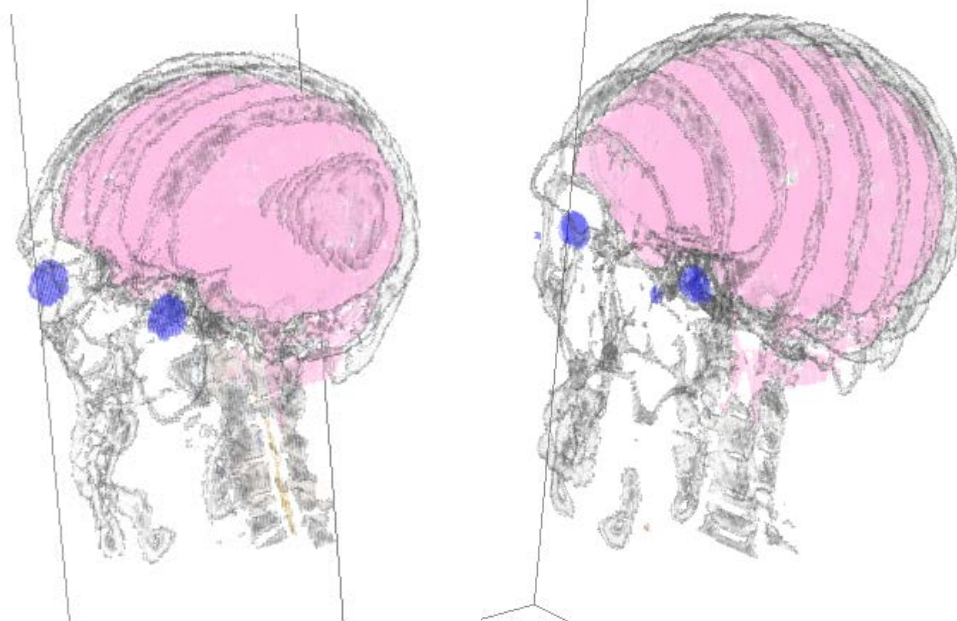
(c) Lateral *Vologram* transformation of a skull.

(d) Sagittal *Vologram* transformation of a skull.

Figure 5.2: *Vologram* transformation of the skull dataset along different directions, viewed from a similar angle.
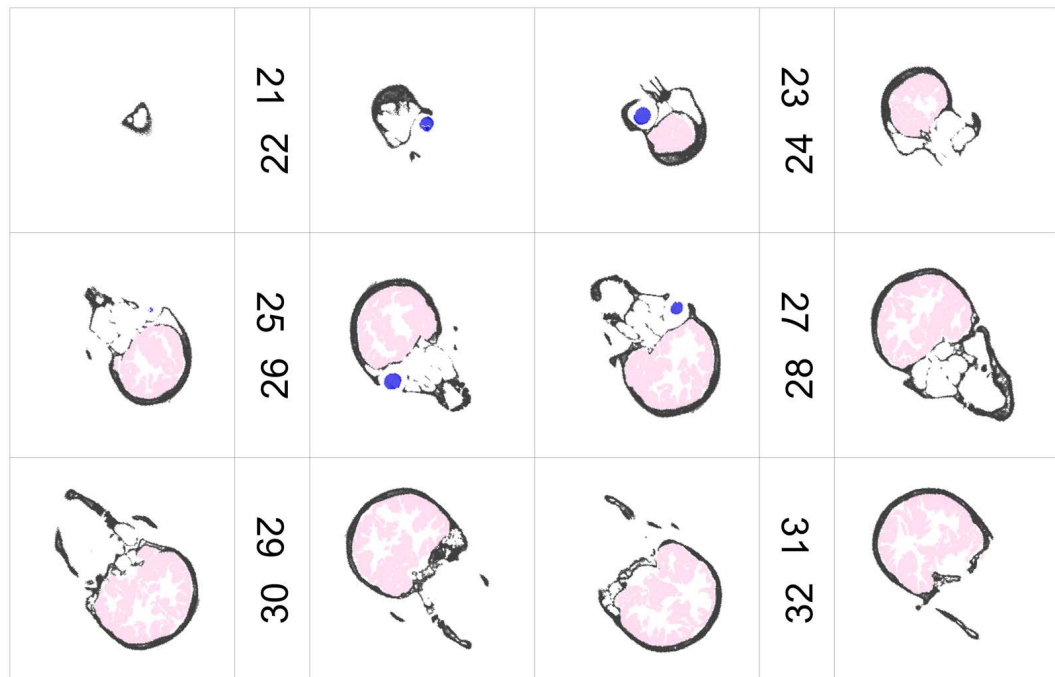
Figure 5.3: Paginated result for the skull *Vologram*. The first non-empty slide has number 21. Slides are arranged head-to-head to save space for the tabs with the numbers inbetween.

After selecting the parameters for the *Vologram*, we used the application to create the printing template. We used the paginator class for $60\,mm \times 60\,mm$ images, which fits 12 images to one page. This led to two pages with a total of 19 slides. The first page is shown in Figure 5.3. The *Vologram* transformation creates a large number of empty slides due to the reslice transformation because the reference grid has to be enlarged for the volume data not to be cropped during the transformation. The application allows users the manual selection of the starting slide index for pagination to avoid creating empty pages. The pagination for the small receptacle arranges subsequent slides along the upper boundary. Tabs are added between the slides to show the numbering.

To demonstrate material differences in available overhead projector slides, we used two different variations. The first is suitable for photocopiers. This is the cheaper variant, costing about 20 € per 100 pages. It can be printed on with laser printers as well, however, the laser printer we had access to only works in black and white. The second variant is printable with inkjet printers but is more expensive at 16 € per 10 pages. We printed the first 12 slides, which corresponds to the first page, twice, once in colour with an inkjet printer and once in monochrome with a laser printer. Figures 5.4a and 5.4c show the

monochrome version, while Figures 5.4b and 5.4d show the coloured version. Besides the fact that the colours help to discriminate between the anatomical structures, additional detail can be seen comparing the two versions. The inkjet sheets have a more opaque surface than the laser sheets. This leads to the visibility of structures on slides behind multiple other sheets suffering more on the inkjet sheets. Using a colour laser printer, one can create *Vologram* sculptures with more slides. The visibility issues can be mitigated by introducing a white background, as well as viewing the sculptures against a light source.

5.1.2 Upper Torso Dataset

The second dataset provided by *Voxel-Man* is a detailed segmentation of the male human torso. We processed the dataset to create filters for the most prominent anatomical structures, like major organs and the skeleton. This section serves to provide an example for filter selection and receptacle placement. Additionally, we compare two distinct rendering techniques.

For this prototype, we excluded the colon, small intestine, and skin to prevent upper torso organs from being obscured. We created two renderings of the same area, with different filtering techniques. The first example uses the realistic volume wrapper, to create a realistic appearance for the outcome. For this, we supply a piece-wise linear volume transfer function [PB13]. The second example uses the discrete illustrative data wrapper, where we provide distinct colours and opacities for each structure, to create a more abstract view of the data [PB13]. Figure 5.5 shows a comparison of the renderings using the different mapping procedures.

For the *Vologram* transformation, the viewing angle from Figure 5.5 was used. We selected the bigger receptacle to fit more of the image on the slides. This physicalization should serve to create an overview of the upper torso organs. To prevent occlusion through the bowel structures, these were excluded using filters. We again used a scale of 1:5 for size. This meant also, that an offset for the rectangle to contain the relevant region had to be selected manually. To reduce the number of slides we increased the inter-slice distance to $4\,mm$. This was meant to prevent the material based occlusion discussed above. The full parametrization can be seen in Table 5.2. The receptacle placement for this is shown in Figure 5.6. It was performed analogously for a realistic and illustrative rendering.

For the larger receptacle, a different paginator class is used. The placement of $90\,mm \times 90\,mm$ slides permits only 6 slides per page. The paginator aligns three images in a row side-by-side. The remaining images are rotated and placed side-by-side at the bottom half of the page. Between both rows, a space for the numbered tabs is left. The pagination with the parameters selected for this *Vologram* sculpture results in 14 slides, arranged

(a) Frontal view monochrome.

(b) Frontal view coloured.

(c) Rear view monochrome.

(d) Rear view coloured.

Figure 5.4: Two variants for the skull *Vologram*. The same printing template was used with two different types of overhead slides and different printers.
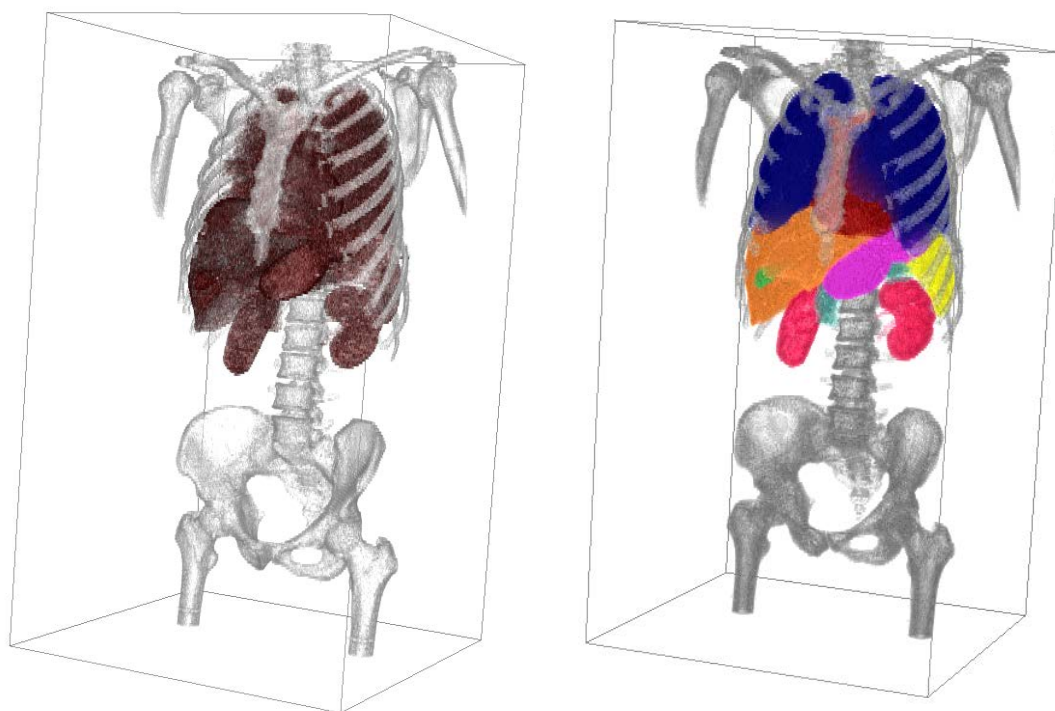
(a) Realistic rendering. (b) Illustrative rendering

Figure 5.5: Comparison of different rendering techniques, defined by the data wrappers. (a) Anatomically realistic direct volume rendering, using a piece-wise linear transfer fucntion. (b) Illustrative volume rendering, using a transfer function generated according to the given parameters. Opacities and colours are assigned to separate structures.

Parameter	Value
Receptacle	$90\,mm \times 90\,mm$
Rendering method	Discrete illustrative and realistic
Scale	1:5
Slice distance	4 mm
Vertical receptacle offset	30 mm
Horizontal receptacle offset	20 mm

Table 5.2: Parametrization of the upper torso *Vologram*

(a) Realistic rendering.

(b) Illustrative rendering.
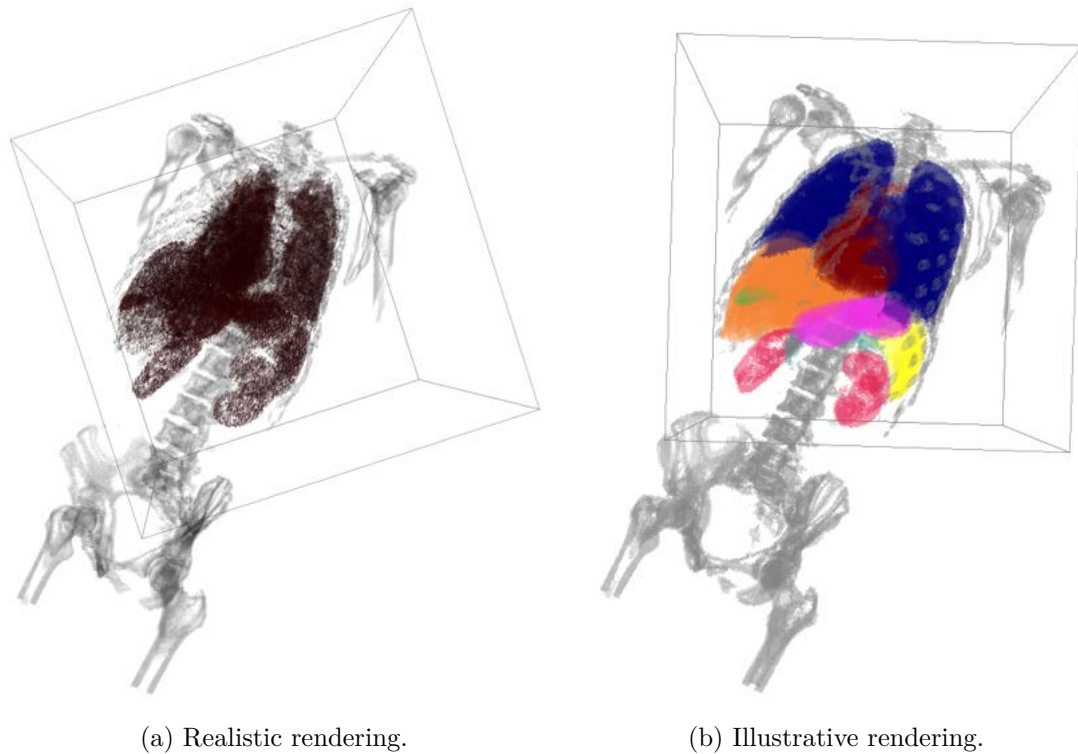
Figure 5.6: Receptacle placement for the upper torso *Vologram*. Frame position is moved to fit the upper torso area.

over three pages in total. Figure 5.7 shows the first pages resulting from pagination for the realistic and illustrative versions of the upper torso *Vologram*.

We constructed both the realistic and the illustrative *Vologram* for the upper torso region. The results show multiple problems with the realistic version of the rendering. Figures 5.8a and 5.8c illustrate these. While in the rendering, through the better resolution, the separate structures can barely be told apart (see Figure 5.5a), this becomes even more difficult in the *Vologram* sculpture. Especially, bordering structures tend to blend into each other, as can be seen in Figure 5.7, where slides 11 to 13 of the left page show this problem. Additionally, the slides indicate that parts of some organs with higher local density are mapped to colours corresponding to higher density areas such as bones. This can be mitigated by altering the transfer function. Meanwhile, the illustrative version of the *Vologram* solves this problem, by using the filter specific transfer functions. Figure 5.7, slides 11 to 13 of the right page show that the different colours assigned per filter simplify inter-organ discrimination. The resulting sculpture, shown in Figures 5.8b and 5.8d, illustrate this as well. Both sculptures were constructed with the inkjet sheets.
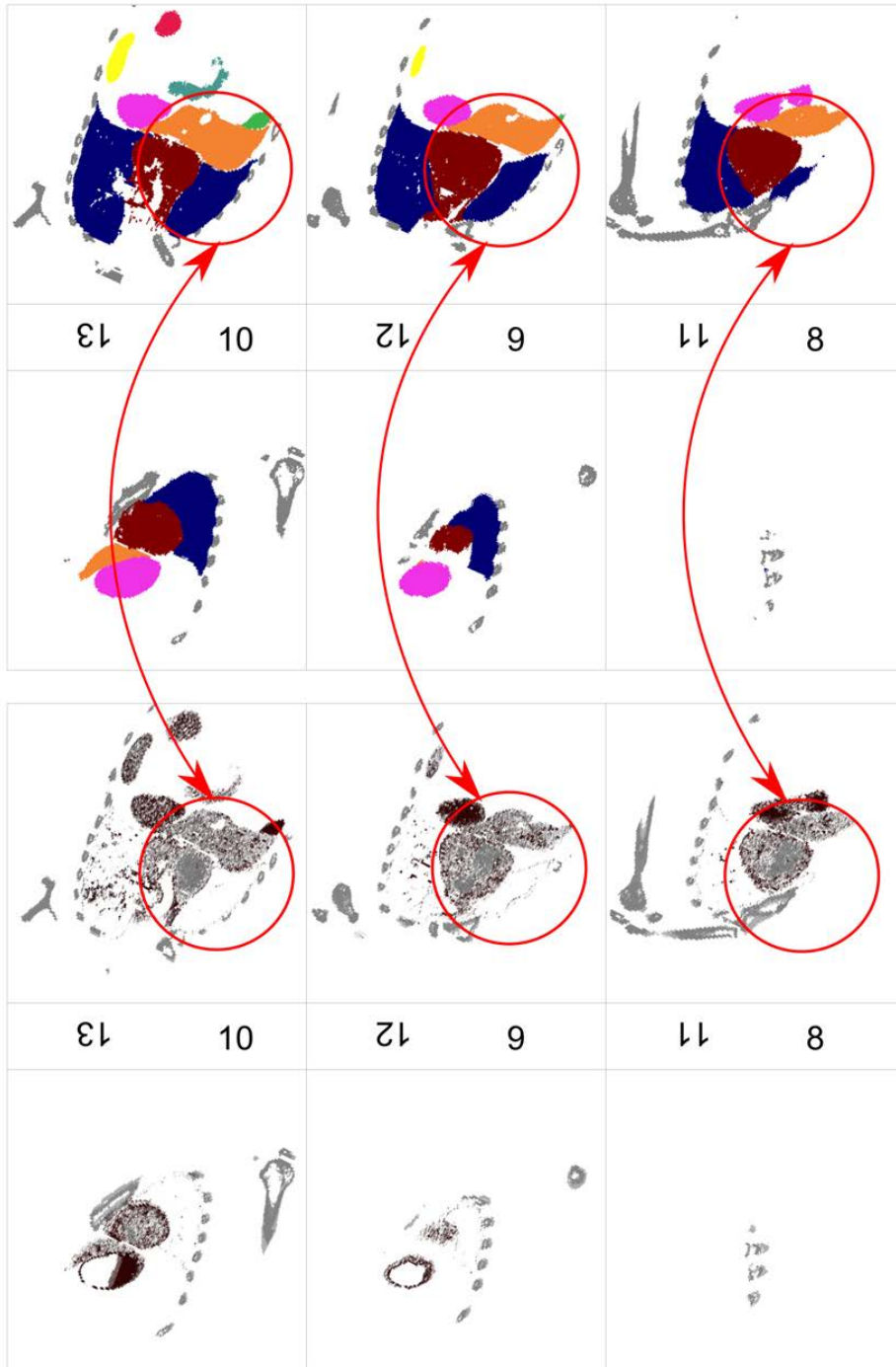
Figure 5.7: Left: First template page for the realistic version of the upper torso *Vologram*. The realistic transfer function is not specific to separate organ structures, higher intensity values of *soft* organs are mapped to the same colour as bone. This can be seen in the bottom row (Slides 11-13), liver and heart are assigned the same colour as bone. Right: First page for the illustrative version. Transfer function and organ discriminability are massively improved through the filter specific colour assignment. Corresponding areas are marked in red.

This leads to the same obstruction effect as in the skull sculpture. Again, this effect is mitigated by placing the sculpture in front of a white background or viewing it in front of a light source, as shown in Figure 5.9a. Alternatively, for more dense sculptures, the inter-slide distance can be increased to improve the visibility of more occluded parts. This is shown in Figure 5.9b, by the example of the upper torso sculpture with half the slides removed.

5.2   Comparative Evaluation

To evaluate the developed concept we performed a small study with 10 laymen participants. The following section serves as an overview of the study design and results.

5.2.1   Study Design

Parameter	Value
Receptacle	$90\,mm \times 90\,mm$
Render method	Discrete illustrative
Scale	1:10
Slice distance	4 mm
Vertical receptacle offset	0 mm
Horizontal receptacle offset	0 mm

Table 5.3: Parametrization of the torso *Vologram* sculpture used for the evaluation

In the course of this thesis, we aimed to investigate the possible advantages of physicalizations over screen-based visualizations in the field of layman anatomy education. For this comparison, we created a visualization and physicalization that are comparable in the following aspects:

1. They use the same source data, without providing filtering methods.

2. They use similar optical cues, such as colours and opacities.

3. They only use interaction methods that are inherent to their nature.

Volcraft, by design, allows users to create physicalization from visualizations of medical data. This means that after the creation of the printing template, the source data can not be filtered. The exploration screen of *Volcraft* serves the purpose for the comparable visualization. The physicalization used for the evaluation study is one created from the shown source data set. The sculpture used for the study is shown in Figure 5.10b. It shows a frontal view of the torso without excluding any organ, in scale 1:10. Transformation parameters are shown in Table 5.3. Participants were asked not to use filtering methods
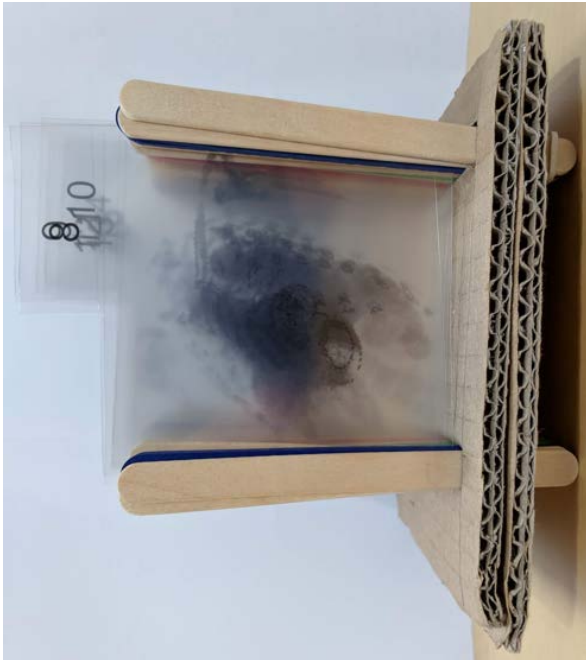
(a) Frontal view realistic *Vologram* sculpture.

(b) Frontal view illustrative *Vologram* sculpture.
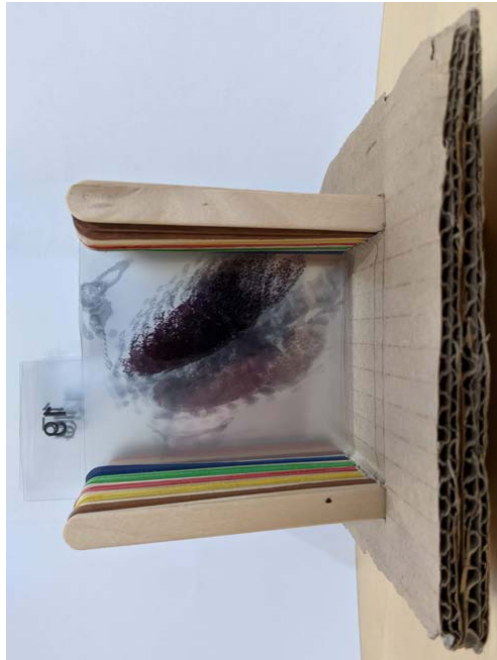
(c) Rear view realistic *Vologram* sculpture.

(d) Rear view illustrative *Vologram* sculpture.

Figure 5.8: Realistic and illustrative *Vologram* sculptures of the same view on the upper torso.

(a) Backlit upper torso sculpture.

(b) Downsampled upper torso sculpture

Figure 5.9: Two methods to improve the visibility of *Vologram* sculptures. The original sculpture is shown in Figure 5.8b (a) Viewing the sculpture in front of a light source improves the visibility of structures in slides further to the back of the figure. (b) Removing every second slide reduces the image resolution along the viewing axis, but structures in the back part of the volume can be seen better.

provided by *Vologram* and we observed them to ensure this was kept. They were still allowed to manipulate the viewpoint of the visualization with a computer mouse, using the *trackball camera* mode, provided by the render window of *vtk*. The initial view of the visualization provided to the participants can be seen in Figure 5.10a. The participants were encouraged to touch and manipulate the physicalization as much as they desired.

We chose to compare the two modalities in the aspects of user performance **(UP)** and user experience **(UX)** as categorized by Lam et al. [LBI+11]. For the user performance evaluation, we use controlled experiments and measure error rates and task completion times of users with the visualization compared to the physicalization. This serves to indicate if either method provides significant advantages through their inherent properties. The user experience evaluation takes the form of interviews and a questionnaire, which should give insight into how users are engaged by the two different modalities.

For the user performance evaluation, we designed a set of tasks for the participants to complete. The participants were asked to find one specific organ, using either the

(a) Illustrative visualization.

(b) Vologram sculpture.
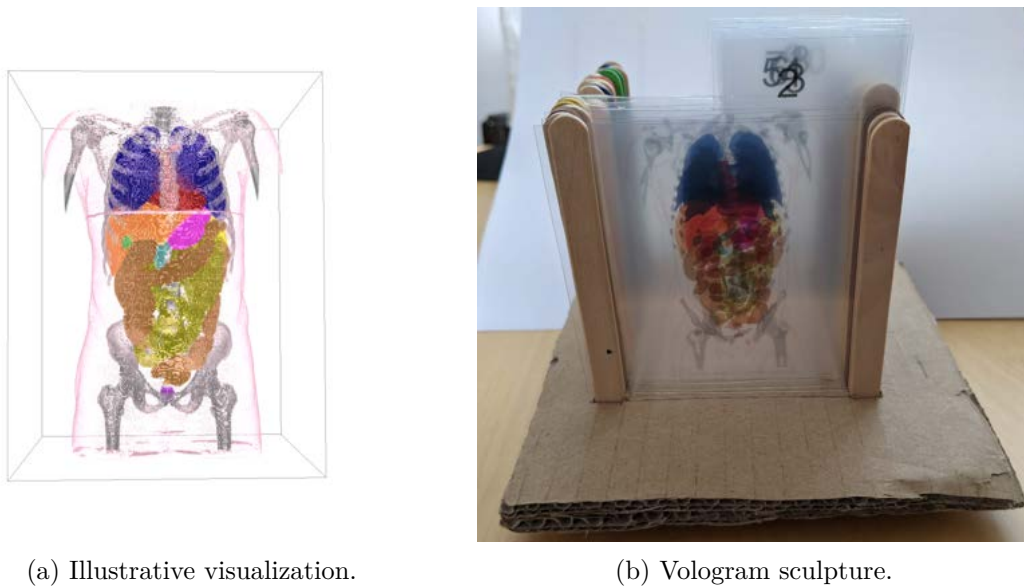
Figure 5.10: Visualization and physicalization used in the evaluation study. Both display the same source data. The visualization (a) serves as the source for the physicalization (b).

physicalization or the visualization. After locating the organ in the respective aid, the participants had to point out the location on a different visualization, created from the same dataset. When the participant located the organ correctly, the timer was stopped, otherwise, we counted an error and continued the clock until the organ could be located successfully. The order of the tasks was randomized and the order of the modalities was alternated, to combat familiarization effects. The setup can be seen in Figure 5.11. We chose organs from the human male torso. The selection was done manually, avoiding more obvious choices like the heart or the lungs, while still requiring the organs to be of a certain size, so they could be located without too much trouble. An additional criterion for the selection was that the viewpoint had to be manipulated to find at least some of them and to test the interaction capabilities of the two modalities. Based on those criteria, the following six organs were subject of the tasks:

- Gallbladder

- Kidneys

- Liver

- Pancreas

- Spleen

- Stomach
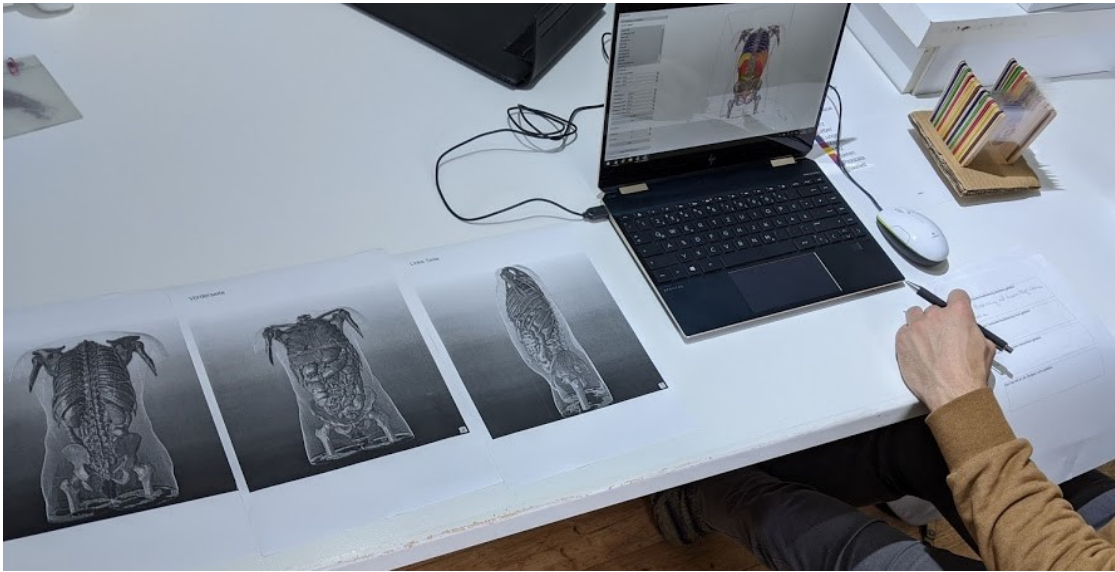
Figure 5.11: Study setup used for user performance evaluation. The participant sits in front of the visualization and physicalization and is asked to complete tasks using either in alternating order. The colour code serves as a reference for both methods. The visualization to point out specific organs can be seen to the left, in black and white.

As another important aspect, next to performance, we investigated user experience. Physicalizations are often employed because they can engage people in a different way than screen-based visualizations. We consider the user experience with the physicalization compared to the visualization an important part of this evaluation. First, the questionnaire serves to collect data about the study demographic such as age and occupation. Then with a short questionnaire, the participant is asked to rate the following statements on a five-point Likert scale [Lik32] from "Strongly Disagree" to "Strongly Agree":

- I am experienced in using computers.

- I have a thorough knowledge of human anatomy.

- I enjoy working with computers.

- I found the computer visualization appealing.

- I found the physicalization appealing.

- I preferred using the physicalization over the visualization.

- The visualisation helped in completing the task.

- The physicalisation helped in completing the task.

Additionally, the questionnaire contains the following open text questions about the user's experience with both concepts:

- What did you like about the visualisation?

- What did you not like about the visualisation?

- What did you like about the physicalization?

- What did you not like about the physicalization?

At the end of their respective trial, we asked users in detail about their experience in the study in a freeform interview. The results are summarized in the following sections.

5.2.2 Study Demographics

Participant	Age	Gender	Occupation	Optical Aid
1	28	Female	Software Developer	Yes
2	56	Female	Government Employee	Yes
3	77	Female	Pensioner	Yes
4	59	Male	Warehouse Manager	Yes
5	36	Male	Software Developer	No
6	27	Male	Mechatronics Engineer	No
7	60	Male	Chemist	Yes
8	36	Male	Camera Operator	No
9	30	Male	Salesperson	No
10	28	Female	Humanities Student	No

Table 5.4: Study Demographics

The test group consisted of 10 people, native German speakers between the Age of 27 and 77. All written material was translated to German for this purpose. No children took part in the study, as this would require a different study design and be supported by children educators, which was not possible at this time. The mean age of the group was 43.7 years, the median lay at 36 years. Four participants are female, six male. Five people wear glasses and five do not require optical aids. None of the participants works in an occupation inside the medical field. Two participants were software developers and two additional participants claimed to have above-average experience with computers. Details about the study's demographics can be seen in Table 5.4.

5.2.3 Results and Discussion

The study was conducted as stated above. Trials took between 15 and 20 minutes per participant and concluded with a short debrief and interview about the participants'

experience. The results for the user performance, as well as the user experience evaluation, are summarized below.

User Performance

Overall the total results for completion times were less than 10 seconds apart, in favour of the visualization. If considered per individual organ, it can be observed that for all organs except the kidneys, the completion time is shorter with the visualization. This might be explained due to the location of the kidneys, being on the back of the body, which can be easily observed by viewing the sculpture from the back. In contrast, the visualization had to be rotated using the mouse control to make the kidneys visible. About half of the participants reported difficulties with the mouse-controlled camera. One participant, in particular, had never used a mouse before. This made it considerably harder for them to rotate the camera compared to the other participants, which were all more experienced with computers. An example to the other extreme was the task to find the spleen, which is located on the left side of the body. Participants that had to use the physicalization to locate it using the sculpture, could not easily locate the organ. This was caused by the static nature of the physicalization. Displaying a frontal view of the body, it could be viewed easily from the front and back, but not from the sides. Multiple participants report that they had to remove individual slices of the sculpture to find the spleen, but had difficulties reassembling it thereafter, which cost them additional time. Considering the error rate, users made more errors, in general, using the physicalization. This can be partly explained by the fixed scale, as compared to the visualization. The screen-based representation allowed the participants to zoom in and out, which they often used to mimic the scale of the reference visualization, therefore making it easier for them to find similar structures. One participant confused the liver repeatedly with parts of the colon while using the sculpture. Overall the standard deviation was relatively high for all tasks, as well as around 30 seconds for both modalities in total. This points to a very different level of understanding of anatomy among all participants. The user performance results can be seen in Table 5.5 and is illustrated as boxplot in Figure 5.12.

User Experience

To evaluate user experience, we observed the study participants during the trials, as well as did individual interviews and handed out a questionnaire afterwards. The first three questions of the inquiry, where thought to shed light on the average computer affinity, as well as anatomy knowledge of the participants. Most participants reported having experience with computers, only very few claimed otherwise. This is exemplified by the median answer to this question which is "strongly agree". However, the study population was evenly divided by the question if they enjoyed working with computers. Here, naturally, the participants with computer-affine occupations, like software developers, answered strongly positive, while some of the participants with more hands-on occupations, as well as the camera person and the pensioner, answered negatively. This was, however, not strongly reflected by the question which of the modalities they prefer.

Organ	Modality	Avg	Med	Std	Errors
Gallbladder	P	50.00	59.00	36.27	1
	V	23.67	16.00	16.86	1
Kidneys	P	20.13	19.50	13.31	1
	V	01:09.00	01:09.00	01:12.12	0
Liver	P	43.33	35.00	18.93	5
	V	17.71	10.00	14.35	0
Pancreas	P	35.40	19.00	28.58	2
	V	15.60	09.00	12.28	0
Spleen	P	58.25	45.00	47.88	0
	V	39.83	27.00	40.42	1
Stomach	P	52.00	25.00	48.51	3
	V	25.71	20.00	16.87	2
Total	P	27.50	40.23	32.41	12
	V	19.00	27.67	28.34	4

Table 5.5: User performance results. Modalities are P for physicalization and V for visualization.

Most participants reported preferring the computer visualization. Only one participant answered to prefer the physicalization, reporting that he *"likes to work with [his] hands"*. None of the participants had seen a 3D medical visualization before being in the study, leading to a positive novelty effect. All of them reported finding the visualization very appealing, while one participant, notably a software engineer, did report of not finding the sculpture appealing. A similar tendency can be seen with the result of the questions regarding the helpfulness of the respective modalities.

In the interviews, as well as in the informal feedback, many participants complimented the colouration of both modalities, which helped them to discriminate between the sculptures. It was stated from different participants that they liked the handy size of the sculpture, as well as the playfulness of the concept. One participant remarked that they would like to show the sculptures to their parents. Another participant, who has young children, said that *"it would be a nice tool for children, they use the computer too much anyway"*. On the negative side, it was often stated that the sculpture seemed a little unstable and that a good view is harder to achieve than on the screen. For the visualization, many participants reported positively about the concept. Participants that managed it well, liked the freedom of movement for the camera controls in the visualization. It was remarked by one participant that he would have liked a slicing mechanism for the visualization, to make it easier to see inside the structures, after seeing the way the physicalization was built. Some participants reported difficulties with the mouse controls. The findings from the questionnaire are presented in Figure 5.13.
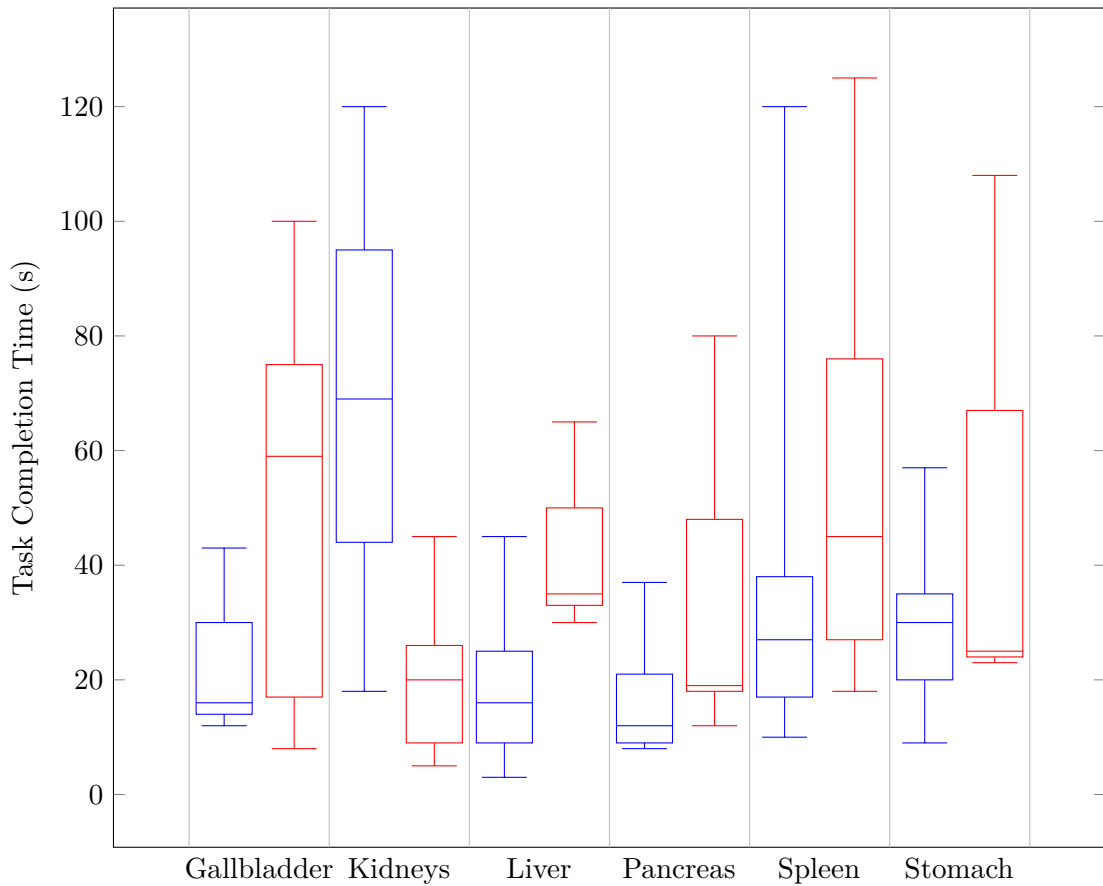
Figure 5.12: User performance per organ statistics. Blue: Visualization performance, Red: Physicalization performance.

Discussion

While the results of the evaluation do not show many advantages of the physicalization over the visualization, we made some interesting discoveries. Our bias was relatively high. We did not expect participants having difficulties finding the locations of some organs that we had naturally learned about in the course of our studies. As the developers of the physicalization as well as the visualization, we had no trouble in handling either. Participants that had never seen a physicalization, had more difficulties with that. It was, however, a positive experience for all participants in an educational sense. Many participants indicated an interest in the results of the tasks, being surprised by the different organs' locations.

We see a big potential for both modalities for laymen education. Both modalities can complement each other fairly well and the addition of the hands-on approach can engage more people than a visualization can on its own. Statements from different
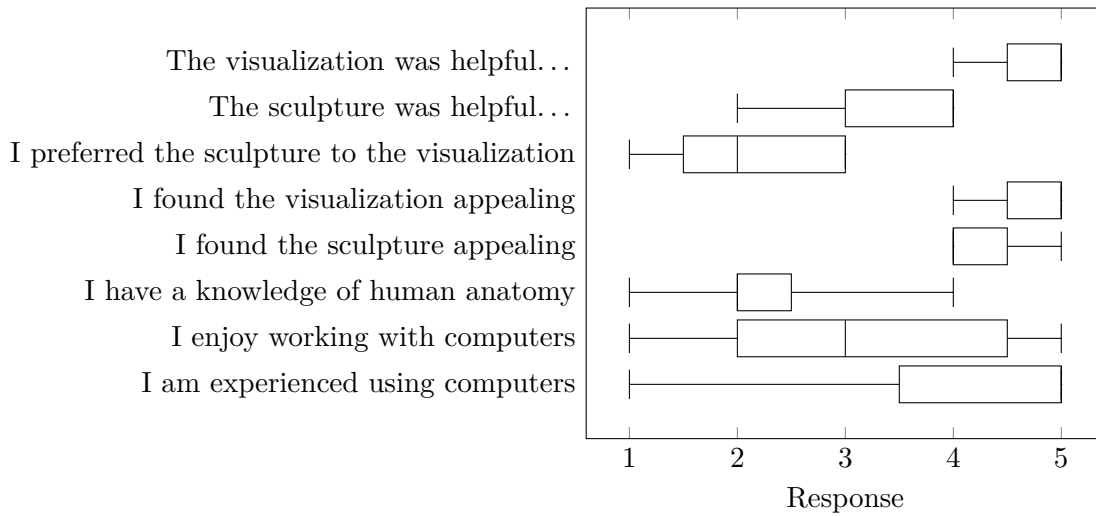
Figure 5.13: Questionnaire response. 1...Strongly Disagree, 5...Strongly Agree

participants also point to an application in children education. While during the time of writing of this thesis we did not have access to a group of children in a suitable age, we think it would be interesting to assess the complimentary use of sculpture and visualization with children around the age of ten and above. Letting children construct their custom physicalizations might also further their engagement in the topic [NMA12].

The study also pointed to a potential use in communicating medical information to elderly patients. One participant stated that doctors confused her understood when they tried to communicate to her the circumstances of their gallbladder removal, using conventional medical images. They reported that with the aid of a 3D method, they would have understood things better. This provides an opportunity for improving patient education, and in turn, their experience during treatment [HL10].

In terms of meeting our requirements, the study shows that the needs of the target group for medical education were sufficiently addressed by *Volcraft* as well as *Vologram* sculptures **(R1)**. Data selection was not part of the study, but the user interface of *Volcraft* neither uses difficult language nor does it require expert visualization or medical knowledge to create meaningful visualizations. It provides an ample amount of pre-processed data, ready for laymen to engage with **(R2)**. The shape and relative positioning of organs in the human body proved to be an interesting and engaging lesson for the participants **(R3)**. Real medical volume data was presented to medical laymen in a way meaningful to them **(R4)**, in both an affordable and easy to construct **(R5, R6)** physical form, and a comparable screen-based visualization **(R7)**.

Conclusion

Concluding this thesis, this chapter summarizes the lessons learned in the course of the work by recounting the contributions that were made. For this we take a look at the research questions we formulated in Chapter 2, and examine how we were able to answer them. Lastly, we will present the current limitations of our approach and list directions for possible future enhancements.

6.1 Summary

Physical representations of data are finding their way into the field of information visualizations for several reasons. Appealing representations of abstract concepts, aside from screen representations [Moe08], have unique ways to engage a layman audience [ZM08]. At the core of the work resides the question of how physicalizations can be used to further the anatomical education of medical laymen **(Q1)**. To find an answer to this, we researched the current state of the art in physicalization of medical data. During this, we found multiple approaches that attempt to use the concept of physicalization for educational purposes. Many concepts for the application of 3D printing technology can be found in this field. To introduce physicalizations to the general public, which often do not have access to expensive technology, like 3D printing, we needed to find cost-effective alternatives. At the moment, only a handful of concepts exist for the application of 2D [SB16], and 3D sculptures for medical education [RGW20]. Due to this, we decided to create a new concept for the creation and construction of physicalizations with means available to a broad audience.

To explore different approaches, we introduced three different concepts to create physical anatomical sculptures out of medical volume data. We especially paid attention to the fact that such a concept should be feasible and affordable to construct for a medical layman audience **(Q2)**. Our three concepts, the *Slicer*, *Cuber*, and *Vologram* are based

on this prerequisites. Taking inspiration from an architectural design concept, the *context model* [HW17], the *Slicer* makes use of the appearance of low-axial-resolution volume data. The *Cuber* concept stems from a similar sculpture, made by a software engineer from his medical imaging data [Fra]. Both of those two initial designs possess some flaws, which we address with the *Vologram* concept. We designed the *Vologram* pipeline, which allows layman users to create personalized physical sculptures, cheaply and quickly from real medical volume data. Similar to previous approaches [RGW20, SB16], we make use of thin, transparent material to create representations of 3D volume data. As opposed to the direct volume rendering approach, as used in the *Slice and Dice* concept, our illustrative renderings represent different structures in different colours. Additionally, through using only parallel slides, *Vologram* sculptures have an optically more coherent appearance, without interrupting the users perspective. The materials used in the workflow are cheap and widely available. Construction of the models takes as little time as possible, due to the possible reuse of the receptacle part. The modular, slide-based appearance of *Vologram* sculptures allows users deeper insight into the human body than a solid 3D model. We present multiple different pre-processing steps for volume data to achieve a variety of different appearances. With this, we contribute to the field of educational medical visualization suitable for layman education, by adding the benefits of physical models to screen-based visualization. This is furthered by customizability of *Vologram* sculptures and the hands-on, do-it-yourself approach, which can add additional engagement to such a concept [NMA12]. Volume data from the *Visible Human* [ASSW95], segmented by the *Voxel-Man* project [AJH+15], is processed in *MeVisLab* to be a suitable source as input data for the workflow. To facilitate interactive and easy parameter selection, and to provide a preview of the outcome of the process, we developed *Volcraft* as a stand-alone *Python* application. Multiple different pre-processing techniques, as well as parameter and material combinations, are explored, to demonstrate the capabilities of *Vologram*.

In the past, different forms of physicalizations, medical or otherwise, have proven to be a worthy addition to screen-based visualizations. To examine the capabilities of *Vologram* sculptures, we performed a study with the target group **(Q3)**. The participants are adult medical laypersons, of a large age variety, with different levels of computer skills. We focused on the evaluation of user-performance and user-experience [LBI+11]. With task-based time measurement, questionnaires, and interviews we examined the impact of *Vologram* sculptures, compared to equivalent screen-based volume renderings. We found that, while most computer-savvy participants navigated a screen-based volume render with ease, people with little computer experience profit from the natural interaction capabilities of the sculpture. In terms of user experience, both modalities were well received. Visualizations as well as physicalizations of medical data had an engaging effect on the study population. While the visualization was received more warmly in total, many remarks regarding the potential of the sculptures were made. Participants hypothesized a possible application for children, as well as potential to engage people with a high degree of technological aversion. From the study data, we conclude that a large potential for the application of both visualizations and physicalizations in laymen

anatomical education exist. The novelty and do-it-yourself approach of *Volvelle* is a promising concept for this, because of the combination of the exploration of anatomical structures in the virtual and physical space.

6.2 Limitations and Future Work

While we examined different approaches for the creation of *Vologram* structures from medical data, limitations of the concept also emerged. This section lists issues with the current approach, possible future additions to address existing problems, as well as interesting future directions for the application.

The physicalization pipeline presented in Chapter 3 shows a complete workflow for creating *Vologram* sculptures from medical imaging data. Our approach is based on the feasibility of executing this pipeline using *vtk* with one single filtered volume dataset. This makes it possible to include the *Vologram* filter directly into a rendering pipeline. The use of the reslice transformation on the volume dataset can lead to visible artefacts in the rendering. Using a single transfer function for the rendering of the volume data prohibits the use of interpolation for smoothing the outcome of the reslice transformation. Using interpolation on volume data, transformed using our illustrative approaches, leads to the assignment of mismatching colours to the individual regions. To achieve a better rendering quality with the help of interpolation, the data transformation part of the pipeline could be reworked. Instead of creating one single volume dataset, a set of actors could be directly created in the filtering process. For the slice extraction *vtk* cutting planes could be used instead of a subsampling of transformed volume dataset.

In *Volcraft*, we present three different methods for volume data preprocessing. Each leads to a different appearance of the resulting rendering and physicalization. The discrete and continuous illustrative [PB13] methods are well-suited to display volume data to laymen. However, the realistic approach, resulting from a similar treatment of the data as in direct volume rendering [PB13] is ill-suited. Structures blend on the individual slides of the sculptures, which is made worse through the reduced resolution. The assignment of colour and opacity values to source-data intensities is not well suited for creating educational sculptures and renderings, because the same colour and intensity values can be assigned to different structures. Future adjustments to the data wrapping in *Volcraft*, using the provided interface structure, could address this problem, by clarifying object boundaries based on the provided filters. Additionally, the development of more complicated transfer functions can limit the optical ambiguity.

Another source of difficulty is the printing material. We found that with access to a laser printer cheaper overhead slides with better transparency could be used. It was not investigated if a more suited version of overhead foils that are printable with inkjet printers exist. Investigations in this area could lead to the discovery of cheaper, better-suited materials for the slides. Likewise, for the other components of the physicalization,

more materials could be examined.

The concept of *Vologram* is based on the possibility to create the same type of physicalization with different sets of materials. We consider slide spacing, scale and receptacle position in the *Volcraft* user interface. The receptacle size is determined by the paginator component in the current version. It would be a worthy addition, to make the receptacle size freely selectable, to account for more diverse ways of construction. For this, a paginator component would have to be designed, according to the provided interface that handles slide placement automatically.

In the current implementation of *Vologram*, users have to select their custom viewpoint. While this enables them to create visualizations from arbitrary views, it might be worth to add an option to limit possible views to a range that shows the maximum possible amount of information. Viola and Gröller's *Smart Visibility* approach [VG05] could be incorporated into *Vologram*. Possible viewpoints could be limited to such that show as many of the selected organ structures as possible. The slicing algorithm used in *Vologram* does not consider the possible loss of visibility for smaller structures. As an alternative to our form of subsampling of the generated volume slices, an octree-based partitioning approach [RGW20] could be used to preserve visibility of such structures.

For the assignment of colours to the structures in the illustrative versions of the pipeline, currently, no interface exists in *Volcraft*. This could be addressed in future iterations of the application. For this, interactive elements could be introduced into the user interface, to customize object-specific colours and opacities. Also, besides the transfer function types, which we use in the application, many alternative types of functions exist [LKG+16]. An examination, which other kinds of transfer functions would be feasible to use for *Vologram*, could prove useful, both for user-customizable functions and automatically generated ones optimized for CT data.

The *MeVisLab* pipeline we use for pre-processing of the volume data is specifically tailored for the *Voxel-Man* segmentation of the *Visible Human* dataset [PHP+01]. For future iterations, it could be interesting to create a more interactive pipeline, suited to prepare arbitrary datasets. Alternatively, pre-processing could be automated directly in the *Vologram* application. Using emerging neural-network-based segmentation methods [MNA16] for segmenting personal medical data could enable users to gain knowledge about their medical conditions.

In this thesis, we presented different *Vologram* sculptures. Examining them, we found that the use of materials with imperfect properties, like the overhead foils with inherent opacity, leads to some visibility issues. Going back to examine these material properties could lead to a formulation of a calibration algorithm, which could mitigate the issues by altering the visual properties of slides impacted by visibility issues. This could be done by, for example, scanning two superimposed pages with a calibration pattern and

calculating necessary corrections for the opacity transfer functions of the individual slides from that.

With the limited size of the *Vologram* sculptures, as well as the slice-based interaction, possibilities for the labelling of anatomical structures, besides using colour codes, are limited. The addition of a digital visualization component could be used to improve this aspect. Modern smartphones are capable of providing camera-based augmented reality technology. With a mobile application, labelling for both the full sculpture, as well as the individual slides, could be introduced as digital augmentation of the sculptures while still providing the actual interactivity in the physical space.

The study was performed on a purely adult target group of a small size. In the course of the interviews, participants remarked that children would benefit from interaction with the sculptures as well. We think this would be an interesting base for a future study. This would, however, need the presence of children educators, to determine a suitable design and scope. It would also be interesting to perform a more focused study on a larger scale. This could provide more insight on how to improve the concept for a larger audience.

In its current form, the concept is already a versatile and engaging tool for its target group. The modular structure of the application leaves ample space for a multitude of future additions. *Vologram* is a further step in bringing medical visualizations out of the screen and into the hands of everyone interested in advancing their anatomical knowledge.

List of Figures

100

101

102

List of Tables

104

Bibliography

[ABKC90]   NM Alpert, JF Bradshaw, D Kennedy, and JA Correia. The principal axes transformation—a method for image registration. *Journal of nuclear medicine*, 31(10):1717–1722, 1990.

[AD09]   Anne MR Agur and Arthur F Dalley. *Grant's atlas of anatomy*. Lippincott Williams & Wilkins, 2009.

[ADS5]   Yousef AbouHashem, Manisha Dayal, Stephane Savanah, and Goran Štrkalj. The application of 3d printing in anatomy education. *Medical Education Online*, 20(1):29847, 2015. PMID: 28229704.

[AJH$^+$15]   Jason Alexander, Yvonne Jansen, Kasper Hornbæk, Johan Kildal, and Abhijit Karnik. Exploring the challenges of making data physical. In *Proceedings of the 33rd Annual ACM Conference Extended Abstracts on Human Factors in Computing Systems*, pages 2417–2420, 2015.

[ASS$^+$19]   Kathleen D Ang, Faramarz F Samavati, Samin Sabokrohiyeh, Julio Garcia, and Mohammed S Elbaz. Physicalizing cardiac blood flow data via 3d printing. *Computers Graphics*, 85:42 – 54, 2019.

[ASSW95]   Michael J Ackerman, Victor M Spitzer, Ann L Scherzinger, and David G Whitlock. The visible human data set: an image resource for anatomical visualization. *Medinfo. MEDINFO*, 8:1195–1198, 1995.

[CB32]   Julius Casserius and Daniel Bucretius. *Tabulae anatomicae LXXIIX, omnes novae nec ante hac visae*. Merianus, 1632.

[CDTJ17]   Long Chen, Thomas W Day, Wen Tang, and Nigel W John. Recent developments and future challenges in medical mixed reality. In *2017 IEEE International Symposium on Mixed and Augmented Reality (ISMAR)*, pages 123–135. IEEE, 2017.

[EB16]   Mohamed Estai and Stuart Bunt. Best teaching practices in anatomy education: A critical review. *Annals of Anatomy-Anatomischer Anzeiger*, 208:151–157, 2016.

[Fra]   Neil fraser. rearrangeable wooden model of brain scan. `https://neil.fraser.name/news/2008/01/04/`. Accessed: 2020-10-23.

[Gei09]   Michael L Geiges. Traces of marion b. sulzberger in the museum of wax moulages in zurich and their importance for the history of dermatology. *Journal of the American Academy of Dermatology*, 60(6):980–984, 2009.

[Gho15]   Sanjib Kumar Ghosh. Human cadaveric dissection: a historical account from ancient greece to the modern era. *Anatomy & cell biology*, 48(3):153–169, 2015.

[gmL]   How GM is saving cash using legos as a data viz tool. `https://www.fastcompany.com/1669468/how-gm-is-saving-cash-using-legos-as-a-data-viz-tool`. Accessed: 2020-04-15.

[Gra09]   Henry Gray. *Gray's anatomy*. Arcturus Publishing, 2009.

[HL10]   Jennifer Fong Ha and Nancy Longnecker. Doctor-patient communication: a review. *Ochsner Journal*, 10(1):38–43, 2010.

[HL16]   Dawn Hui and Richard Lee. Scan, plan, print, practice, perform: A disruptive technology? *The Journal of Thoracic and Cardiovascular Surgery*, 153, 09 2016.

[HW17]   Carmen Hull and Wesley Willett. Building with data: Architectural models as inspiration for data physicalization. In *Proceedings of the 2017 CHI Conference on Human Factors in Computing Systems*, pages 1217–1264, 2017.

[JD13]   Yvonne Jansen and Pierre Dragicevic. An interaction model for visualizations beyond the desktop. *IEEE Transactions on Visualization and Computer Graphics*, 19(12):2396–2405, 2013.

[JDF13]   Yvonne Jansen, Pierre Dragicevic, and Jean-Daniel Fekete. Evaluating the efficiency of physical visualizations. In *Proceedings of the SIGCHI Conference on Human Factors in Computing Systems*, pages 2593–2602, 2013.

[JDI+15]   Yvonne Jansen, Pierre Dragicevic, Petra Isenberg, Jason Alexander, Abhijit Karnik, Johan Kildal, Sriram Subramanian, and Kasper Hornbæk. Opportunities and challenges for data physicalization. In *Proceedings of the 33rd Annual ACM Conference on Human Factors in Computing Systems*, pages 3227–3236, 2015.

[JVJB17]   Susan Jang, Jonathan M Vitale, Robert W Jyung, and John B Black. Direct manipulation is better than passive viewing for learning anatomy in

a three-dimensional virtual reality environment. *Computers & Education*, 106:150–165, 2017.

[KNSV15]   Harikrishnan K N, Bennett Samuel, and Joseph Vettukattil. Hybrid 3d printing: A game-changer in personalized cardiac medicine? *Expert Review of Cardiovascular Therapy*, 13, 10 2015.

[LBI+11]   Heidi Lam, Enrico Bertini, Petra Isenberg, Catherine Plaisant, and Sheelagh Carpendale. Empirical studies in information visualization: Seven scenarios. *IEEE transactions on visualization and computer graphics*, 18(9):1520–1536, 2011.

[Lee83]   Jong-Sen Lee. Digital image smoothing and the sigma filter. *Computer vision, graphics, and image processing*, 24(2):255–269, 1983.

[Let]   Original campus model finds new home. `https://www.uleth.ca/masterplan/stories/original-campus-model-finds-new-home`. Accessed: 2020-10-23.

[Lik32]   Rensis Likert. A technique for the measurement of attitudes. *Archives of psychology*, 1932.

[LKG+16]   Patric Ljung, Jens Krüger, Eduard Gröller, Markus Hadwiger, Charles D Hansen, and Anders Ynnerman. State of the art in transfer functions for direct volume rendering. In *Computer Graphics Forum*, volume 35, pages 669–691. Wiley Online Library, 2016.

[LLG+16]   Kah Heng Alexander Lim, Zhou Yaw Loo, Stephen J Goldie, Justin W Adams, and Paul G McMenamin. Use of 3d printed models in medical education: a randomized control trial comparing 3d prints versus cadaveric materials for learning external cardiac anatomy. *Anatomical sciences education*, 9(3):213–221, 2016.

[LVPI18]   Kai Lawonn, Ivan Viola, Bernhard Preim, and Tobias Isenberg. A survey of surface-based illustrative rendering for visualization. In *Computer Graphics Forum*, volume 37, pages 205–234. Wiley Online Library, 2018.

[Mev]   Mevislab. `https://www.mevislab.de/`. Accessed: 2020-11-04.

[MMŽ10]   Danica Marković and Bojana Marković Živković. Development of anatomical models-chronology. *Acta Medica Medianae*, 49(2), 2010.

[MNA16]   Fausto Milletari, Nassir Navab, and Seyed-Ahmad Ahmadi. V-net: Fully convolutional neural networks for volumetric medical image segmentation. In *2016 fourth international conference on 3D vision (3DV)*, pages 565–571. IEEE, 2016.

[Moe08]   Andrew Vande Moere. Beyond the tyranny of the pixel: Exploring the physicality of information visualization. In *2008 12th International Conference Information Visualisation*, pages 469–474. IEEE, 2008.

[Mou]   Portal für moulagen und medizinische wachsmodelle, universitätsmedizin berlin. `https://www.moulagen.de/sammlungen/oesterreich/`. Accessed: 2020-11-19.

[MQMA14]   Paul G McMenamin, Michelle R Quayle, Colin R McHenry, and Justin W Adams. The production of anatomical teaching resources using three-dimensional (3d) printing technology. *Anatomical sciences education*, 7(6):479–486, 2014.

[NCFD06]   Daren T Nicholson, Colin Chalk, W Robert J Funnell, and Sam J Daniel. Can virtual reality improve anatomy education? a randomised controlled study of a computer-generated three-dimensional anatomical ear model. *Medical education*, 40(11):1081–1087, 2006.

[NMA12]   Michael I Norton, Daniel Mochon, and Dan Ariely. The IKEA effect: When labor leads to love. *Journal of consumer psychology*, 22(3):453–460, 2012.

[num]   Numpy. `https://numpy.org/`. Accessed: 2020-11-04.

[ODHHL95]   Lucille ML Ong, Johanna CJM De Haes, Alaysia M Hoos, and Frits B Lammes. Doctor-patient communication: a review of the literature. *Social science & medicine*, 40(7):903–918, 1995.

[PB13]   Bernhard Preim and Charl P Botha. *Visual computing for medicine: theory, algorithms, and applications*. Newnes, 2013.

[PHP+01]   Andreas Pommert, Karl Heinz Höhne, Bernhard Pflesser, Ernst Richter, Martin Riemer, Thomas Schiemann, Rainer Schubert, Udo Schumacher, and Ulf Tiede. Creating a high-resolution spatial/symbolic model of the inner organs based on the visible human. *Medical Image Analysis*, 5(3):221–228, 2001.

[PIL]   Pillow. `https://pillow.readthedocs.io/en/stable/`. Accessed: 2020-11-04.

[PS18]   Bernhard Preim and Patrick Saalfeld. A survey of virtual human anatomy education systems. *Computers & Graphics*, 71:132–153, 2018.

[pyq]   Pyqt5. `https://pypi.org/project/PyQt5/`. Accessed: 2020-11-04.

[Pyt]   Python. `https://www.python.org/`. Accessed: 2020-11-04.

108

[RCSL10]   Alessandro Riva, Gabriele Conti, Paola Solinas, and Francesco Loy. The evolution of anatomical illustration and wax modelling in Italy from the 16th to early 19th centuries. *Journal of anatomy*, 216(2):209–222, 2010.

[RGW20]   Renata Georgia Raidou, Eduard Gröller, and Hsiang-Yun Wu. Slice and Dice: A Physicalization Workflow for Anatomical Edutainment. *Computer Graphics Forum*, 2020.

[RMVTK+10] F Rengier, Amit Mehndiratta, Hendrik Von Tengg-Kobligk, Christian Zechmann, Roland Unterhinninghofen, Hans-Ulrich Kauczor, and Frederik Giesel. 3d printing based on imaging data: Review of medical applications. *International Journal of Computer Assisted Radiology and Surgery*, 5:335–341, 07 2010.

[SAK10]   Kapil Sugand, Peter Abrahams, and Ashish Khurana. The anatomy of anatomy: a review for its modernization. *Anatomical sciences education*, 3(2):83–93, 2010.

[SB16]   Sergej Stoppel and Stefan Bruckner. Vol 2 velle: Printable interactive volume visualization. *IEEE transactions on visualization and computer graphics*, 23(1):861–870, 2016.

[SCS17]   Dolores Steinman, Peter Coppin, and David Steinman. Data physicalization for improving communication and memorization. In *16º Encontro Internacional de Arte e Tecnologia 16th International Meeting of Art and Technology*, page 512, 2017.

[SML06]   Will Schroeder, Ken Martin, and Bill Lorensen. *The Visualization Toolkit*. Kitware, 2006.

[SSPOJ16]   Patrick Saalfeld, Aleksandar Stojnic, Bernhard Preim, and Steffen Oeltze-Jafra. Semi-immersive 3d sketching of vascular structures for medical education. In *VCBM*, pages 123–132, 2016.

[SWO+14]   Philipp Stefan, Patrick Wucherer, Yuji Oyamada, Meng Ma, Alexander Schoch, Motoko Kanegae, Naoki Shimizu, Tatsuya Kodera, Sebastien Cahier, Matthias Weigl, et al. An AR edutainment system supporting bone anatomy learning. In *2014 IEEE Virtual Reality (VR)*, pages 113–114. IEEE, 2014.

[SWR20]   Marwin Schindler, Hsiang-Yun Wu, and Renata Georgia Raidou. The anatomical edutainer. 2020.

[Ves47]   Johann Vesling. *Syntagma anatomicum*. Frambottus, 1647.

[VF+09]   O Rebecca Vincent, Olusegun Folorunso, et al. A descriptive algorithm for Sobel image edge detection. In *Proceedings of Informing Science &*
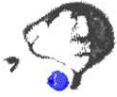
IT Education Conference (InSITE), volume 40, pages 97–107. Informing Science Institute California, 2009.

[VG05]   Ivan Viola and M Eduard Gröller. Smart visibility in visualization. In *Computational aesthetics*, pages 209–216, 2005.

[Vis]   The visible human project. `https://www.nlm.nih.gov/research/visible/`. Accessed: 2020-11-04.

[VMML17]   Marija Vukicevic, Bobak Mosadegh, James K Min, and Stephen H Little. Cardiac 3d printing and its future directions. *JACC: Cardiovascular Imaging*, 10(2):171 – 184, 2017.

[Voxa]   Segmented inner organs of the visible human. `https://www.voxel-man.com/sio`. Accessed: 2020-11-04.

[Voxb]   Voxel-man. `https://www.voxel-man.com/`. Accessed: 2020-11-04.

[VTK]   The visualization toolkit (vtk). `https://vtk.org/`. Accessed: 2020-11-04.

[WPF$^+$15]   Peter Weinstock, Sanjay P Prabhu, Katie Flynn, Darren B Orbach, and Edward Smith. Optimizing cerebrovascular surgical and endovascular procedures in children via personalized 3d printing. *Journal of Neurosurgery: Pediatrics PED*, 16(5), 2015.

[ZM08]   Jack Zhao and Andrew Vande Moere. Embodiment in data sculpture: a model of the physical visualization of information. In *Proceedings of the 3rd international conference on Digital Interactive Media in Entertainment and Arts*, pages 343–350, 2008.

Appendix A: *Vologram* Templates
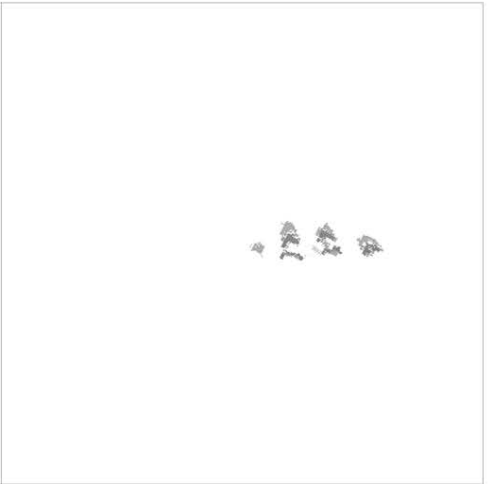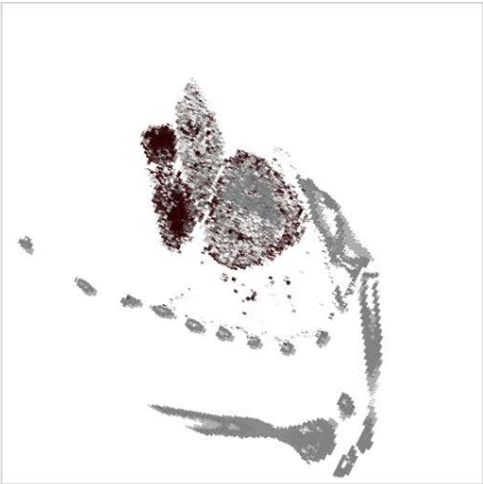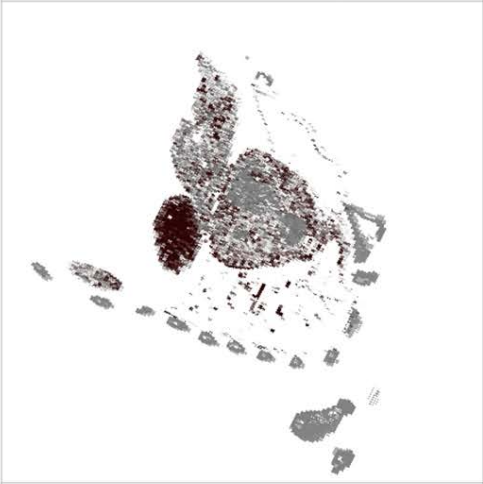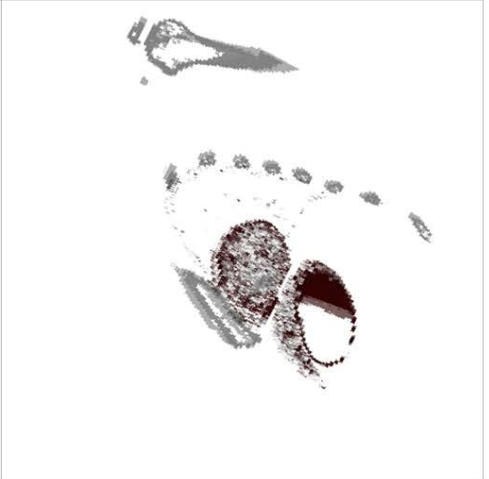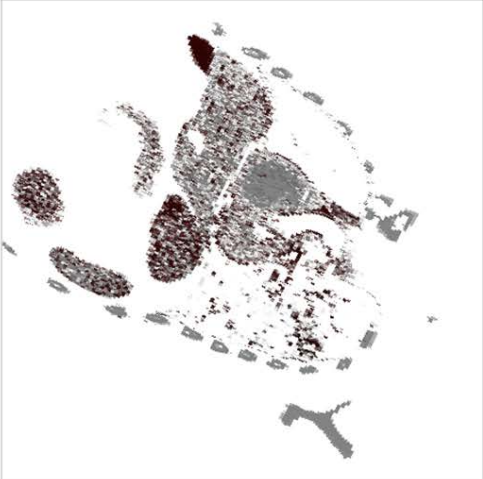
Skull
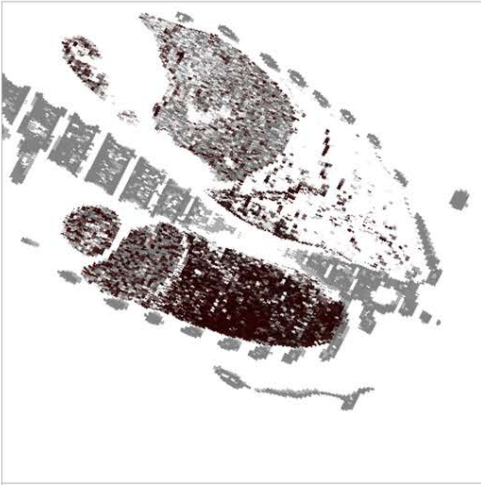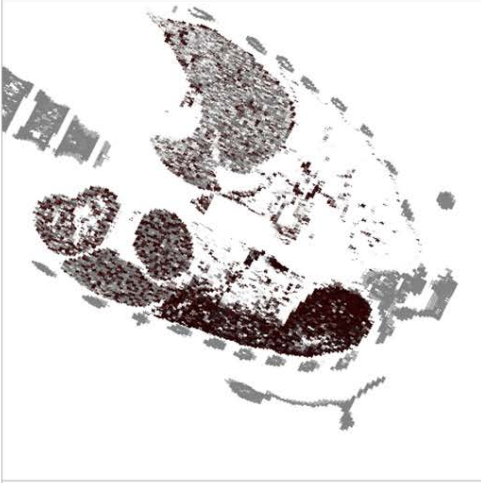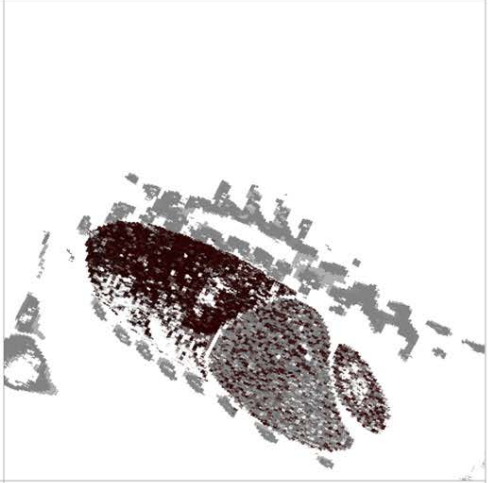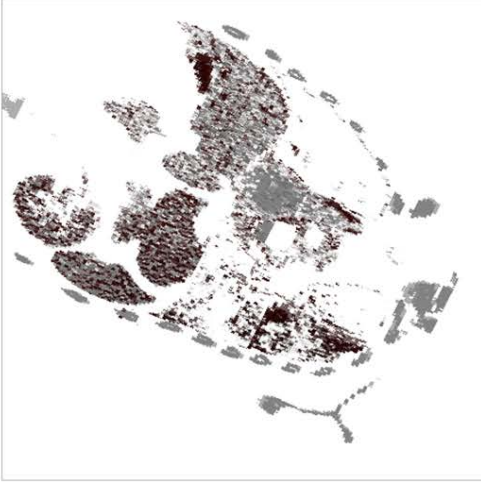
Upper Torso Realistic
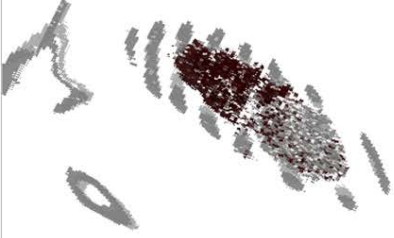
Upper Torso Illustrative
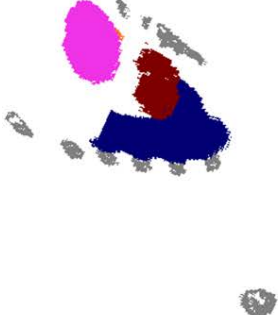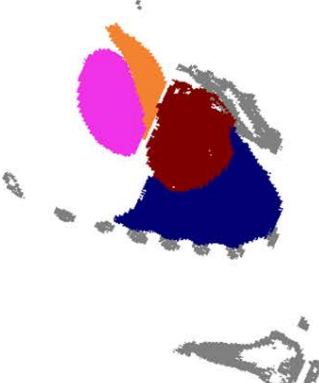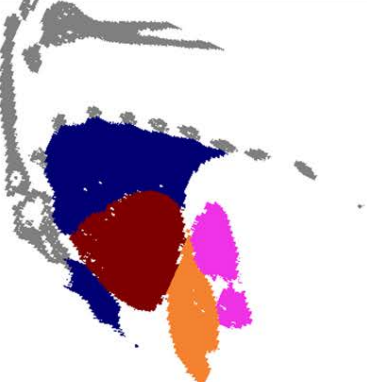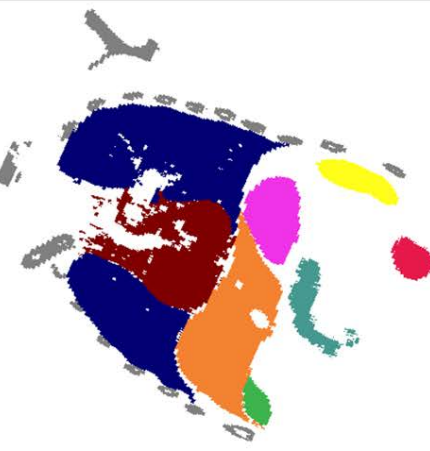
30 29
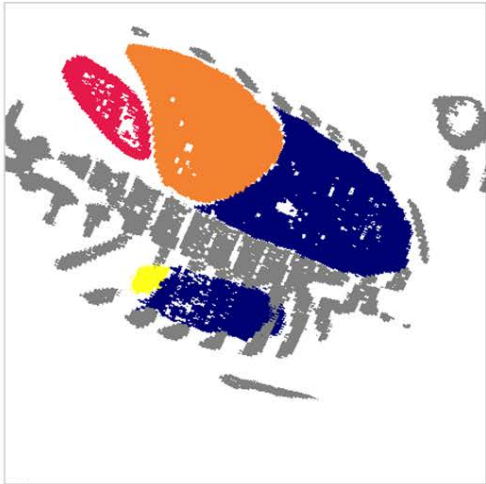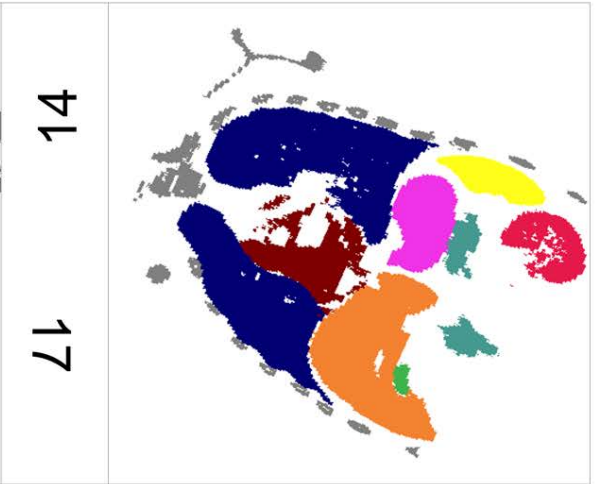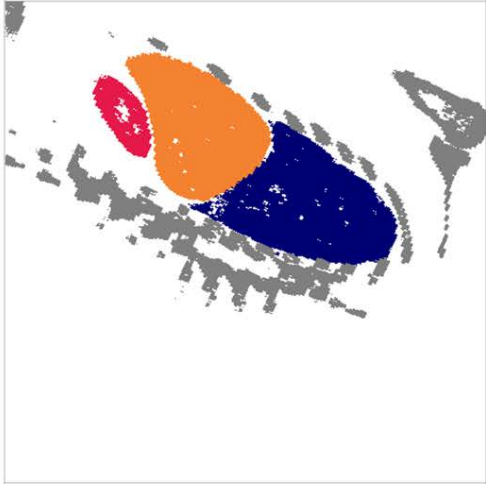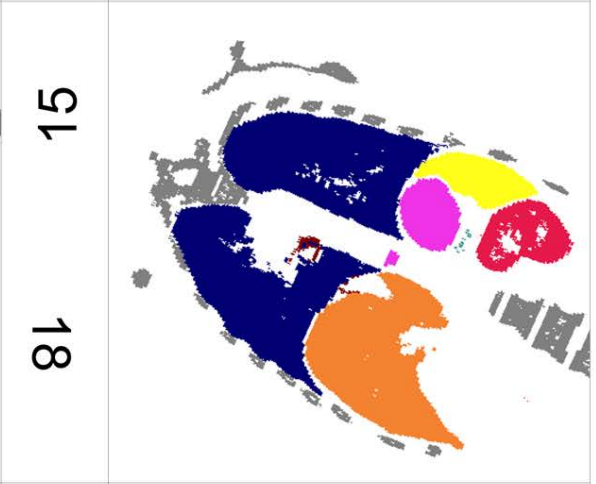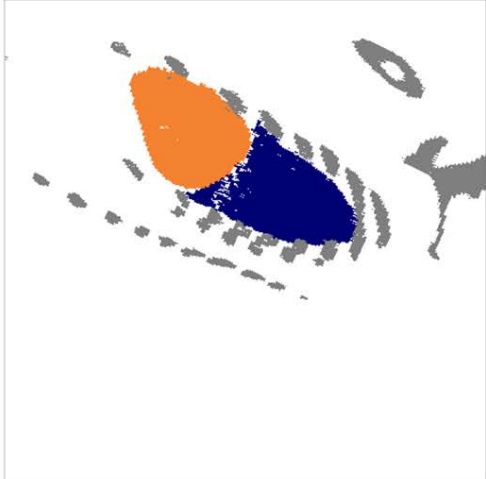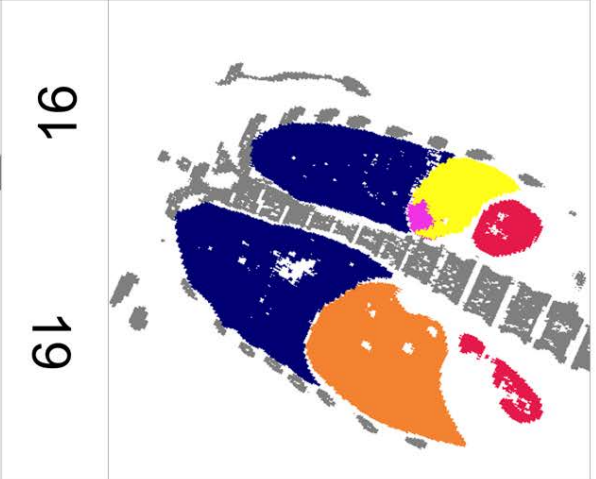
26 25

22 21

32 31

28 27

24 23

112

8 11

6 12

10 13

19   16

18   15

17   14

14   15   16

17   18   19

118

Appendix B: Study Materials

Reference Visualization

Front

122

Back

Left

Right

Colour Key

Labels

■ Colon
■ Gallbladder
■ Heart
■ Kidneys
■ Liver
■ Lung
■ Pancreas
■ Prostate
■ Skeleton
■ Skin
■ Small Intestine
■ Spleen
■ Stomach

Questionnaire

Questionnaire   Participant

Age:

Occupation:

I am experienced in using computers.				
Strongly Disagree	Disagree	Neutral	Agree	Strongly Agree

I have a thorough knowledge of human anatomy.				
Strongly Disagree	Disagree	Neutral	Agree	Strongly Agree

I enjoy working with computers.				
Strongly Disagree	Disagree	Neutral	Agree	Strongly Agree

I found the computer visualization appealing.				
Strongly Disagree	Disagree	Neutral	Agree	Strongly Agree

I found the physicalization appealing.				
Strongly Disagree	Disagree	Neutral	Agree	Strongly Agree

The visualisation was helpful completing the task.				
Strongly Disagree	Disagree	Neutral	Agree	Strongly Agree

The physicalisation was helpful completing the task.				
Strongly Disagree	Disagree	Neutral	Agree	Strongly Agree

I preferred using the phyiscalization over using the visualization.				
Strongly Disagree	Disagree	Neutral	Agree	Strongly Agree

What did you like about the visualization?

What did you not like about the visualization?

What did you like about the physicalization?

What did you not like about the physicalization?